PAEDIATRIC HIV INFECTION
FROM A MATHEMATICAL PERSPECTIVE
taking care of every child

JULIANE SCHRÖTER

Paediatric HIV infection from a mathematical perspective

Taking care of every child

Juliane Schröter

Paediatric HIV infection
from a mathematical perspective
Taking care of every child

Hiv-infectie bij kinderen vanuit een wiskundig perspectief
Elk kind telt

(met een samenvatting in het Nederlands)

Pädiatrische HIV-Infektion aus einer mathematischen Persepktive
Jedes Kind zählt

(mit einer Zusammenfassung auf Deutsch)

Proefschrift

ter verkrijging van de graad van doctor aan de
Universiteit Utrecht
op gezag van de
rector magnificus, prof. dr. H.R.B.M. Kummeling,
ingevolge het besluit van het college voor promoties
in het openbaar te verdedigen op

woensdag **19 oktober 2022** des middags te **4.15 uur**

door

Juliane Schröter

geboren op 21 april 1989 te Rastatt, Duitsland

Promotor: Prof. dr. Rob J. de Boer

Beoordelingscommissie:

Prof. dr. Becca Asquith

Prof. dr. José A.M. Borghans

Prof. dr. Nigel Klein

Prof. dr. Roland R. Regös

Prof. dr. Ruy M. Ribeiro

Preface

If you ask me about my favourite subjects at high school, the answer will be math and biology. A combination of both results in "biomathematics". This is exactly what a google search revealed to me almost 15 years ago, which had a major impact on my study subject of choice and has been the foundation of the work I am presenting here.

While at the beginning it was mainly pure math courses with some sprinkles of biology, ranging from genetics over molecular biology and zoology to botany, I quickly developed a deep interest for the interdisciplinary work. I wanted to apply math in the biomedical field, I wanted to use it as a tool to answer medicine-related questions, I wanted to compare, quantify, and determine numbers from human derived data, and I wanted to know where the data I am working with is coming from and how exactly it is generated. My PhD project in the field of theoretical immunology has ticked all these boxes.

Nevertheless, an interdisciplinary approach also bears its very own challenges. "As a biomathematician you understand more biology than any mathematician, and more math than any biologist". These words I was told during my bachelor's study, and they are still reverberating. As a biomathematician, I have been equipped with the basic knowledge to speak and understand both scientific languages, but you can also quickly become the odd one out. Unfortunately, this is something I have learnt the hard way through trial and error, and it took me along a bumpy road until I ended up at the Theoretical Biology & Bioinformatics (TBB) group in Utrecht, where I found my place in a group full of like-minded people. Their support, trust and encouragement were also urgently needed when I was facing the so-called interdisciplinary curse.

To develop mathematical models not just in theory, I have relied on the willingness and help of others to share and allow me access to their data. Working in the interdisciplinary and international consortium of EPIICAL ensured that there was a common interest to share clinical data, but accessing that data still proved to be difficult. Different countries, different institutions, different expectations, and on top human data – all together involves a lot of negotiations and

bureaucracy: ethical agreements have to be passed, contracts have to be signed, patient privacy has to be asserted. It was tedious sometimes and required quite some perseverance.

An important milestone in my PhD was my research stay in South Africa at the Family Centre for Research with Ubuntu (FAMCRU) at Tygerberg Hospital (Cape Town), and the Perinatal HIV Research Unit (PHRU) at Chris Hani Baragwanath Hospital (Soweto, Johannesburg). This stay did not only help to develop an understanding and interest for each other's work between the collaborating researchers, but it also broke down many interpersonal barriers which removed some hurdles in the jungle of bureaucracy. Even the fruits of my research stay have sadly not directly made it into this thesis because of time constraints, this trip was also personally a great experience that I would not want to miss. Especially, it showed me the importance and the meaning of my work, as HIV is a much more prominent problem in South Africa than it is in Europe. I encourage everyone who is working interdisciplinary to visit their collaborators as often as possible and to get hands-on experience with each other's work very early on, as this can prevent quite some struggles in the process of collaboration.

For the successful performance of interdisciplinary work and to bridge the gap between different disciplines, more than just pure knowledge is required. Communication and networking skills have been the key aspect during my PhD, and the development of such soft skills should not be missed out or neglected in any PhD journey. As more and more data are generated, bearing more information than one discipline by itself can tackle, interdisciplinary work has become crucial. Interdisciplinary work benefits from the connection of different perspectives, including misunderstandings and confrontation, which should not repel anybody from working in an interdisciplinary field. Working interdisciplinary can be really fun!

With this booklet I can now proudly present the achievements of my collaborations and results of the work done in the last couple of years. While reading this booklet now, keep in mind that a PhD thesis only presents the tip of the iceberg. The struggles, efforts and accomplishments along the way are nicely hidden behind the words you are going to read.

Utrecht, September 2022

Contents

1

General Introduction

According to the World Health Organisation (WHO), 1.5 million people newly acquired Human Immunodeficiency Virus (HIV) in 2020 and every 10th person was a child below the age of 15 years [UNAIDS, 2020]. Children acquire HIV via mother-to-child-transmission (MTCT) during pregnancy (in utero), labour (intrapartum) or after birth (postpartum), for example, due to breastfeeding [Newell, 1998; Tobin and Aldrovandi, 2013]. Once positively diagnosed, children depend usually on lifelong treatment (antiretroviral treatment, ART) to control the HIV infection and to prevent further disease progression towards the **A**cquired **I**mmune **D**eficiency **S**yndrome (AIDS). A functional cure for HIV is not yet available.

In 2013, the case of the "Mississippi Baby" rose to attention and the hope for an HIV cure increased [Persaud et al., 2013]. A newborn received an HIV diagnosis within 30 hours of birth and started treatment immediately. Treatment initiation led to a rapid control of the virus, so that viral genetic material (ribonucleic acid, RNA) was undetectable in blood. The treatment was continued for 18 months, after which it was stopped (medically unplanned) by the mother. After a medical visit half a year later, the child was once again tested for HIV RNA, and to the surprise of everyone there was still no evidence for any viral load (VL) [Persaud et al., 2013]. The question rose if this child was indeed HIV free and if the early treatment onset led to a cure of HIV [Palma et al., 2015, 2019]. Unfortunately, the virus rebounded two years later [Luzuriaga et al., 2015]. But paediatric HIV research has been since amazed by this long treatment-free viral suppression [Shiau et al., 2018].

So far, there are only two other cases reporting children in which early treatment initiation followed by an interruption has resulted in successful HIV remission off treatment - both children are now over 10 years off treatment (11 and 18 years) [Violari et al., 2019; Sáez-Cirión et al., 2013; Frange et al., 2016]. These are exceptional cases, but the question remains whether treatment-free HIV remission in children is indeed possible, and if early-treated children are a hypothetical target population for a potential HIV cure. To be able to answer these very ambitious questions, we first have to understand the viral and immunological dynamics before and after early treatment initiation in children with perinatally-acquired HIV.

This thesis investigates paediatric HIV infections from a mathematical perspective by quantifying viral and immunological dynamics during untreated infections and during treatment. The focus is on the two main measures/read-outs (biomarkers) of an HIV infection: Plasma HIV RNA (VL) (**Chapter 2 and 5**) as an indicator for the presence of replicating virus, and CD4+ T-cell levels (**Chapter 3 and 4**)

as an indicator for the health status of the immune system. We make use of existing cohort studies and focus on early-treated children in response to ART. We depart from conventional statistical approaches that typically describe a population average or the median of all measured data. Throughout this thesis we follow an individual approach and "take care of every child" individually. In this introductory **Chapter 1**, the relevance of the VL and CD4+ T-cell levels (counts and percentages) in the context of an HIV infection and its treatment is outlined. A special focus is on paediatric HIV, challenges of treatment, and the breakthrough of early treatment onset. The field of viral dynamics and its importance is also introduced, as well as the goal and scope of this thesis are explained.

HIV pathogenesis and treatment: HIV reservoir is the hurdle to cure

HIV is not a death sentence anymore. Thanks to ART, HIV replication can nowadays be controlled (Figure 1.1), which allows individuals living with HIV to have a normal and "healthy" life. HIV infects cells of the immune system, mainly activated CD4+ T cells (Figure 1.1). It enters the cells via the CCR5 or CxCR4 co-receptors and integrates its genomic blueprint in the host DNA. HIV therefore makes use of the replication machinery of the host cells to reproduce. Infected T-cells produce new virus particles which can be detected and fought by the host's immune system. HIV mutates rapidly, which allows the virus to escape from established immune responses. Constant immune activation and the virus-induced depletion of CD4+ T helper cells weaken and damage the immune system, and make the host more susceptible to other infections, eventually leading to AIDS. In contrast to adults, who can have a chronic HIV infection for more than 10 years before progressing to AIDS, untreated infants typically show a very rapid disease progression. They develop AIDS within one year after infection, and often do not survive beyond their second birthday [Babiker et al., 2000].

ART prevents new viral infection of target cells, blocks viral replication, and allows the immune system to maintain or regenerate. The major problem is that ART cannot eliminate latently HIV-infected cells, in which HIV is already genetically imprinted but probably not actively replicated [Finzi et al., 1999]. These cells form the HIV reservoir, which is seeded very early during an HIV infection [Frenkel et al., 2003; Joos et al., 2008], and can be stochastically reactivated. The interruption of ART would therefore ultimately lead to a viral rebound and a continuation of the HIV infection. Thus, the HIV reservoir creates the major hurdle towards an HIV cure.
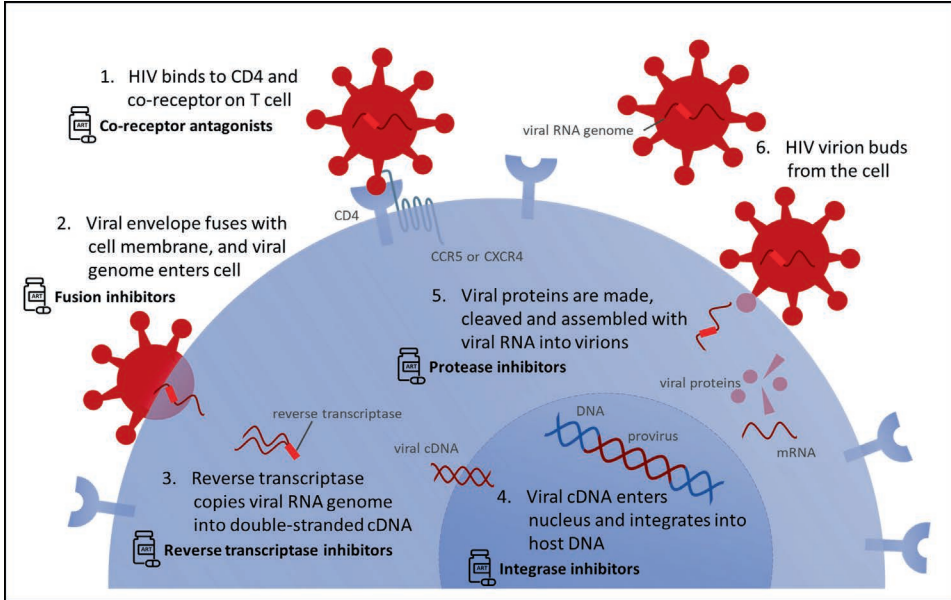
1

Figure 1.1: Illustration of HIV life cycle and targeted sites of the antiretroviral drugs. The figure is modified from [Parham, 2013].

A milestone in paediatric HIV research: Early ART initiation is life saving

The results of the **C**hildren with **H**IV **E**arly Anti**R**etroviral (CHER) randomised trail in 2008 marked a turning point in paediatric HIV research. The timing of treatment initiation in children with parentally acquired HIV and the duration of treatment was studied [Violari et al., 2008; Cotton et al., 2013]. The results showed that an early initiation of treatment soon after the HIV diagnosis is life saving for children with HIV. This led to a change in international guidelines on when to start treatment in young children with HIV - namely straight after a positive HIV diagnosis [National Institutes of Health, 2022]. Before the CHER trial, ART was only administrated to children once CD4+ T-cell levels were low, or children showed first symptoms of AIDS as an advanced stage of the infection.

The CHER study also investigated the potential of ART interruption after 1 or 2 years of early-initiated continuous ART, because ART is a very harsh treatment associated with toxicity and numerous side effects. In the majority of cases, HIV rapidly rebounded after treatment interruption and all children besides one had to re-start ART shortly thereafter [Violari et al., 2008; Cotton et al., 2013; Violari et al., 2019]. The CHER study showed that an early onset of treatment,

independent of CD4+ T-cell levels and the stage of the disease, reduced morbidity and mortality of young children with perinatally acquired HIV, compared to delayed and continuous ART [Violari et al., 2008; Cotton et al., 2013]. Thanks to an early onset of treatment many more children with perinatally acquired HIV are nowadays reaching adolescence, however they also seem to rely on lifelong ART to control the infection.

Challenging ART adherence - is there an alternative?

Even though ART interruptions are not recommended by international guidelines, they are often not avoidable and frequently occur in clinical practice. ART is a combination of antiretroviral drugs from different drug classes, which act against different stages of the viral integration and replication process (Figure 1.1). Therapy schedules are therefore complicated, and have to be followed and monitored carefully to ensure a successful HIV control. Even though there are more and better antiretroviral drugs becoming available and drug administration is facilitated for infants, these drugs have numerous side effects, high potential for toxicity and drug-drug interactions. Consequently, treatment is often interrupted unplanned and treatment regimes have to be adjusted and changed, particularly for the youngest. Discontinued treatment increases the risk of drug resistance, reducing the options of treating and controlling HIV for an individual. The adherence of ART is challenging, and not only requires the willingness and commitment of the patient but also their primary caregivers (with respect to paediatric HIV). Thus, there is an urgent need for alternative treatment strategies.

Current research is searching for an effective way of completely eliminating HIV infection or for a functional cure, i.e. suppressing the virus in the absence of antiretroviral therapy and allowing, therefore, "drug holidays". Therapeutic HIV vaccines and other immunotherapeutics, such as broadly neutralizing antibodies and/or innate-immune-enhancing agents, are options that are currently considered [Terrade et al., 2021]. In combination with early initiated ART, these new approaches have been shown to be successful in non-human primates with simian immunodeficiency virus (SIV) and simian-human immunodeficiency virus (SHIV) infections by limiting the viral reservoir, virus persistence in tissue, and delaying viral rebounds during ART interruptions [Byrareddy et al., 2016; Whitney et al., 2018; Okoye et al., 2018]. The hope is that these or similar novel curative therapies eventually translate into a cure of HIV.

1

Using cohort data to study paediatric ART response dynamics

The EPIICAL (**E**arly-treated **P**erinatally HIV-infected **I**ndividuals: **I**mproving **C**hildren's **A**ctual **L**ife with Novel Immunotherapeutic Strategies, www.epiical.org) project has been formed as an international and interdisciplinary collaboration establishing novel immunotherapeutic strategies to achieve ART-free HIV remission in children [Palma et al., 2015, 2019]. Its greater purpose is to investigate in which terms novel strategies could be implemented in children who perinatally acquired HIV and who have started ART early, as curative strategies are often combined with early initiated ART [Palma et al., 2019; Terrade et al., 2021]. Furthermore, EPIICAL aims to figure out which children are ideal and potential candidates for additional or alternative curative strategies to ART. As the focus is on early treated children with perinatally acquired HIV, it seems natural to ask what we know about ART response dynamics in this special target population at this stage.

There are a few examples of children who showed a fast VL suppression after initiating ART early [Persaud et al., 2013; Sáez-Cirión et al., 2013; Luzuriaga et al., 2015; Frange et al., 2016; Shiau et al., 2018]. Children seem to have barely any HIV specific immune response. However, the immunological damage caused by the virus seems to be minor in the long term, as these children typically show normal immunological development [Palma et al., 2015]. Information is often drawn from cohort studies, in which specific time points of interest, like time to viral suppression (TTS) or immunological status after 3 to 5 years, are used to make generalised predictions for the population of early treated children [Lewis et al., 2012; Picat et al., 2013; Lewis et al., 2017; EPPICC and EPIICAL, 2019]. However, these predictions are not applicable for every child, as only a fraction of children follow the average observations. Therefore, we aim to get insights into the individual virological and immunological dynamics in response to early initiated ART:

- How fast does an infant suppress the virus?
- What kind of VL decay pattern do early-treated children show, and how do their VL decay patterns differ from each other?
- What effect do VL decay patterns have on the time to viral suppression?
- How fast do CD4+ T-cells recover? How does the recovery depend on the VL decay pattern?
- Do depleted CD4+ T-cell levels recover back to healthy values?
- Is age an independent variable influencing ART response dynamics?

In this thesis, we try to address these open questions by modelling the data

from early-treated children. The knowledge gained from our novel analyses of viral and immunological dynamics of these children during early-initiated ART hopefully paves the way for a more rationalised timing of subsequent novel treatment options.

The studies in this thesis and the data that we analyse are mainly part of the EPIICAL consortium. EPIICAL has facilitated our access to collected cohort studies participating in the **E**uropean **P**regnancy and **P**aediatric H**I**V **C**ohort **C**ollaboration (EPPICC), on which we have performed our analyses. The EPPICC studies contain observational data that was collected for the purpose of epidemiological research on the prognosis and outcome of HIV-infected pregnant women and their children across Europe and Thailand [EPPICC, 2011, 2018]. We have worked with the data from the EPPICC Paediatric merger 2014, which contains routine demographics, clinical, laboratory and treatment related data collected between 1998 and 2013 [EPPICC, 2018; EPPICC and EPIICAL, 2019]. Since most of the data was collected before the era of early treatment initiation in paediatric HIV, we had to select those children in the EPPICC cohorts starting ART early - meaning within half a year of age. EPPICC contains a large amount of longitudinal and clinically processed data. This type of data is rare in the field of paediatric HIV, and/or difficult to access for non-clinicians (even though regular clinical monitoring is essential).

Viral load and CD4+ T-cell measurements and dynamics inform about disease status and treatment efficiency

Plasma HIV RNA (also referred to as "viral load", VL) and CD4+ T-cell measurements are surrogate and approved biomarkers for HIV infection, which are regularly measured and monitored. Detectable viral load, measured in copies per millilitre (mL) of blood, indicates the presence of reproductive virus; the higher the values the more virus is actively produced. Undetectable VLs do not indicate the absence of virus but show that the active viral production is under control. Depending on the used assay the limit of detection may vary between 20 and 400 copies/mL. The more recent assays are more exact but to be consistent we define 400 copies/mL as the detection limit in the context of this thesis. Effective treatment rapidly suppresses and sustains the VL to undetectable levels. Viral suppression is generally defined after having two sequential undetectable VL measurements. Virological failure of the treatment

occurs when ART fails to reduce the VL or to sustain viral suppression, and requires a switch in treatment.

The CD4+ T-cell levels reflect the status of the immune system. As HIV disease progresses CD4+ T-cells gradually decline partly caused by the cytotoxic effect of HIV and partly due to the activated immune response. A successful treatment response is usually reflected by stable or rising CD4+ T-cell levels. Immunological failure of the treatment occurs when CD4+ T-cells further degrade despite being on ART. Thus, the monitoring of both biomarkers together and their dynamics over time inform us not only about disease progression but also about the adherence and effectiveness of treatment. Such data has been collected in the EPPICC cohorts, which dataset forms the basic data source for this thesis.

In an acute HIV infection, VL rapidly increases and reaches a peak after 2 to 4 weeks [Lindbäck et al., 2000; Richardson et al., 2003]. This peak is about an order of magnitude higher in children than in adults [McIntosh et al., 1996; Richardson et al., 2003]. VL then decreases to a constant lower "setpoint" level over the next few weeks. Setpoint VLs in very young untreated children are usually higher compared to adults and somewhat older children, as their degree of viral contraction is much lower (see Figure 1.2) [Richardson et al., 2003]. **Chapter 5** addresses this difference in setpoint VLs between adults and children in more detail. High setpoint VLs generally predict a fast disease progression [Kelley et al., 2007; Fraser et al., 2007], as seen in children. An HIV infection is accompanied by a gradual loss of CD4+ T-cells. Once levels of CD4+ T cells become too low, the immune system starts to respond poorly to pathogens, leading to opportunistic infections, which status is defined as AIDS. As many children are already exposed to HIV in utero, they are often born with high VLs and/or low CD4+ T-cell levels. The time needed to suppress their VL to undetectable levels has been associated with the VL, CD4+ T-cell level and age at start of treatment [EPPICC and EPIICAL, 2019]. Thus, treatment initiation leads to heterogeneous decline in VL and usually facilitates an asymptotic CD4 recovery, on which we will focus in **Chapters 2 and 4**.

Studies of an infant immune system requires CD4 normalisation

In young children with HIV we have to be careful with the interpretation of their CD4+ T-cell dynamics, as CD4+ T-cell measurements in a microlitre (μl) of blood naturally change with age - not only in numbers but also in their functionality. An infant immune system is immature and develops with age, impacting the T-cell compartments. These natural and healthy dynamics are most dominant in early
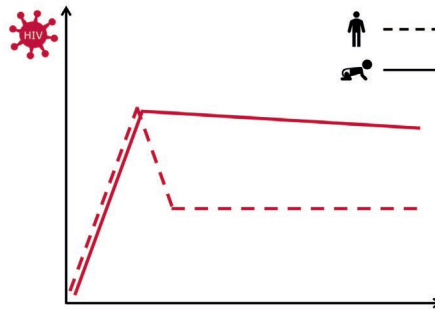
Figure 1.2: Schematic illustration of the difference in VL dynamics between adults and children during acute HIV infection.

childhood and reaching constant levels in adulthood. An infant immune system develops a responsiveness to infections but some cells of the immune system still have to be produced. While describing CD4+ T-cell dynamics in children with HIV, as done in **Chapter 4,** it is therefore important to account for these natural dynamics and to not assume the steady state of an adult immune system.

Thus, a decline in CD4+ T cell measurements is a natural feature of an infant's immune system, for example due to body growth, and is not necessarily caused by the HIV infection alone. To correct for these natural changes in the T-cell compartments, it is necessary to have standardised "healthy" CD4+ T-cell dynamics over age at hand. Such reference normalisation functions are provided in **Chapter 3** of this thesis and allow us to quantify T-cell dynamics independent of age.

Viral dynamics - Mathematical modelling in HIV research to gain quantities

Mathematical modelling has been a useful tool to capture the fundamental viral and immunological dynamics of HIV infection, and the response to treatment [Perelson and Nelson, 1999; Nowak and May, 2000; Perelson, 2002; Hill et al., 2018]. Known biological processes of the virus-host-interactions (Figure 1.3A) are translated into simple equations [Nowak and Bangham, 1996; Bonhoeffer et al., 1997; Wodarz and Nowak, 2002]. Typical models of an HIV infection within an individual consider uninfected target CD4+ T cells (T) that are newly produced at a constant rate σ and die at a rate d (where $1/d$ is the lifespan of uninfected CD4+ T-cells). Due to the infection by the virus population (V), target cells become

infected cells (I) at a rate β, after which they leave the compartment of uninfected cells and enter the compartment of infected cells. Infected cells die with a rate δ. As infected cells are recognised and killed by the immune system, their lifetime is usually short and δ is faster than d. Infected cells produce free virus at a rate p and the clearance rate of free viral particles in blood plasma is c. The changes for each of these three populations (T, I and V) over time t in a μL of blood can be written into the following set of ordinary differential equations (ODEs):

$$\frac{dT}{dt} = \sigma - dT - \beta\,T\,V, \tag{1.1}$$

$$\frac{dI}{dt} = \beta\,T\,V - \delta I, \tag{1.2}$$

$$\frac{dV}{dt} = pI - cV. \tag{1.3}$$

This system (1.1)-(1.3) forms the classic viral dynamic model for HIV infection, which tracks the levels of the virus and CD4+ T-cells during a typical course of an HIV infection (Figure 1.3B). The model can be extended (e.g. by an immune response, and/or a latently and/or other infected cells population) and modified (e.g. to simulate the onset of treatment by setting $\beta = 0$), and thus allows one to study many qualitative features of an HIV infection [Nowak and May, 2000]. Since this model (1.1)-(1.3) is "mechanistic", it allows one to make assumptions about underlying mechanism explaining real-world scenarios, which cannot be directly derived from measurements alone.

Example: Analysis of viral decay after treatment initiation - a breakthrough in HIV research

A famous application of this model (1.1)-(1.3) was the analysis of ART [Perelson et al., 1996; Perelson, 2002; Nowak and May, 2000; Hill et al., 2018], which revealed that the productively infected cells are turning over rapidly. As the viral dynamics occur on a much faster time scale than the dynamics of uninfected and infected cells, one typically assumes a quasi steady state (QSS) for the viral population (Equation 1.3). In mathematical terms this means that the change in the virus population over time should be equal to zero, $\frac{dV}{dt} \overset{!}{=} 0$, which implies that fast production of the virus ($p\,I$) and the clearance of the virus ($c\,V$) balance out. Hence, V is proportional to I and Equation (1.3) can be replaced by

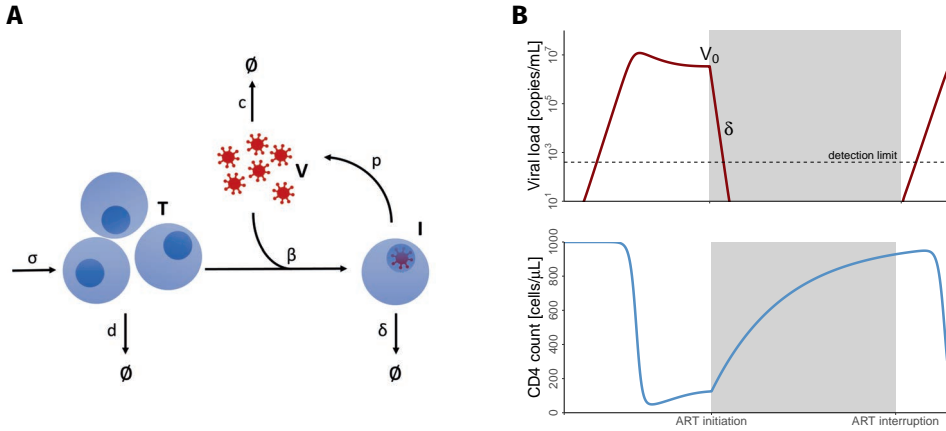$$V(t) = \frac{p}{c}I(t). \tag{1.4}$$

Figure 1.3: The basic viral dynamics model of HIV. (A) Flow diagram of known virus-host interactions that underlie the model (1.1)-(1.3). (B) Example trajectories of an acute/chronic HIV infection and the effect of treatment initiation. Upper panel represents the viral and lower panel the CD4+ T-cell dynamics. Grey shaded area shows the treatment window. Dashed horizontal line depicts the viral load detection limit of 400 copies/mL. V_0 shows the initial VL at start of treatment and δ represents the decay parameter, according to Equation (1.8)).

Introduction of treatment can be simulated by setting $\beta = 0$, reducing the above system (1.1)-(1.3) to

$$\frac{dT}{dt} = \sigma - dT, \tag{1.5}$$

$$\frac{dI}{dt} = -\delta I. \tag{1.6}$$

The infected cell Equation (1.6) is now decoupled from the target cell Equation (1.5) and can be analytically solved:

$$I(t) = I_0\, e^{-\delta t}, \tag{1.7}$$

where I_0 are the number of infected cells at the start of treatment. Number of infected cells are impossible to measure, instead VL measurements are usually available. Equation (1.4) can be used to rewrite Equation (1.7) into

$$V(t) = V_0\, e^{-\delta t}, \tag{1.8}$$

where we receive an equation describing the VL dynamics as response to treatment initiation. The initial VL at start of treatment is given by V_0, which declines exponentially at the rate δ, where $1/\delta$ refers to the expected life span of

1

infected cells. A rapid exponential decay has been observed in VL measurements immediately following treatment initiation, establishing that productively infected cells are short-lived (with $\delta \approx 1/\text{day}$). Due to the short generation time, HIV was identified as a fast mutating virus quickly escaping established immune responses and occupying the immune system [Ho et al., 1995; Wei et al., 1995].

Parameter estimation and identifiability requires model simplification

A mathematical model can, in principle, be calibrated (fitted) to observed data by estimating its parameters. This procedure of "parameter estimation" allows one to quantify processes and dynamics of an HIV infection. Parameters within a system often depend on each other, and if various sets of parameters result in similar trajectories, parameters will be difficult to uniquely identify. To not run into the problem of overfitting, (many) more measurements must be available than parameters. This can, however, not always be guaranteed. Particularly human data is often sparse. Alternatively, individual parameters can be obtained from other experimental measurements, e.g. individual parameters can be determined by breaking down processes, like the above described viral decline analysis after treatment initiation [Perelson et al., 1996]. Also the dependency of variables can be considered, and the intrinsic influence between VL and CD4+ dynamics can be factored in. Thus, additional information can reduce the number of free parameters that need to be estimated, avoiding the overfitting of parameters.

However, often models require further simplifications, for example, by lumping parameters together. On closer consideration, the decline of viral load directly after treatment initiation, depends not only on one, but on several, populations of infected cells with different lifespans [Perelson et al., 1997]. Additionally, the viral clearance rate also contribute to the viral decay. Thus, VL decay is mechanistically considered to be a multi-phasic process. As these different decay rates are difficult to identify, we describe the exponential VL decay after treatment in a more phenomenological way like in **Chapter 2**. Hence, we have to acknowledge that our mathematical model is a rigorous simplification of reality. The art of mathematical modelling is to find the right model to address one or a set of particular questions given the data at hand.

Scope and aim of this thesis

In this thesis, we apply mathematical modelling to quantitatively describe viral load and CD4+ T-cell dynamics in very young children during HIV infection and during early-initiated ART. The analysed data has been retrieved from existing (already published) cohort studies. We focused on children who perinatally acquired HIV around birth and started treatment early within their first 6 months of life. The aim of this thesis is to characterise successful response kinetics of early treated children, to learn how to identify candidates for alternative treatment strategies and to evaluate if this particular target population might assert the hope for a potential HIV cure.

In **Chapter 2**, we focus on viral decay dynamics of children directly after their first treatment initiation. We qualitatively describe VL decay patterns and quantify viral suppression. We use a simplified exponential decay model for VL decay after treatment initiation and determine time to viral suppression mathematically. As age has been assessed to be an independent factor associated with time to viral suppression [EPPICC and EPIICAL, 2019], we especially investigated the contribution of a child's age on both the HIV disease progression, and on the viral suppression upon treatment initiation.

Chapter 3 addresses the natural dynamics in T-lymphocytes over age. As standardised functions for T-lymphocytes of children barely exist, or are only based on a few measurements, we improve on this by fitting a phenomenological model to a large dataset of healthy Dutch individuals. A special focus is on the period younger than 1 year of age, which is of special interest in this thesis. Continuous T-lymphocyte reference functions are required for comparison and quantification of T-cell dynamics to correct for age-differences, like for children living with HIV.

In **Chapter 4**, we investigate CD4+ T-cell recovery upon treatment initiation. Using the standardised functions from Chapter 3, we normalise CD4+ T-cell measurements and quantify their recovery in every individual child. We here focus again on early-treated children, who successfully suppress HIV. We describe recovery phenomenologically by an increasing linear function approaching an asymptotic level. So, next to the recovery rate, we establish the level of recovery, and the time to reach this recovery level. We also investigate whether CD4 recovery is linked to viral suppression.

1

As the contraction ratio from peak VL to setpoint VL is low in children, we investigate this ratio in **Chapter 5**. Using classical mechanistic mathematical models, we perform parameter sweeps to identify mechanistic explanations for the large difference in this VL contraction ratio between young children and adults (or somewhat older children). We group parameters into host, virus and immune response associated, observe their impact on the peak, setpoint VL and their ratio, and find that differences in immune associated parameters explain the observations most parsimoniously.

Chapter 6 concludes this thesis with a general discussion. We focus on the selection criteria of the children we have studied, and on the limitations of the data used in the analyses. We close with an outlook on how quantitative knowledge of the VL and CD4+ T-cell dynamics during a paediatric HIV infection, before and during ART, might help the selection of potential candidates for novel alternative treatment strategies towards an HIV cure.

2

Time to viral suppression in perinatally HIV-infected infants depends on the viral load and CD4 T-cell percentage at the start of treatment

Juliane Schröter [1], Anet J.N. Anelone [1], Andrew J. Yates [2] & Rob J. de Boer [1]
on behalf of the EPIICAL Consortium

[1] Theoretical Biology & Bioinformatics, Utrecht University, Utrecht, NL
[2] Department of Pathology & Cell Biology, Columbia University, New York City, USA

Abstract

Background: Interventions aiming for an HIV cure would benefit from rapid elimination of virus after the onset of antiretroviral treatment (ART), by keeping the latent HIV reservoir small.

Setting: We investigated HIV suppression in 312 perinatally infected infants starting ART within 6 months after birth from the EPPICC (European Pregnancy and Paediatric HIV Cohort Collaboration).

Methods: To better understand kinetic differences in HIV suppression among infants, we investigated their individual viral loads (VL) decay dynamics. We identified VL decay patterns and determined times to viral suppression (TTS). For infants with strictly declining VLs (n=188), we used parameter fitting methods to estimate baseline VLs, decay rates and TTS. We subsequently identified the parameters determining TTS by linear modelling.

Results: The majority of infants suppress HIV VL after the onset of ART. Some children experienced a long TTS due to an "erratic" VL decay pattern. We cannot exclude that this is partly due to treatment complications and subsequent treatment changes, but these children were characterised by significantly lower CD4 percentages (CD4%) at start of treatment compared to those with a "clean" VL decline. Focusing on this "clean" subset, the TTS could be predicted by mathematical modelling, and we identified baseline VL and CD4% as the major factors determining the TTS.

Conclusion: As VL steeply increases and CD4% constantly decreases in untreated HIV-infected infants, the progression of an HIV infection is largely determined by these 2 factors. To prevent a further disease progression, treatment should be initiated early after contracting HIV, which consequently shortens TTS.

Keywords: virological suppression, decay dynamics, perinatal HIV, early ART, mathematical model, mechanisms

Introduction

Since the discovery of HIV in the 1980s, there is still no cure for HIV [Barré-Sinoussi et al., 1983]. HIV research has resulted in effective antiretroviral therapy (ART) in which a combination of drugs successfully controls the virus. ART reduces HIV replication [Ho et al., 1995; Wei et al., 1995] and allows for the recovery of target cells (largely CD4+ T-cells) [Zhang et al., 1999]. Once HIV infects a $CD4^+$ T cell, it either uses the cell for active replication or inserts viral DNA into the host's DNA and forms a latent reservoir. Since the virus is quiescent in the latent reservoir, ART fails to affect these established reservoirs, and once treatment stops, latent HIV reservoirs can get reactivated leading to the production of new HIV particles [Finzi et al., 1999]. Latent HIV reservoirs are the main hurdle in achieving HIV cure.

Current HIV research aims to prevent the establishment of viral reservoir and to reduce its size and diversity. An HIV reservoir is established during the early stages of an HIV infection [Chun et al., 1998]. To keep the reservoir small and homogenous, it seems essential to keep the viral exposure time to a minimum by an early starting of ART [Hecht et al., 2006]. An ART initiation soon after contracting the infection can be accomplished in perinatally HIV-infected infants who are tested and diagnosed soon after birth if the HIV status of the mother is known [Goulder et al., 2016]. Thus, perinatally HIV-infected infants are the ideal target group for an early-ART initiation [Palma et al., 2015], resulting in the reduction of the viral reservoir size in these infants [Goulder et al., 2016; Tagarro et al., 2018b].

Although early-ART typically reduces the viral load (VL), the time to viral suppression (TTS) varies in infants. In 23 reviewed infant studies, the percentage of infants achieving viral suppression ranged from 19% to 81% with an median TTS of 6 months [Shiau et al., 2018]. Significant predictors of a fast TTS in infants have been founded to be age, VL, and CD4 percentage (CD4%) at start of ART (baseline) [EPPICC and EPIICAL, 2019]. The mechanisms underlying these differences in viral suppression in infants are unknown. As a follow-up to previous epidemiological analyses [Shiau et al., 2018; EPPICC and EPIICAL, 2019], we aimed to understand how the baseline factors age, VL, and CD4% contribute to the observed differences in TTS among infants on ART. Therefore, we investigated individual VL decay dynamics from the beginning of treatment until viral suppression was established in perinatally HIV-infected infants receiving ART within the first 6

months of life. These longitudinal measurements were collected by the European Pregnancy and Paediatric HIV Cohort Collaboration (EPPICC) [EPPICC and EPIICAL, 2019; EPPICC, 2011].

Material & Methods

Study inclusion criteria

We received virological, immunological, sociodemographic, and treatment-related data of 499 infants born between 1997 and 2013 from the EPPICC [EPPICC and EPIICAL, 2019; EPPICC, 2011]. These infants were perinatally infected with HIV-1, and 469 started standard ART within 6 months of age. The standard ART regime was composed of either a boosted protease inhibitor or non-nucleoside reverse transcriptase inhibitor and 2 or 3 nucleoside reverse transcriptase inhibitor [EPPICC and EPIICAL, 2019]. To study VL dynamics shortly after the initiation of ART, we required at least one VL measurement within 90 days after the first ART initiation. This requirement was fulfilled by a subset of 312 infants (see Figure S2.1).

Defining baseline values, viral suppression and decay dynamics

For each infant we determined age, VL and CD4+ T-cells as a percentage of total lymphocytes (CD4%) at baseline. As the EPPICC was an observational study, baseline VL and baseline CD4% measurements were not available for most infants. To enrich the baseline information, we extrapolated missing measurements of baseline VL and baseline CD4% from the closest measurement within 10 days before ART initiation (see Table S2.1. We chose a short period of 10 days because the VL changes rapidly during acute infections, making more extended extrapolations unreliable.

We restricted our analysis of VL dynamics to the time points before viral suppression. Viral suppression is defined as 2 consecutive VL measurement below 400 HIV RNA copies/mL [EPPICC and EPIICAL, 2019]. We defined the "time to viral suppression" (TTS) as the time to the first measurement <400 copies/mL and considered the second measurement <400 copies/mL to be the endpoint of our investigation. We further characterised three VL decay patterns describing the VL dynamics from ART initiation to TTS: "immediate" VL suppression reached TTS at the first measurement after ART initiation, "monotonic" VL suppression reached

TTS with strictly decreasing VL measurements over all consecutive time points, and "erratic" VL suppression reached TTS in a nonmonotonic manner, including increasing VL measurements that increased between consecutive time points. Infants showing an immediate and monotonic VL decay pattern are referred to as the "clean" subset.

Mathematical model and Statistics

For infants with a "clean" VL decay pattern, we applied parametric fitting methods to estimate baseline VL and to mathematically determine the TTS for each infant. We used Monolix (2018R1, www.lixoft.com) to perform a nonlinear mixed-effects analysis and fitted a phenomenological model of exponential decay to the logarithmically transformed ($\log_{10}$) VL measurements:

$$V = V_0\, e^{-\gamma t}, \tag{2.1}$$

where V_0 is the baseline $\log_{10}$(VL) and γ is the decay rate of $\log_{10}$(VL). This model, adapted from Ásbjörnsdóttir et al. [2016], can capture the typical "biphasic" decline of the HIV VL during treatment [Perelson et al., 1996]. We applied random effects on both parameters and obtained for each infant a mean estimate and standard deviation (SD) for each parameter. These individual parameter sets were used to calculate an expected TTS by solving Equation (2.1) for the time at which the threshold of $\log_{10}$(400 copies/mL) is reached. We opted for this phenomenological model because the data for some infants were too sparse to fit the classical mechanistic biexponential model [Perelson et al., 1996].

Statistical analyses were performed with R (Version 3.4.4, R Core Team 2018, https://www.r-project.org). We used linear regression and Spearman correlation test to examine the associations between the different parameters. We quote Spearman correlation coefficients ρ with a significance level of 5%. We assessed cross-sectional time courses with locally estimated scatterplot smoothing (LOESS regressions). Differences in decay patterns were compared using two-sided Wilcoxon-tests. Pearson correlation tests were used to compare estimates derived from fits to experimental measurements. In these cases, we quote the coefficients of determination, R^2, with a significance level of 5%. Finally, we performed multivariable linear models with the inclusion of intercepts, by first performing univariate analyses, and subsequently considering all univariably significant variables in a multivariable model. We then performed backward stepwise regression, selecting on the basis of the Akaike information criterion. For all cases, we quote β-coefficients and p-values to the significant value of 5%.
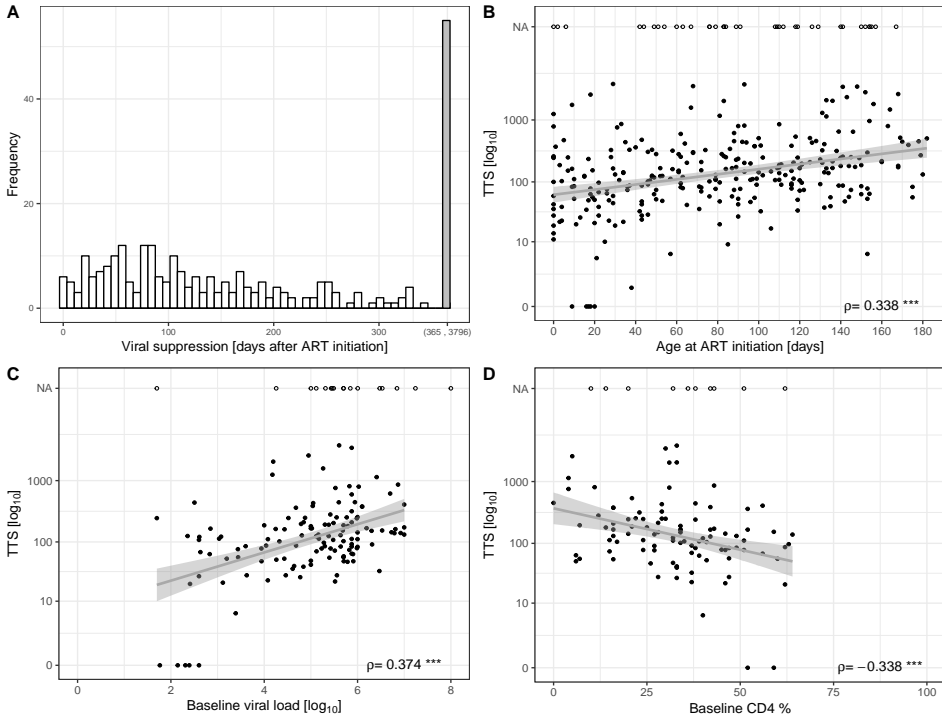
Figure 2.1: TTS is associated with baseline measurements. (A) Histogram of TTS with a bin-width of 7 days. TTS longer than one year are summarised in one bin. (B-D) TTS correlations with (B) age, (C) observed VL, and (D) observed CD4% at ART initiation. To cover the wide range TTS is shown on a logarithmic scale. Filled circles represent infants experiencing viral suppression; open circles represent infants not achieving viral suppression, their TTS is noted with NA. Linear regressions with 95% confidence intervals are shown in grey. The Spearman correlation test was performed and significant correlation coefficients ρ are given (p-value<0.001: ***).

Results

Early-treated infants differ in their TTS

From 312 infants of the EPPICC cohorts fulfilling our inclusion criteria (see Methods), 276 infants showed viral suppression (see Figure S2.1. These infants started standard ART at a median age of 82 days (interquartile range, IQR=[34,121]) with median baseline values of 5.3 $\log_{10}$(VL) (IQR=[4.2,5.9], n=128) and 33 CD4% (IQR=[22.5,42.5], n=99), and were virally suppressed within a median 132 days (IQR=[64,283], Figure 2.1A). Their distribution of baseline values and sociodemo-

graphic characteristics was indistinguishable from the 36 infants who showed no viral suppression in the data available (age: p=0.105, VL: p=0.047, CD4%: p=0.671, open circles in Figure 2.1B–D and see Table S2.1). We excluded these 36 infants from the further analysis, as our objective was to study the VL dynamics from first treatment initiation until viral suppression. Thus, the majority of infants (88%) in the EPPICC cohorts starting early ART suppressed their VLs, but they did not suppress VLs equally rapidly. We aimed to understand these differences.

Baseline conditions and VL decay pattern lead to differences in TTS

To understand the wide range of observed TTS, we assessed differences among the 267 viral suppressors. First, we examined correlations between TTS and baseline measurements. Infants with a shorter TTS started treatment at a younger age ($p<9x10^{-9}$, Figure 2.1B), a lower baseline VL ($p<2x10^{-5}$, Figure 2.1C), and a higher baseline CD4% ($p<7x10^{-4}$, Figure1D). All these associations are in agreement with a previous analysis by the EPIICAL consortium, using a somewhat larger selection of infants from the same cohorts [EPPICC and EPIICAL, 2019]. Thus, the age, VL, and CD4% at which infants start treatment are clearly correlated with differences in TTS.

We then studied how individual VL decay dynamics lead to viral suppression. We classified the data into 3 decay patterns (Figure 2.2A): 47 infants showed immediate VL suppression after ART initiation (immediate), 141 infants had a VL declining in a strictly monotonic manner (monotonic), and 88 infants showed an "erratic" VL with irregular and intermittent increases in the VL (erratic). As expected, infants with an "clean" (immediate or monotonic) decay pattern suppressed the virus in a significantly shorter time than infants with an erratic decay pattern ($p<2.2x10^{-16}$, Figure 2.2B). Infants with erratic decay patterns had, according to their medical records, more changes in treatment (mean=2.89, SD=2.26, $p<2.2x10^{-16}$) and accumulated treatment interruptions (mean=0.28, SD=0.55), suggesting treatment-related challenges such as poor adherence, drug resistance, toxicity or irregular drug administration. Thus, long TTS in infants with an erratic VL declines are at least partly due to treatment complications. Consequently, the VL dynamics of infants with erratic VL decay patterns provide no reliable information regarding the factors associated with VL suppression after first ART initiation because we cannot exclude the possibility that the observed TTS might be a response to later initiated ART. Therefore, we removed these infants from the analysis.

2
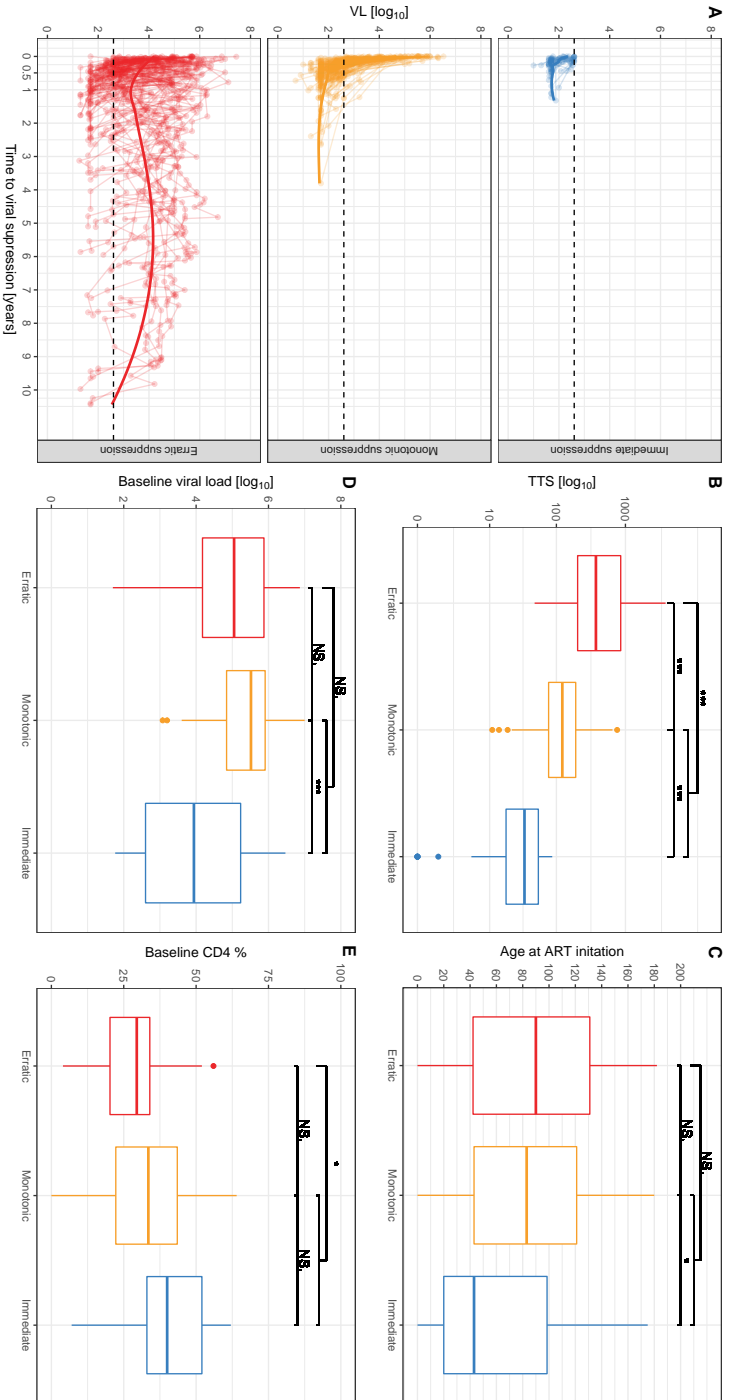
Figure 2.2: Association of VL decay patterns with TTS, age, baseline VL, and baseline CD4%. (A) The initial VL decay after initiation of standard ART is shown for 276 infants distinguished by their decay pattern: immediate (blue, n=47), monotonic (yellow, n=141) and erratic suppression (red, n=88). The measurements belonging to the same individual are connected by lines. The dashed line represents the threshold VL of 400 copies/mL and the thick lines represent the LOESS regressions for each category. (B)-(E) Boxplots distinguished by VL decay pattern (red: erratic, yellow: monotone, blue: immediate) show differences in the distribution of (B) time to viral suppression (TTS), (C) age, (D) observed baseline VL, and (E) observed baseline CD4% at ART initiation. Two-sided Wilcoxon tests were performed and significance levels are shown (p-value≥0.05: NS, p-value<0.05: *, p-value<0.01: **, p-value<0.001: ***).

Erratic VL patterns are associated with significantly lower baseline CD4%

Next, we asked whether the exclusion of infants with erratic VL decay dynamics would introduce a bias in our analysis regarding the baseline conditions. To address this issue, we compared the different decay patterns by the age and the conditions at which infants started treatment. Although the age at start of treatment (p=0.213, Figure 2.2C) and baseline VL (p=0.465, Figure 2.2D) were comparable between infants with erratic and clean VL declines, infants with an erratic decay pattern started treatment with a significantly lower baseline CD4% (p=0.032, Figure 2.2E). We found no significant differences in baseline CD4% between immediate suppressors and infants with a monotonic decay pattern (p=0.065, Figure 2.2E). Infants with an immediate suppression started treatment significantly earlier (p=0.015, Figure 2.2C) and with a significantly lower baseline VL (p<7x10^{-5}, Figure 2.2D) than monotonic decliners. Thus, we acknowledge that infants with an erratic decay pattern are likely biased towards significantly lower baseline CD4% than infants with an immediate or monotonic VL suppression.

Mathematical modelling estimates missing baseline VL and determines TTS more precisely

To further determine with more precision which factors determine TTS during a successful initial ART, we focused on the "clean" subsets of infants with an immediate or monotonic decay pattern. To estimate additional parameters describing these VL decay dynamics, and to more precisely determine their TTS rather than defining it as the time of the first measurement of VL <400 copies/mL, we performed mathematical modelling (see Figure S2.2). By fitting the phenomenological model (Equation (2.1)), we inferred the baseline VL for all 188 infants with a "clean" VL decay kinetic (population estimate V0, fixed ± SD of the random effect: 4.52±0.196); these estimated VLs were in good correspondence with the available measured values (R^2=0.85, p<2.2x10^{-16}, n=87, Figure S2.3A). We also estimated the slope parameter γ, which is the readout for the VL decline, showing huge individual variability (population estimate γ, fixed ± SD of the random effect: 0.01±0.705). The residuals of both parameter estimates were uncorrelated (see Figure S2.3B). From these parameters, we calculated a TTS; these were (as expected) shorter than those derived from the measurement times (R^2=0.52, p<2.2x10^{-16}, Figure S2.3C), as viral suppression occurs before an undetectable measurement. The median estimated TTS for the

Table 2.1: Baseline VL and baseline CD4% determine TTS.

	univariable		multivariable		stepwise	
	β	p-value	β	p-value	β	p-value
slope (γ)						
age	-5.31×10^{-5}	**< 0.001**	-4.11×10^{-6}	0.805	-	-
V_0	-4.82×10^{-3}	**< 0.001**	-3.63×10^{-3}	**0.002**	-3.72×10^{-3}	**< 0.001**
CD4%	1.07×10^{-4}	**0.022**	5.81×10^{-5}	0.227	6.28×10^{-5}	0.154
TTS						
age	0.44	**< 0.001**	0.08	0.554	-	-
V_0	46.25	**< 0.001**	35.02	**< 0.001**	36.96	**< 0.001**
CD4%	-1.05	**0.01**	-0.52	0.204	-0.62	0.101

Linear regression models for slope parameter γ and for TTS. The independent variables are age at start of ART, estimated VL (V_0), and observed baseline CD4%. The regression coefficients β and the p-values are given for a univariable, multivariable model, and the final model resulting from a stepwise approach. Significant p-values are marked in bold.

clean subset was 54 days (IQR=[32,82], Figure S2.3D). We confirmed the previously observed correlations of age (p=4.793x10^{-12}, Figure S2.4A), estimated baseline VL (p<2.2x10^{-16}, Figure S2.4B) and measured baseline CD4% (p=0.005, n=69, Figure S2.4C) with the TTS estimated by data fitting [EPPICC and EPIICAL, 2019]. In addition, TTS negatively correlated with the slope parameter (p<2.2x10^{-16}, Figure S2.4D). All these parameters are highly correlated with each other (see Figure S2.4-S2.6). Thus, mathematical modelling provides additional information in infants with monotonic VL decay dynamics, allowing us to identify factors driving the TTS.

A low baseline VL and a high baseline CD4% lead to a short TTS

The slope parameter γ has the strongest correlation with TTS (Figure S2.5) and is a phenomenological parameter describing the "quality" of suppression. We used linear regression analysis to assess which biological parameters (age, VL or CD4%) were the best predictors of the slope parameter γ. Although a univariable model confirmed the Spearman correlations from Figure S2.5, the results of a multivariable model highlighted a significant effect of the estimated baseline VL on the slope parameter γ (Table 2.1). This significance further increased in a subsequent stepwise model. Here the factor age dropped out, whereas the estimated baseline VL and measured baseline CD4% remained as biological factors explaining the slope parameter γ. We then performed a similar linear regression analysis for the estimated TTS (Table 2.1). Again age, baseline VL and baseline CD4% were significantly associated with TTS in an univariable model.
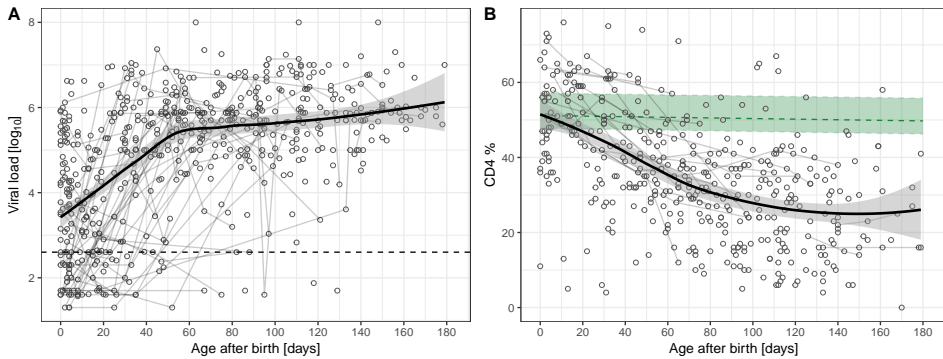
Figure 2.3: Cross-sectional time course of HIV infection before treatment: VL increases and CD4% decreases as HIV infection progresses. (A) From 360 infants in the EPPICC database, we obtained 580 VL measurements before any treatment was applied. These VL measurements are plotted against age on a logarithmic scale. The dashed line represents the threshold VL of 400 copies/mL. (B) From 309 infants in the EPPICC database, we obtained 427 CD4% measurements before treatment. These CD4% measurements are plotted against age. In green reference values and 95% confidence intervals of natural CD4% decline in healthy children are represented (data retrieved from Huenecke et al. [2008]). LOESS regression with 95% confidence interval is shown in black. Infants with more than 3 follow-up measurements are represented by connected grey lines.

In a multivariable model, baseline VL was the only remaining significant factor. This remained the case in a subsequent stepwise model, in which the CD4% was also retained. Thus, TTS depends mainly on the baseline VL and CD4%, and the effect of age might be indirect as it affects baseline VL and baseline CD4%.

Perinatal HIV infection progresses rapidly in untreated infants

To study how age affects VL and CD4% we considered the natural course of HIV infection before the onset of treatment. We used all pretreatment measurements of infants from the EPPICC cohorts to form a cross-sectional time-course of VL and CD4% (Figure 2.3). In general, infants have very low or undetectable VLs at birth. As they grow older, their HIV infection progresses in the absence of treatment. VL measurements increase within a few weeks to reach a plateau around 6 $\log_{10}$(VL) after approximately 50 days (Figure 2.3A). In contrast to adults, infants maintain this high setpoint VL for at least half a year [Palma et al., 2015; Shearer et al., 1997]. The measured CD4% then exhibits a constant decline as HIV infection progresses (Figure 2.3B). We used the raw baseline CD4% measurements and did not normalize them to correct for the natural CD4% decline because
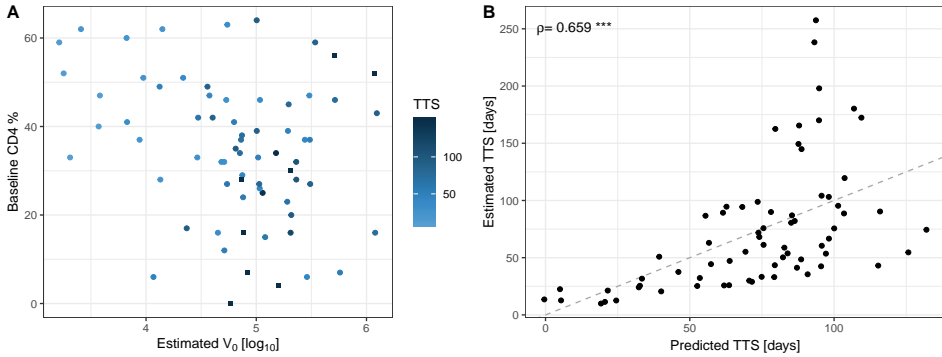
Figure 2.4: Baseline VL and baseline CD4% predict TTS. (A) Estimated TTS in dependence of estimated VL and baseline CD4% measurements (n=69). Increasing intensity of the colour bar represent longer TTS. TTS greater than 150 days are marked by squares. (B) Correlation plot between predicted and estimated TTS. TTS was estimated by fitting data, and TTS was predicted with model of Equation (2.2). The dashed line represents the diagonal. Spearman's correlation coefficient ρ is given with a p-value < 0.001 (***).

the natural CD4% barely shows a decline during the first 6 months of life (see the green dashed band in Figure 2.3B) [Huenecke et al., 2008]. The observed decline in CD4% is much steeper than the natural decline in infants (Figure 2.3B). Thus, age markedly affects the VL and CD4%, as infants starting treatment late are expected to have a high VL and a low CD4%. Consequently, these infants are expected to have a long TTS (Table 2.1). Note that the effect of age on the VL vanishes after 6-8 weeks, when most infants have approached a plateau level, while the effect of CD4% persists (Figure 2.3). Summarising, we find that baseline VL and CD4% are the main drivers of TTS and that age operates indirectly by increasing VL and decreasing CD4%. Although at an early stage of an HIV infection age increases TTS by increasing VL and decreasing CD4%, at a later stage, the effect of the VL stabilises and the deteriorated immune system reflected by declining CD4% determined prolonged TTS (see also Figure 2.4A).

Baseline VL and baseline CD4% predict TTS

Finally, we checked how well the results of the stepwise linear model (Table 2.1), i.e.

$$TTS = 36.96 \times V_0 - 0.62 \times CD4_0 - 82.81 \tag{2.2}$$

could be used to predict TTS. Our model (Equation (2.2)), including an intercept (p=0.085), predicts the TTS estimated by the model of Equation (2.1) reasonably

well (Figure 2.4B, $p<2.2 \times 10^{-16}$), using the estimated baseline VL (V_0, $p<7 \times 10^{-5}$) and the measured baseline CD4% ($CD4_0$, $p=0.101$) as input values. We decided for the estimated VL baseline values as we had more data available, but the results with the measured VL baseline values performed equally good. The TTS could be well predicted with Equation (2.2), if the baseline VL was within the increasing VL phase of a natural HIV infection course (Figure 2.3A) because the baseline VL is the major predictor (Table 2.1). Once the VL plateau is reached, the model (Equation (2.2)) underestimates the TTS. These skewed model predictions for late times to suppression suggest that the effect of CD4% is nonlinear and might play a more dominant role in predicting TTS at a later stage of an HIV infection. This prediction, therefore, provides a lower bound for the expected TTS at the start of treatment. Equation (2.2) could be used as a diagnostic tool for early treated infants that are responding poorly to their treatment.

Discussion

We studied "clean" VL decay dynamics of early treated perinatally HIV-infected infants from a heterogeneous database (EPPICC) to identify the major factors underlying TTS during the first treatment. We identified low baseline VL and high baseline CD4% as the major factors contributing to fast TTS. Because VL might be regarded as a trivial factor influencing TTS, the contribution of CD4% at start of ART is our most interesting and surprising result, although the association with TTS is not significant at the 5% level (Table 2.1). In addition, high CD4 levels are likely to be protective because the CD4% was also significantly lower in infants experiencing an erratic response. The exact mechanisms by which CD4 T-cell levels affect viral suppression remain elusive, but our results suggest that the status of the deteriorating immune system at the onset of treatment influences the TTS. Further immunological studies, considering different immune compartments, e.g., levels of $CD8^+$ T cells or innate immune cells, are required to investigate and clarify the contribution of the immune system to viral suppression.

In contrast to a previous analysis of a somewhat larger subset of the same EPPICC cohort [EPPICC and EPIICAL, 2019], we cannot confirm an independent effect of age on TTS. A major difference is that we selected for a subset of infants with "clean" VL decay dynamics to ensure that our analysis was not confounded by inefficient or ineffective treatment. In the previous studies [Shiau et al., 2018; EPPICC and EPIICAL, 2019], the TTS need not be the response to the initial

treatment and could also be the response to a later initiated treatment because of subsequent changes in treatment. Note that we have not generated an age bias by excluding infants with an "erratic" VL decay dynamics (see Table S2.1). Thus, we find that age describes the TTS in an indirect manner (via baseline VL and CD4%).

The age at start of treatment need not reflect the time period of progression of an HIV infection. With improving diagnosis and treatment of pregnant women, increasing proportions of infants are in-utero infected as opposed to intrapartum infected, and although infants usually start ART soon after birth, they might have progressed already in their HIV infection. In-utero infections might, therefore, confound the age effect on TTS, and baseline VL and baseline CD4% are more appropriate covariates in this setting. Unfortunately, we lacked any information about time of infection (in-utero or intrapartum). To determine whether a separate age contribution affects TTS, comparisons between in-utero versus intrapartum-infected infants are necessary, which will require more detailed studies addressing virological and immunological dynamics in young infants (e.g., the EARTH study by EPIICAL).

We based our analyses on a simple phenomenological mathematical model describing the decay in the VL during treatment. Typically, a mechanistic model is used to capture the multiphase decay dynamic of HIV [Perelson et al., 1996], but the sparseness of virological measurements did not allow proper identification of all parameters of this mechanistic model. The EPPICC database is a collection of observational studies and was not specifically designed to investigate TTS. Available virological and immunological measurements were sparse, and baseline measurements, and regular measurements during the initial VL decay, were often missing. The sparse datum is a generic problem in studies with infants. According to the WHO recommendations, only a limited volume of blood can be extracted from infants, which reduces the variety of medical tests that can be performed. To counter these issues, we used an exponential fit to the log-transformed VL data to predict missing baseline VLs and to estimate decay rates reflecting multiphase VL decay dynamics phenomenologically. In addition, we used a nonlinear mixed-effect model approach to compensate for missing data with a population mean. By combining phenomenological and mixed-effect approaches, we dealt with the sparseness of the data and nevertheless obtained individual estimates for infants in a heterogeneous data set allowing us to precisely determine individual TTS.

In conclusion, the data presented here support the fact that age at start of ART is less helpful than markers of infection such as VL and CD4% to determine TTS. Thus, an early ART initiation not only prevents disease progression but also shortens TTS. In addition to a low VL and a high CD4% at start of treatment, a "clean" VL decay pattern might predict an initially successful treatment responses resulting in fast TTS. Early ART initiation combined with a fast viral suppression may lead to the reduction of the early established latent viral reservoir by shortening the viral exposure time, which may allow for temporarily sustained VL suppression during treatment interruptions as seen in cases such as the Mississippi baby [Persaud et al., 2013] and the VISCONTI child [Sáez-Cirión et al., 2013]. The opportunity to schedule treatment interruptions for perinatally HIV-infected infants has been investigated in the CHER trial [Violari et al., 2008; Cotton et al., 2013]. However, only a minority of early treated children achieved a prolonged viral suppression without ART [Cotton et al., 2013; Violari et al., 2019], and novel therapeutic strategies are needed to obtain viral remission [Palma et al., 2019]. Testing novel immunotherapeutic approaches in the early treated HIV-infected children is the challenge of the EPIICAL network, of which we are part of [Palma et al., 2015]. Potential candidates for such treatment interruptions studies should be chosen on an individual basis. Our results provide a first step for such selection criteria, namely early ART initiation, low baseline VL, high baseline CD4%, and a "clean" VL decay pattern to suppression. As a next step, the effect of these criteria on sustained VL suppression has to be investigated.

Author Contributions

JS performed the mathematical analysis and drafted the manuscript with support from AJNA and RJdB. AJY critically reviewed the development of this manuscript. RJdB supervised this project. All co-authors contributed to the concept and the design of this work, participated in discussions about interpretation of findings, and contributed to the final version of this manuscript.

Acknowledgements

The EPIICAL Consortium study team: Nigel Klein, Diana Gibb, Sarah Watters, Man Chan, Laura McCoy, Abdel Babiker (University College London, United Kingdom); Anne-Genevieve Marcelin, Vincent Calvez (Université Pierre et Marie Curie, France); Maria Angeles Munoz (Servicio Madrileño de Salud-Hospital General Universitario Gregorio Marañon, Spain); Britta Wahren (Karolinska Institutet, Sweden); Caroline Foster (Imperial College Healthcare NHS Trust, London, United Kingdom); Mark Cotton (Stellenbosch University-Faculty of Medicine and Health Sciences, South Africa); Merlin Robb, Jintanat Ananworanich (The Henry M. Jackson Foundation for the Advancement of Military Medicine, Maryland); Polly Claiden (HIV i-Base, United Kingdom); Deenan Pillay (University of KwaZulu-Natal Africa Center, South Africa); Deborah Persaud (Johns Hopkins University); Rob J De Boer, Juliane Schröter, Anet J.N. Anelone (University of Utrecht, Netherlands); Thanyawee Puthanakit (Thai Red Cross AIDS-Research Centre, Thailand); Adriana Ceci, Viviana Giannuzzi (Consorzio per Valutazioni Biologiche e Farmacologiche, Italy); Kathrine Luzuriaga (University of Massachusetts Medical School, Worcester, Massachusetts); Nicolas Chomont (Centre de Recherche du Centre Hospitalier de l'Universitè de Montreal-University of Montreal, Canada); Mark Cameron (Case Western Reserve University, Cleveland, Ohio); Caterina Cancrini (Università degli Studi di Roma Tor Vergata, Italy); Andrew Yates, Louise Kuhn (Columbia University, New York); Avy Violari, Kennedy Otwombe (University of the Witwatersrand, Johannesburg [PHRU] South Africa); Ilaria Pepponi, Francesca Rocchi (Children's Hospital "Bambino Gesu," Rome, Italy); Stefano Rinaldi (University of Miami, Miller School of Medicine, Florida); Alfredo Tagarro (Hospital 12 de Octubre, Universidad Complutense, Madrid, Spain); Maria Grazia Lain, Paula Vaz (Fundação Ariel Glaser contra o SIDA Pediátrico, Mozambique); Elisa Lopez, Tacita Nhampossa (Fundação Manhiça, Mozambique).

Supplementary Tables and Figures

```
┌──────────────────────────────────────────┐
│                    499                     │
│            Started ART ≤ 6 months          │
└──────────────────────────────────────────┘
                                Excluded ──→ ┌────────────────────────────┐
                                             │             30             │
                                             │   Started on non-standard ART │
                                             └────────────────────────────┘
┌──────────────────────────────────────────┐
│                    469                     │
│  Started on standard ART (bPI or NNRTI + 2-3 NRTI) │
└──────────────────────────────────────────┘
                                Excluded ──→ ┌────────────────────────────┐
                                             │            157             │
                                             │   No VL measurement within  │
                                             │    90 days after ART start  │
                                             └────────────────────────────┘
┌──────────────────────────────────────────┐
│                    312                     │
│  > 1 VL measurement within 90 days after ART start │
└──────────────────────────────────────────┘
                                Excluded ──→ ┌────────────────────────────┐
                                             │             36             │
                                             │   No viral suppression within │
                                             │       observation time       │
                                             └────────────────────────────┘
┌──────────────────────────────────────────┐
│                    276                     │
│     Viral suppression within observation time │
│ (2 consecuitve VL measurements < 400 copies/m ) │
└──────────────────────────────────────────┘
                  Excluded from modelling ──→ ┌────────────────────────────┐
                                              │             36             │
                                              │    "erratic" VL suppression │
                                              └────────────────────────────┘
┌──────────────────────────────────────────┐
│                    188                     │
│  "clean"  VL suppression (considered for modelling) │
├────────────────────┬─────────────────────┤
│        47          │         141          │
│ "immediate" VL     │  "monotonic" VL      │
│  suppression       │   suppression        │
└────────────────────┴─────────────────────┘
```
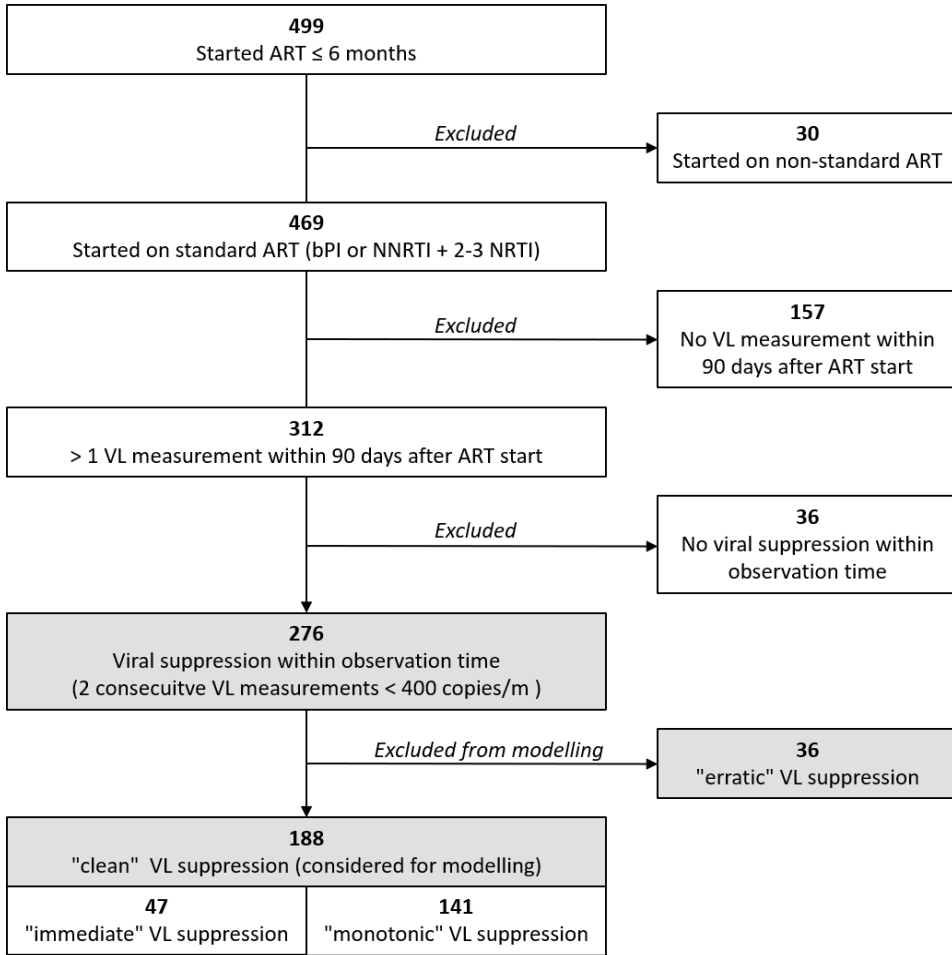
Figure S2.1: Study inclusion criteria. This flow chart shows the selection of infants from 499 infants of the EPPICC who started ART within 6 months after birth. Those subsets considered for our study are grey shaded.

Table S2.1: Baseline study characteristics.

Variables	Total (n=312)		Suppressor (n=276)		Clean (n=188)		Erratic (n=88)	
	n	%	n	%	n	%	n	%
Gender								
Female	187	59.9	164	59.4	112	59.6	52	59.1
Male	125	40.1	112	40.6	76	40.4	36	40.9
Ethnicity								
White	92	29.5	79	28.6	58	30.9	21	23.9
Black	107	34.3	100	36.2	63	33.5	37	42
Other (Asian)	9	2.9	8	2.9	4	2.1	4	4.5
Unknown	104	33.3	89	32.2	63	33.5	26	29.5
Geographical region								
Central and Western Europe	188	60.3	166	60.1	123	65.4	43	48.9
UK/Ireland	98	31.4	94	34.1	56	29.8	38	43.2
Eastern Europe	21	6.7	12	4.3	8	4.3	4	4.5
Thailand	5	1.6	4	1.4	1	0.5	3	3.4
ART regime								
bPI + ≥ 2 NRTI	129	41.3	105	38	79	42	26	29.5
NNRTI + 2 NRTI	116	37.2	109	39.5	66	35.1	43	48.9
NNRTI + 3 NRTI	67	21.5	62	22.5	43	22.9	19	21.6
Age at ART start (in days)								
median [IQR]	83	[38, 121]	82	[34, 121]	79	[31, 120]	83	[43, 121]
Baseline $\log_{10}$(VL) (copies/ml) [a][b]	145	46.5	128	46.4	87	46.3	41	46.6
median [IQR]	5.4	[4.3, 5.9]	5.3	[4.2, 5.9]	5.4	[4.4, 5.9]	5.0	[4.2, 5.9]
Baseline CD4 counts (cells/µl) [a][b]	117	37.5	104	37.7	72	38.3	32	36.4
median [IQR]	1592	[816, 2350]	1600	[868, 2429]	1648	[1016, 2465]	1530	[529, 2163]
Baseline CD4% [a][b][c]	109	34.9	99	35.9	69	36.7	30	34.1
median [IQR]	33	[22.0, 43.0]	33	[22.5, 42.5]	35	[26.0, 46.0]	29.5	[20.3, 34.0]

bPI, boosted protease inhibitor; NRTI, nucleoside reverse transcriptase inhibitor; NNRTI, non-nucleoside reverse transcriptase inhibitor

[a] baseline measurements within 10 days prior to ART start

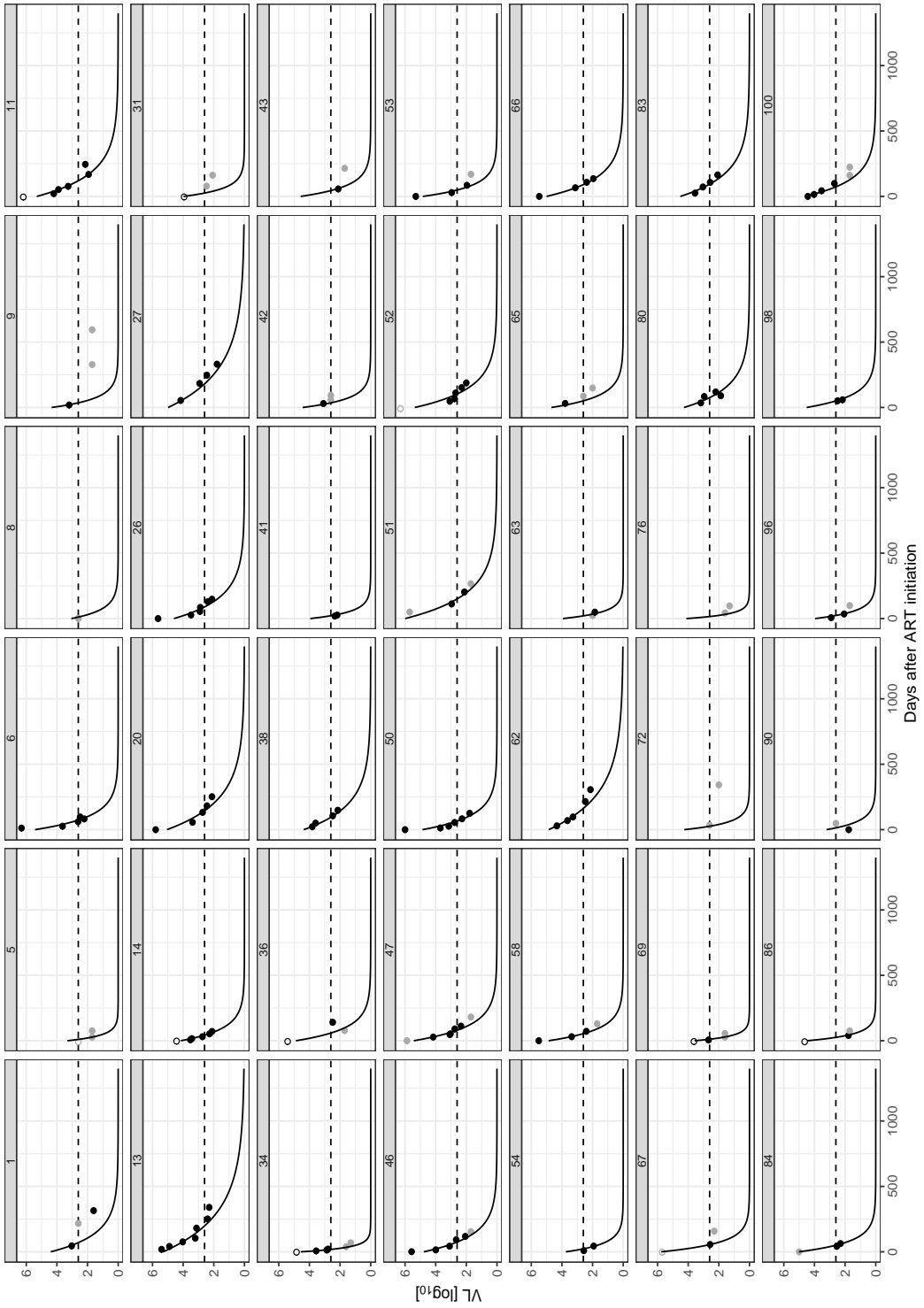[b] Number of available data is shown
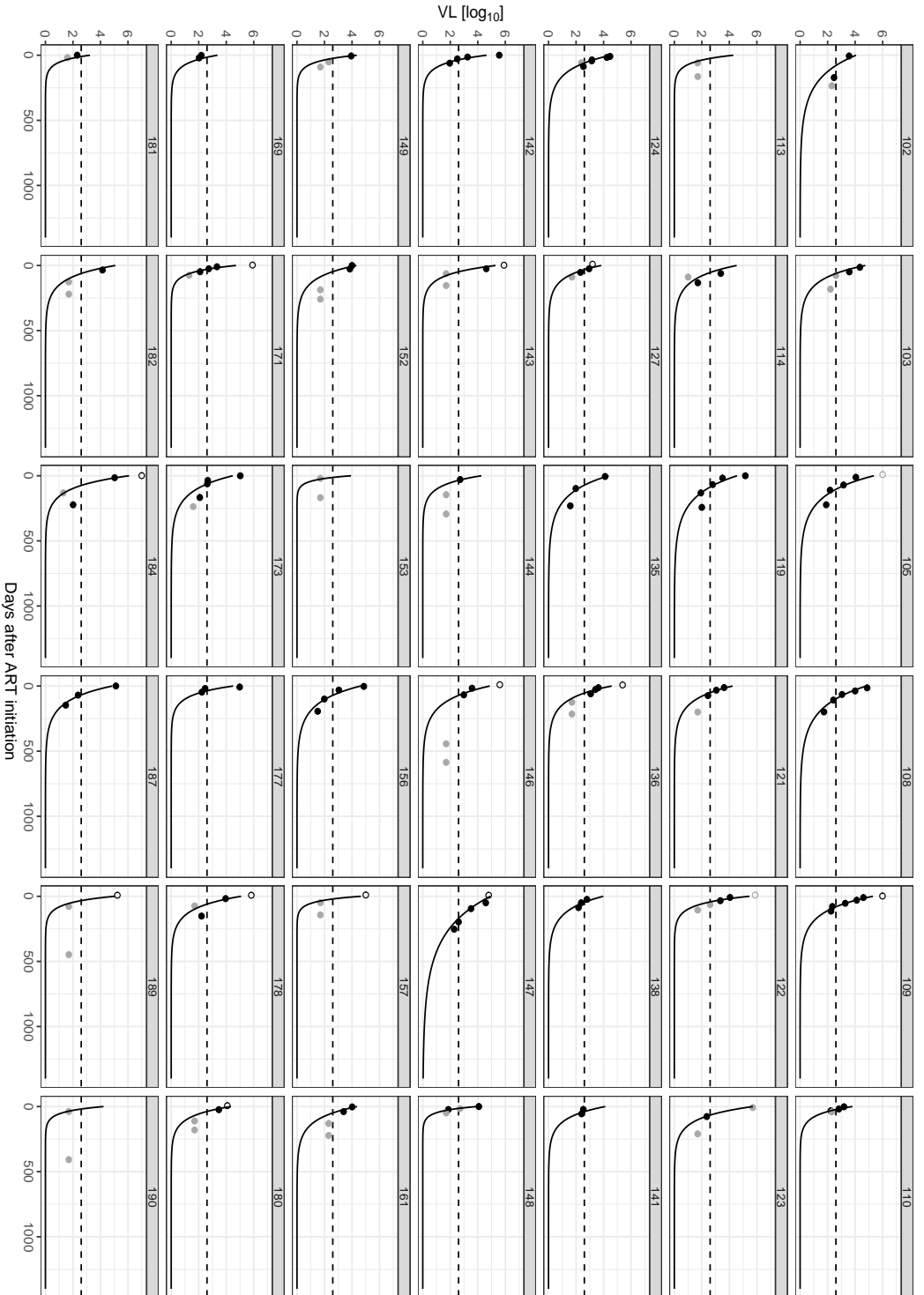
[c] CD4% of total lymphocytes

2

Figure S2.2: Continued.
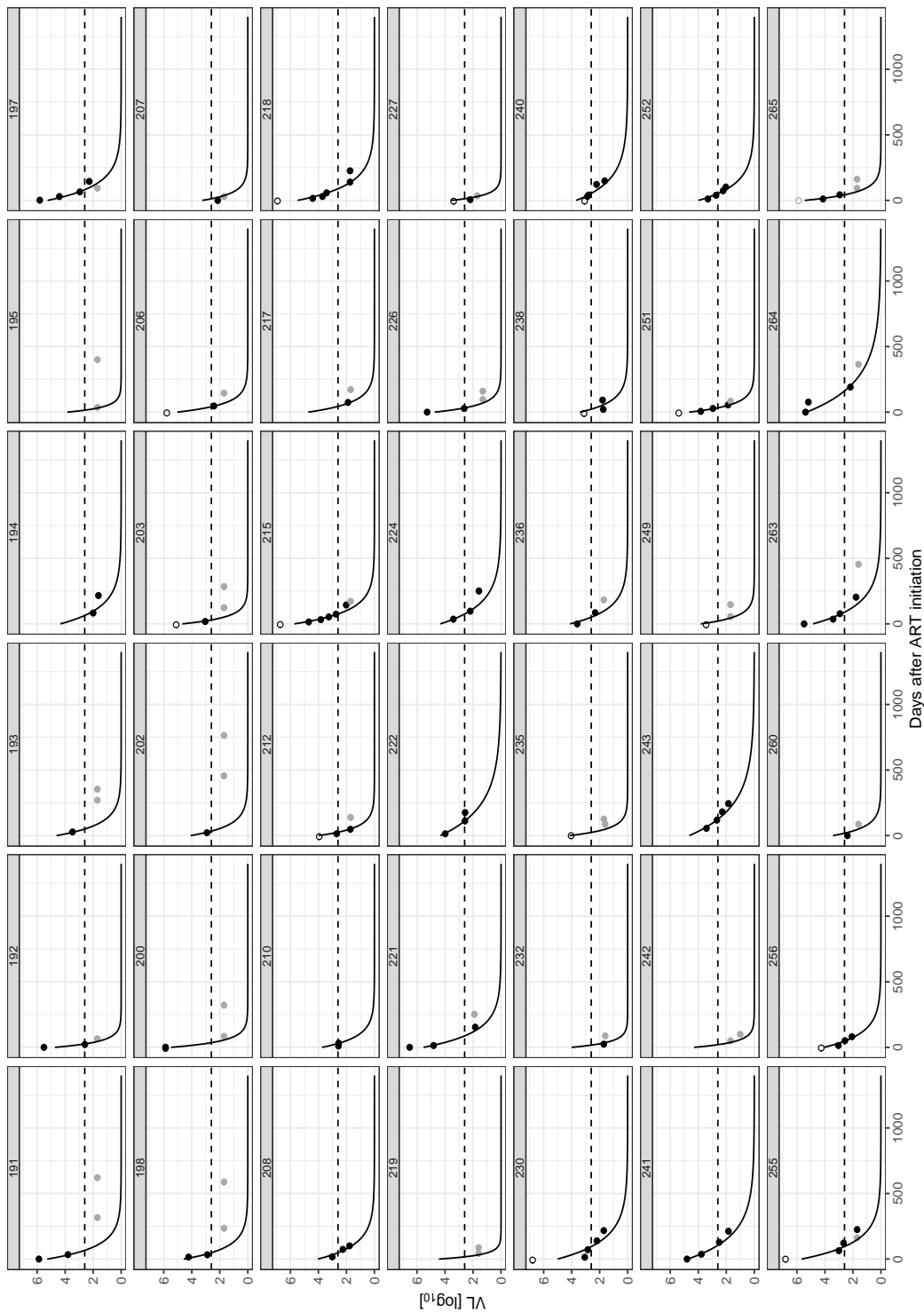
Figure S2.2: Continued.
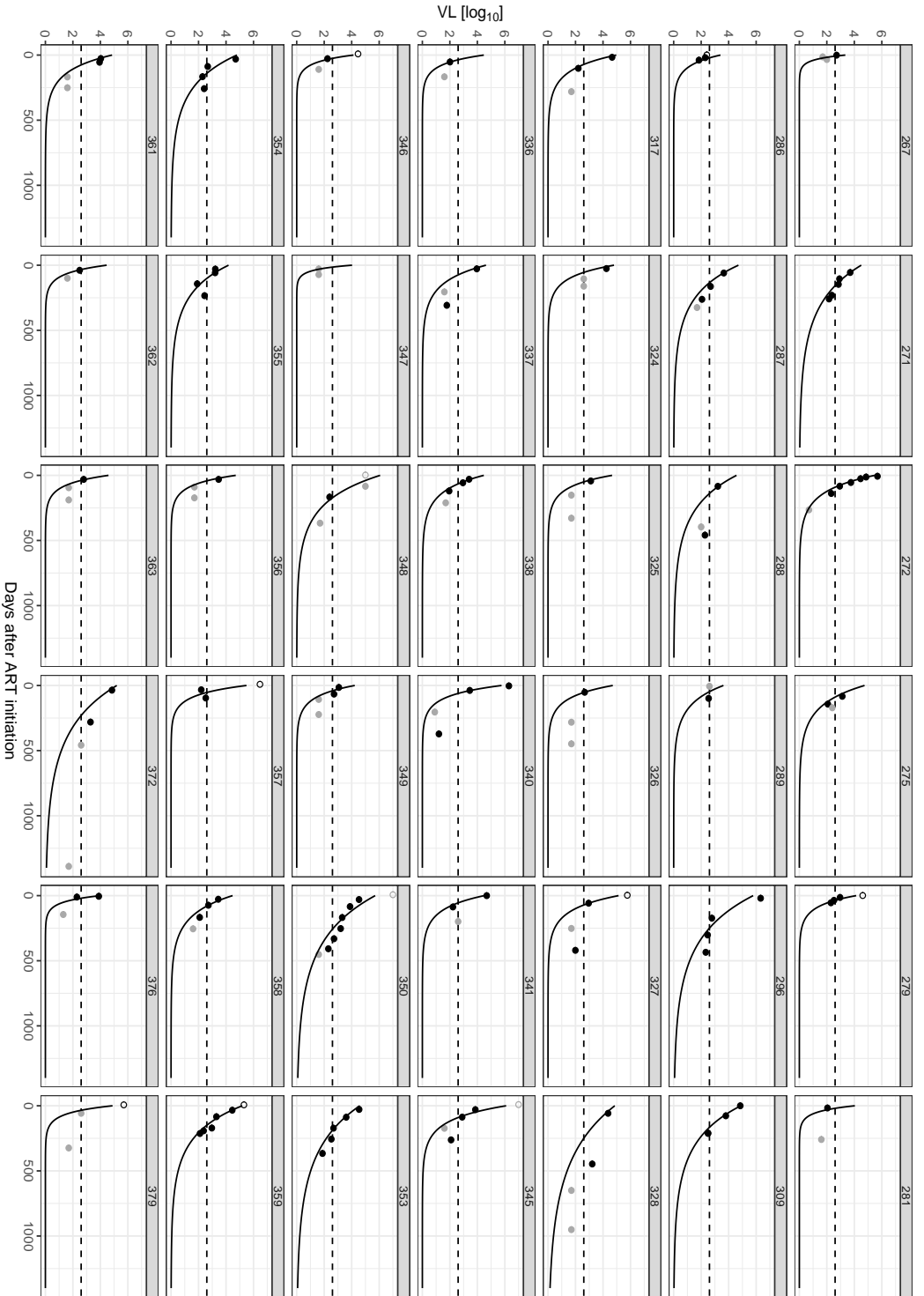
Figure S2.2: Continued.
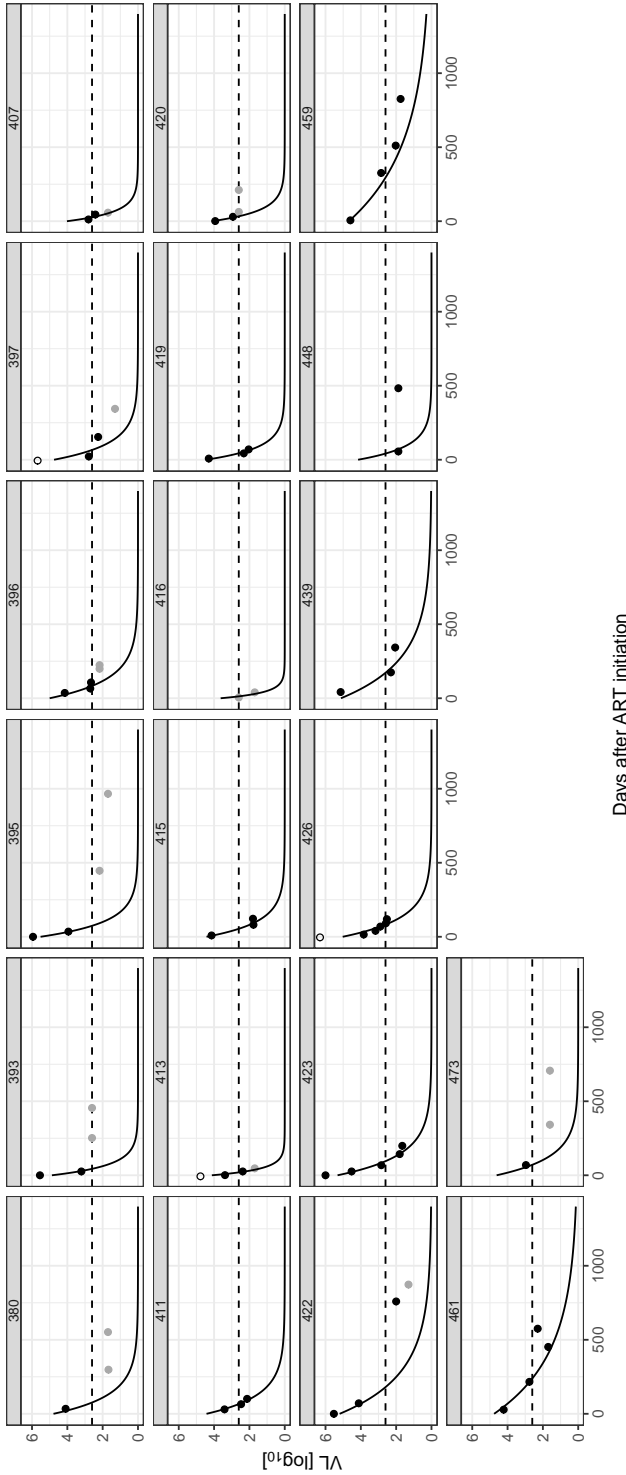
2

Figure S2.2: Continued.

Figure S2.2: Non-linear mixed effect model fits "clean" VL decay of 188 infants. Each panel represents a different infant labelled with its ID. Dots represent VL measurements: black dots are exact measurements; grey dots are censored and below or above the RNA-assay detection threshold. Open circles indicated that the baseline measurements are extrapolated from the closest measurements within 10 days prior to ART initiation. The solid black lines represent the model fit and the horizontal dashed line marks the threshold criteria for VL suppression (400 RNA copies/ml).
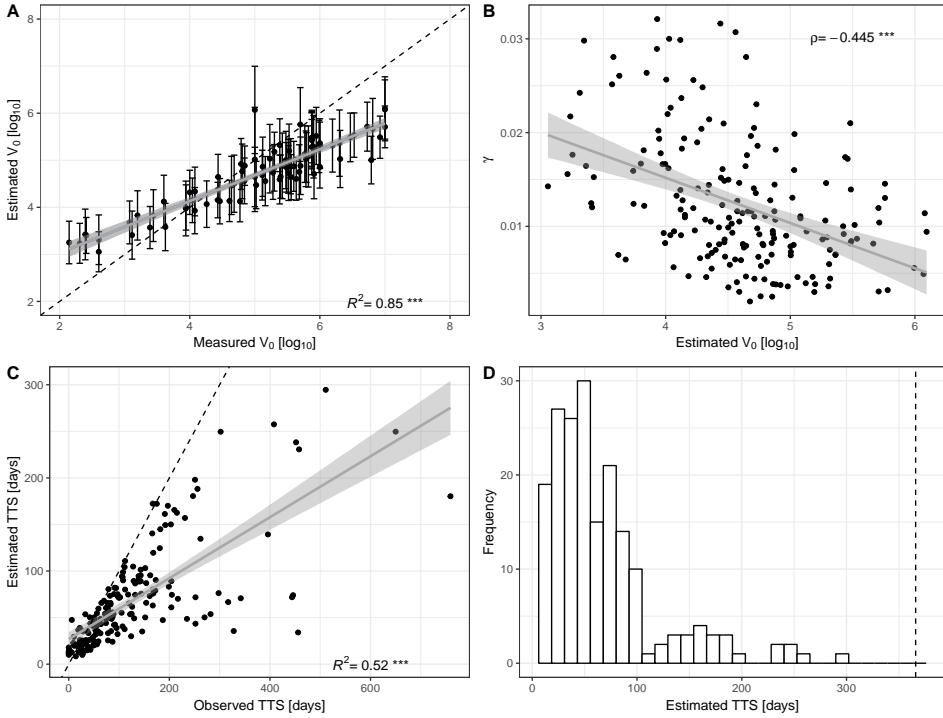
Figure S2.3: Estimated TTS of "clean" mVL decays is shorter than observed TTS. Sensitivity check of model parameters: Correlation plots between (A) measured and mean estimated baseline viral load V_0 and (C) observed and predicted time to viral suppression (TTS) are shown. The dashed lines present the diagonal. The linear regression lines and the 95% confidence intervals are shown in grey. We performed a Pearson correlation test and the R^2 are given (***, p-value < 0.001). In (A) the error bars represent the standard derivation of the estimated V_0. In (B) the correlation between the mean estimated V_0 and the slope parameter γ is shown. Spearman's correlation coefficient ρ is given (***, p-value < 0.001). (D) shows the distribution of the estimated times to viral suppression (TTS) in a histogram. The dashed line represents one year.
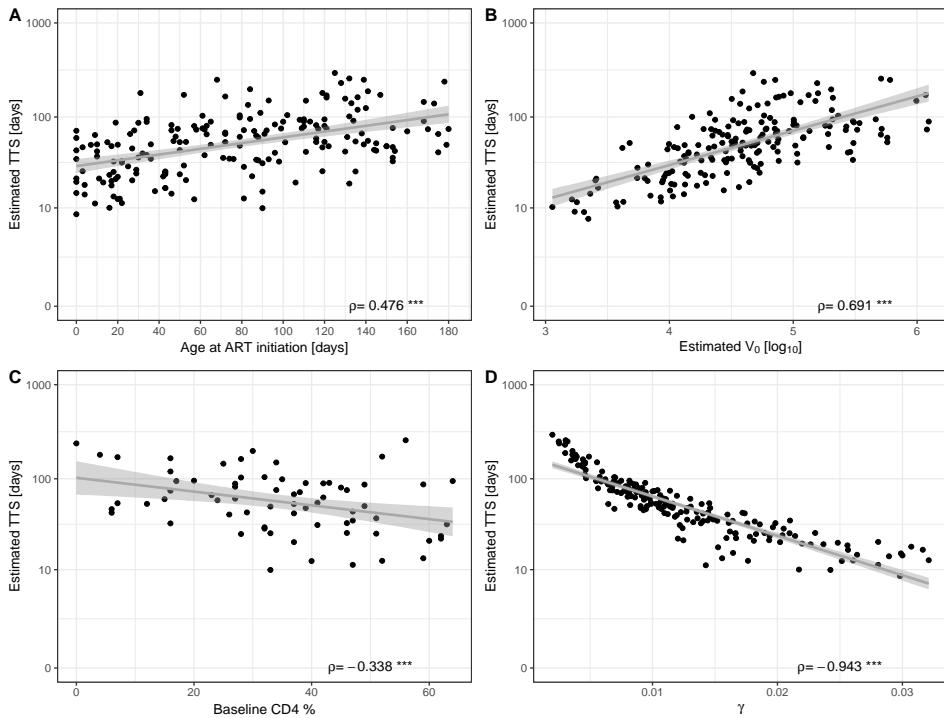
Figure S2.4: TTS correlates with baseline measurements and model parameters. Plots show estimated time to viral suppression (TTS) as a function of (A) age at ART initiation, (B) mean estimated baseline viral load V_0, (C) measured baseline CD4% at ART initiation, and (D) the slope parameter γ. The linear regression lines with their 95% confidence intervals are shown in grey. Spearman's correlation tests were performed and correlation coefficients ρ are given (***, p-value < 0.001).
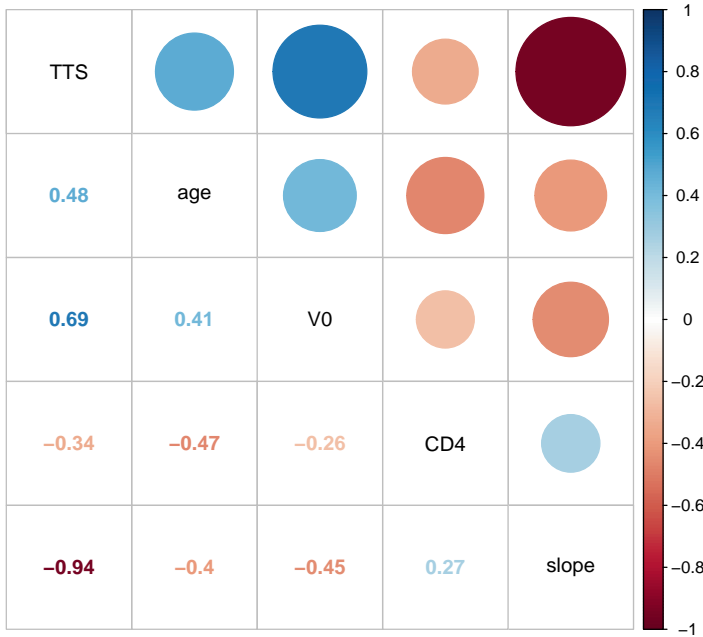
2

Figure S2.5: Parameters determining TTS highly intercorrelate. Correlation matrix of time to viral suppression (TTS), age at ART initiation, estimated baseline V_0, estimated slope parameter γ and measured baseline CD4%. We performed Spearman's correlation tests, the correlation coefficients ρ are given in the lower triangular. The strengths of the correlation are represented by the size of the circle and their colour intensity in the upper triangular. A negative correlation is shown in red, a positive correlation is shown in blue. All correlations have a p-values < 0.05.
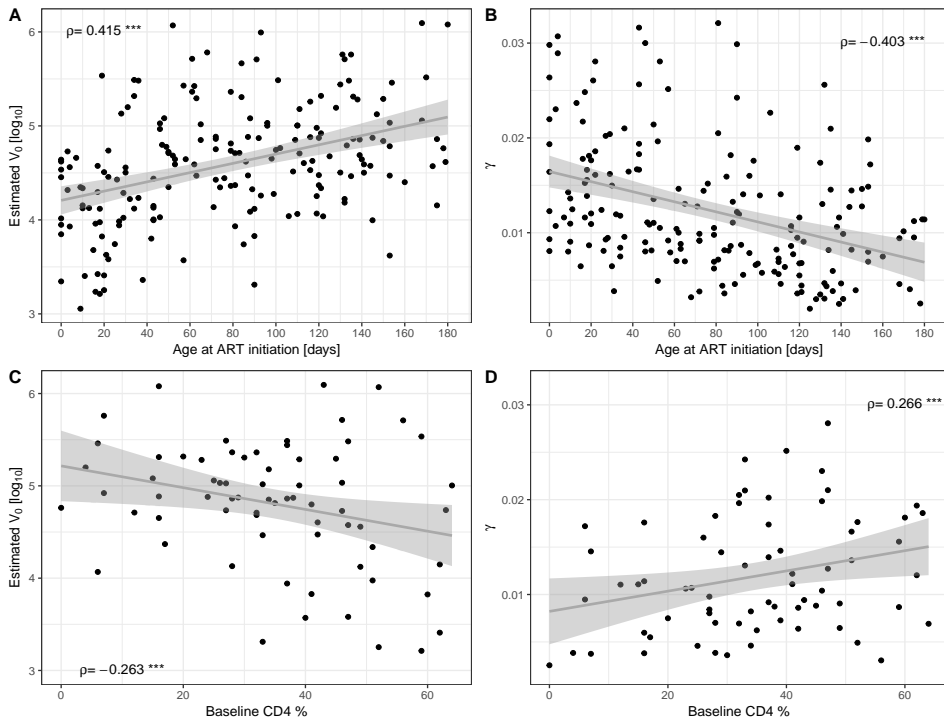
Figure S2.6: Parameters associated with TTS highly intercorrelate. Panel (A) shows mean estimated V_0 and (B) shows the slope parameter γ for each infant against age at ART initiation. The correlation of measured baseline CD4% with mean estimated V_0 is shown in (C) and with slope parameter γ is shown in (D). The linear regression lines with their 95% confidence interval are shown in grey. Spearman's correlation tests were performed and correlation coefficients ρ are given (***, p-value < 0.001).

3

Age-dependent normalisation functions for T-lymphocytes in healthy individuals

Juliane Schröter [1], José A. M. Borghans [2], W. Marieke Bitter [3], Jacques J. M. van Dongen [3] & Rob J. de Boer [1] in collaboration with the EPIICAL Consortium

[1] *Theoretical Biology & Bioinformatics, Utrecht University, NL*
[2] *Center for Translational Immunology, University Medical Center Utrecht, NL*
[3] *Department of Immunology, Leiden University Medical Center, NL*

Abstract

Lymphocyte numbers naturally change through age. Normalisation functions to account for this are sparse, and mostly disregard measurements from children in which these changes are most prominent. In this study, we analyse cross-sectional numbers of mainly T-lymphocytes ($CD3^+$, $CD3^+CD4^+$ and $CD3^+CD8^+$) and their subpopulations (naive and memory) from 673 healthy Dutch individuals ranging from infancy to adulthood (0-62 years). We fitted the data by a delayed exponential function and estimated parameters for each lymphocyte subset. Our modelling approach follows general laboratory measurement procedures in which absolute cell counts of T-lymphocyte subsets are calculated from observed percentages within a reference population that is truly counted (typically the total lymphocyte count). Consequently, we obtain one set of parameter estimates per T-cell subset representing both the trajectories of their counts and percentages. We allow for an initial time delay of half a year before the total lymphocyte counts per μL of blood start to change exponentially, and we find that T-lymphocyte trajectories tend to increase during the first half a year of life. Thus, our study provides functions describing the general trajectories of T-lymphocyte counts and percentages of the Dutch population. These functions provide important references to study T-lymphocyte dynamics in disease, and allow one to quantify losses and gains in longitudinal data, such as the $CD4^+$ T-cell decline in HIV-infected children, and/or the rate of T-cell recovery after the onset of treatment.

Introduction

Lymphocyte numbers experience dynamical changes over a lifetime – known as a hallmark of a maturing and subsequently ageing immune system [Wade and Ades, 1994; Hulstaert et al., 1994; Bains et al., 2009b; Valiathan et al., 2016; van den Heuvel et al., 2017]. These dynamics are more prominent in childhood than in adulthood, as a child's immune system is maturing and has not yet approached steady state. These natural changes over time have to be considered while determining the immunological health status of an individual.

To define an individual's immunological health status, cell counts and percentages of various lymphocyte subsets are measured and compared to reference values of healthy individuals [Picat et al., 2013; Ásbjörnsdóttir et al., 2016; Lewis et al., 2017; Salzmann-Manrique et al., 2018; Schröter et al., 2020]. For this reason, lymphocyte data of healthy individuals have been presented in contiguous age-categories, combining lymphocyte measurements from several months to several years into bins [Shearer et al., 2003; Comans-Bitter et al., 1997; van Gent et al., 2009; Lawrie et al., 2015; Blanco et al., 2018; van Dongen et al., 2019]. These age-intervals allow clinicians to classify the health status of an individual at a given age.

As these bins often cover a broad age range and the lymphocyte numbers themselves are variable, continuous and gradual changes in lymphocytes over time during a disease – such as the decline in CD4+ T cell numbers during HIV infection, and/or their recovery after the onset of treatment – are difficult to quantify. Instead of binning the data into age categories, one can also define continuous normalisation functions as healthy references. By providing a finer time scale, such functions allow a better quantification of lymphocyte dynamics.

To our knowledge, only few publications present estimates describing lymphocyte data of healthy individuals in a continuous manner [Wade and Ades, 1994; Huenecke et al., 2008; Payne et al., 2020]. The often cited paper from Huenecke et al. [2008] describes the trajectories of several T-lymphocyte subsets and their subpopulations based on 100 healthy German individuals by fitting an exponential function, decaying towards an asymptote. Unfortunately, this dataset only includes 14 children under the age of one year, which is the time frame during which one expects major dynamical changes. Moreover, this paper neglects an initial increase within the first half a year of age as observed by

longitudinal analyses and in large cohort studies [de Vries et al., 1998; van den Heuvel et al., 2017; Li et al., 2020]. Additionally, Huenecke et al. [2008] provides neither parameters for the total lymphocyte counts, nor for the $CD4^+$ and $CD8^+$ percentages. Percentages usually show less variability than the cell counts per μL of blood [Goicoechea and Haubrich, 2005], and they are easier and cheaper to obtain through flow cytometry analysis [Comans-Bitter et al., 1997]. Thus, percentages are more commonly reported than counts. As percentages cannot replace the information retrieved from count data, normalisation functions for both counts and percentages are required.

To extent on this and to obtain a much more detailed description of the T-lymphocyte dynamics during the first year of life, we fitted cross-sectional age-matched total lymphocyte and T-lymphocyte measurements from 673 healthy Dutch individuals (ranging from 0 to 62 years), including 268 individuals under the age of one year. As a statistical improvement, our methods follow laboratory measurement procedures, where most cell counts are calculated from observed percentages within a truly counted reference population. We therefore fit percentage data, while receiving parameters describing the cell count data. Thus, we provide new standard functions expressing both absolute and relative data for several T-lymphocyte subsets and their subpopulations of the Dutch population.

Method

Data

We accessed the age-matched raw data of two published Dutch cohorts: Dutch I (presented by bullets (●) in all figures) [Comans-Bitter et al., 1997] and Dutch II (presented by triangles (▲) in all figures) [van Gent et al., 2009]. Both publications presented their lymphocyte data in age-categories. The data presented in Dutch I are typically used as standard reference intervals for the Netherlands and Europe [Shearer et al., 2003; Huenecke et al., 2008; Payne et al., 2020]. For Dutch I, we had measurements from 426 individuals including total lymphocyte counts (TLC) as well as the counts and percentages of the $CD3^+$, $CD3^+CD4^+$ and $CD3^+CD8^+$ subsets within the total lymphocyte gate. For Dutch II, we had measurements from 112 children and adolescents including total lymphocyte counts as well as the counts and percentages of the $CD3^+CD4^+$, $CD3^+CD8^+$, naive CD4+ ($CD27^+$ $CD45RO^-$ $CD4^+$), memory CD4+ ($CD45RO^+$ $CD4^+$), effector CD4+ ($CD27^-$ $CD45RO^-$ $CD4^+$), naive CD8+ ($CD27^+$ $CD45RO^-$ $CD8^+$), memory CD8+ ($CD45RO^+$ $CD8^+$), and
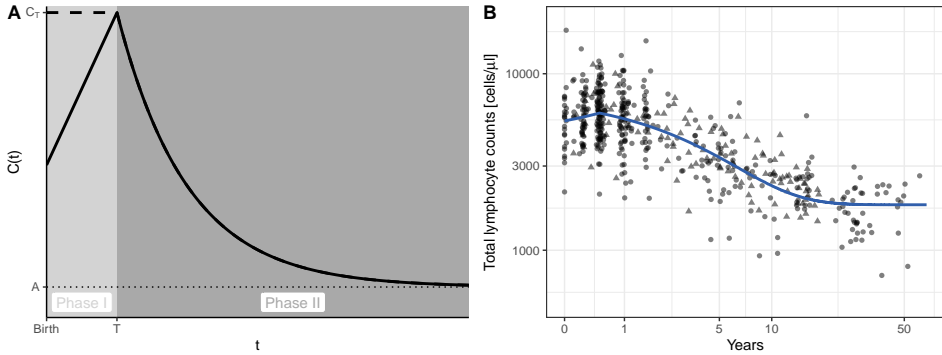
Figure 3.1: Lymphocyte trajectory follows a delayed exponential decay towards and asymptote. (A) Schematic illustration of the mathematical model (3.1) with a flat (dashed line) and an increasing (solid line) initial linear phases (I) lasting until time T, followed by an exponential declining phase (II) from the value at T (C_T) towards an asymptote A (dotted line). (B) Measured total lymphocyte cell counts/μL blood over age ($\bullet$: Dutch I, ▲: Dutch II) are shown along with the best fit of model (3.1) to the data (blue line).

effector CD8+ (CD27$^-$ CD45RO$^-$ CD8$^+$) subsets. To cover the naive, memory, and effector subpopulations until late adulthood, we accessed a third dataset (Dutch III; presented by squares (■) in all figures) with an additional 135 individuals [Veel et al., 2018]. For Dutch III, percentages and count data are given for the CD4+ and CD8+ T-cell naive, memory, and effector subpopulations, but only count data is provided for CD4+ and CD8+ T-cell subsets. Even though the cohorts were collected a decade apart in different laboratories, their quantifications of count data were based on similar methods (in Dutch I with a Coulter Counter model Z1, and in Dutch II/III with a Cell-Dyn Sapphire™ Hematology Analyzer) and we do not observe major differences by visual inspection of cross-sectional illustrations of the data (Figure 3.1-3.3). Thus, we combined the three cohorts for our analysis and refer to them from now on as the Dutch cohorts (see also Table S3.1).

Model

Absolute cell counts

The natural decline of lymphocyte counts over age has previously been described phenomenologically by an exponential decay towards an asymptote [Huenecke et al., 2008]. To allow for a different initial phase, which has been observed in longitudinal data and large cohort studies [de Vries et al., 1998; van den Heuvel

et al., 2017; Li et al., 2020], we extend the original model by defining two phases for the absolute cell counts per μL blood, $C(t)$, depending on time t in years (Figure 3.1A). The initial phase (Phase I) is described by a linear function which lasts until time T, and is succeeded by a second phase (Phase II) describing the exponential towards an asymptote as reported by Huenecke et al. [2008]:

$$\begin{aligned}
C(t) &= C_0 + \alpha\, t & \text{if } t \leq T, \\
C(t) &= (C_T - A) \times e^{-\lambda\,(t-T)} + A & \text{otherwise.}
\end{aligned}$$

(3.1)

For any lymphocyte subset, C_0 is the initial cell count per μL blood at birth, which changes linearly until time T to a value C_T with a slope α (cells per year). From time T onwards the counts change exponentially from C_T at a rate λ (per year), and eventually approach an asymptote A (cells per μL blood), which corresponds to the normal homeostatic level as seen in healthy adults. Depending on the initial value, C_0, and the ultimate asymptote, A, our model (3.1) can describe either overall increasing or declining dynamics of different lymphocyte subsets. The exponential, λ, can be expressed as a half-life or doubling time, $t_{1/2} = \frac{\ln 2}{\lambda}$, giving an indication for the time required to approach the homeostatic level, A, from the level at time T, C_T. Since this is independent of the difference, $C_T - A$, in cell numbers, we also report the quantity $\lambda(C_T - A)$, which is the initial slope after the early initial phase in terms of 'cells per μL per year'. Model (3.1) can be fitted to the absolute cell count data of any lymphocyte subset.

From percentages to absolute cell counts

In immunology, one is typically interested in both the absolute cell counts and the relative fractions (typically presented as percentages) of lymphocytes subsets. Since percentages are easier and cheaper to measure by flow cytometry than counting cells directly, the data representing the percentages are more commonly gathered than the cell counts of a given subset. In experiments, one typically counts some reference population in a μL blood, like total lymphocytes, and estimates the fractions of various subsets within that reference population by flow cytometry. The cell counts of the subsets are then calculated by multiplying these observed fractions with the observed cell count of the reference population. We decided to fit the data according to this experimental procedure, and refrain from the conventional way of fitting model (3.1) directly to the, from now on referred, *"calculated"* cell counts.

Instead, we first fit model (3.1) to the cell counts of the reference population, $C_R(t)$ (in our case total lymphocytes). Keeping the estimated parameters of the

reference population, we then fit the observed percentages, $P(t)$, of a particular subset, by reversing the calculation of the cell counts from the measurement procedure, i.e.,

$$P(t) = \frac{C(t)}{C_R(t)} \times 100, \qquad (3.2)$$

while fitting the parameters of model (3.1) to describe the unobserved cell counts, $C(t)$, of the subset of interest (e.g., CD4+ T cells; see also Box 3.1). The advantages of this procedure are that (i) we stay close to the experimental measurement procedures, that (ii) we use the same parameters to describe the percentages and the cell counts of a particular subset, and that (iii) we can describe complicated trajectories of percentages that are decreasing and subsequently increasing over time with a very simple model. As a sanity check, we will show that fitting the "calculated" cell count data directly with model (3.1) provides similar estimates (see Figure S3.2, Table S3.3).

Algorithm and confidence intervals

To fit the models to the data, we use the Grind wrapper that is based on the FME package in R (version 4.0.2) [R Development Core Team, 2003; Soetaert and Petzoldt, 2010]. Parameter estimates are obtained based on the Levenberg-Marquardt algorithm by minimising the sum of squared residuals. We fit the logarithmically transformed data to account for the measurement variance of several magnitudes over age (particularly in the count data) and to receive normally distributed residuals. Parameter estimates are constrained to be positive, and are tested on being significantly different from zero by the F-test at a significance level of 0.05 (as provided by the algorithm in the FME package). We additionally apply a bootstrapping method to obtain 95% confidence intervals for each parameter estimate, by resampling the data 1000 times. The 95% confidence ranges for the parameters are displayed in Table S3.1 and Table S3.3.

Results

No direct decline in lymphocyte counts after birth

We modelled lymphocyte dynamics from birth to 60 years of age with a simple delayed exponential function (Equation (3.1), Figure 3.1A). We accessed published reference lymphocyte data of two Dutch cohorts. Together they included measurements from 538 healthy individuals covering the full age range. Measurements are enriched for individuals under the age of one year (n=253),

Table 3.1: Parameter estimates and their 95% confidence intervals to obtain fits for count data via model (3.1). The 95% confidence intervals for each parameter are received from bootstrapping the data 1000 times. The delay T was fixed to 0.5 years. The dimensions of the parameters are as follows, C_0, A: cells per μL, α: cells per μL per year, λ: per year, $(C_T - A)\lambda$: cells per μL per year, and $t_{1/2}$: years.

Subset		C_0	α	λ	A	$(C_T - A)\lambda$	$t_{1/2}$
Total lymphocyte count	Estimate	5405.5	1165.1	0.221	1810.1	923.33	3.14
	95% CI	[4794.0 - 5954.5]	[0.0 - 2785.9]	[0.174- 0.287]	[1625.4 - 1986.5]	-	-
CD3+ T-cell count	Estimate	3439.9	796.1	0.238	1287.0	607.13	2.91
	95% CI	[3221.1 - 3654.2]	[299.2 - 1326.3]	[0.218 - 0.262]	[1242.4 - 1330.0	-	-
CD4+ T-cell count	Estimate	2424.7	490.1	0.380	788.9	714.72	1.82
	95% CI	[2202.8 - 2622.8]	[0.0 - 987.6]	[0.341 - 0.427]	[755.5 - 821.5]	-	-
CD8+ T-cell count	Estimate	963.7	211.8	0.156	386.5	106.56	4.44
	95% CI	[866.0 - 1057.9]	[0.0 - 440.5]	[0.133 - 0.179]	[350.5 - 418.6]	-	-
naive CD4+ T-cell count	Estimate	1733.1	0.0	0.162	428.1	211.41	4.28
	95% CI	[1447.6 - 2122.1]	[0.0 - 0.0]	[0.104 - 0.299]	[340.5 - 548.4]	-	-
memory CD4+ T-cell count	Estimate	140.4	167.2	0.600	332.1	-64.86	1.16
	95% CI	[49.2 - 228.3]	[0.0 - 454.4]	[0.004 - 10.476]	[309.9 - 999.9]*	-	-
effector CD4+ T-cell count	Estimate	6.8	0.0	0.000	6.8	0.00	-
	95% CI	[5.8 - 8.0]	-	-	[5.8 - 8.0]	-	-
naive CD8+ T-cell count	Estimate	607.5	208.9	0.079	169.6	42.85	8.77
	95% CI	[311.3 - 762.3]	[0.0 - 877.5]	[0.049 - 0.114]	[92.0 - 223.3]	-	-
memory CD8+ T-cell count	Estimate	22.2	57.3	0.468	122.4	-33.49	1.48
	95% CI	[0.0 - 55.3]	[0.0 - 156.9]	[0.037 - 1.073]	[109.8 - 175.2]	-	-
effector CD8+ T-cell count	Estimate	8.4	0.0	0.488	35.3	-13.13	1.42
	95% CI	[4.8 - 13.7]	[0.0 - 0.0]	[0.164 - 1.010	[29.2 - 45.2]	-	-

*Pararmeter was constraint to an upper limit of 1000 cells/μl

which allowed us to focus on T-lymphocyte dynamics in the very early phase of life, when changes are largest. Longitudinal data and large cohort studies [de Vries et al., 1998; van den Heuvel et al., 2017; Li et al., 2020] report an initial increase in lymphocyte counts during the first half a year of age (rather than the typically assumed exponential decline from birth onwards [Huenecke et al., 2008]). Visual inspection of our data (see Figure 3.1B, Figure 3.2, Figure 3.3) and linear regression analyses, resulting in positive slope estimates for the data covering the first year of life (see Table S3.2), support these observations. Consequently, we have extended the conventional exponential model [Huenecke et al., 2008] with an initial phase allowing for an early increase (Equation (3.1), Figure 3.1A).

Fitting total lymphocyte counts (TLC) as a reference population

An attempt to freely fit all five parameters of the model (3.1) to the cross-sectional total lymphocyte counts (TLC) resulted in high correlations of the parameters

describing the first phase (C_0, α and T). Thus, these 3 parameters are no identifiable from our data. We therefore decided to fix T to the in literature reported minimum value of T=0.5 years [de Vries et al., 1998; van den Heuvel et al., 2017; Li et al., 2020], which reduces the number of free parameters in the model (3.1) from five to four. The best fit of the TLC data results in an linearly increasing phase over the first half a year from C_0=5406 cells/μL to C_T=5988 cells/μL, before the TLC starts to decline exponentially at a rate of λ=0.221 per year towards an asymptotic level of A=1810 cells/μL (Figure 3.1B, Table 3.1). Identifying the slope α of the initial phase remains difficult (see Table 3.1), because α correlates with the initial value C_0, and α is not significantly different from zero. This is due to the wide spread of the cross-sectional data suggesting inter-individual variabilities. Given the good evidence for an initial increase in [de Vries et al., 1998; van den Heuvel et al., 2017; Li et al., 2020], we continued with the non-zero α= 1165 cells/μL, as we aimed to provide a TLC reference function for the Dutch population including the additional knowledge of an early increase. The parameters of the best fit implemented into model (3.1) result in a smooth trajectory describing the overall dynamics of the TLC data reasonably well (Figure 3.1B, Table 3.1). This smooth TLC trajectory served as the reference to obtain the following estimations for the trajectories of the CD3+, CD4+ and CD8+ T-cell subsets via model (3.2).

Fitting non-monotonic percentages to predict cell counts

In contrast to the TLC, absolute counts of lymphocyte subsets, such as CD3+, CD4+, CD8+ T cells are typically calculated from the observed fraction within the lymphocyte gate, i.e., they are not directly counted. While the calculated count data obey the trajectories described by model (3.1), the observed percentages of several lymphocyte subsets change in a more complicated manner over time, with an increasing and a decreasing phase (Figure 3.2 left panels), which is more challenging to model. By following typical experimental procedures, and using model (3.2) with the TLC as a reference, we can describe these non-monotonic trajectories with a rather simple function (Figure 3.2 left panels). Thus, each trajectory can be estimated by four additional free parameters (C_0, α, λ, and A), predicting the corresponding T-cell counts by inserting them into model (3.1) (see Box 3.1).

Taking the CD4% as an example (Figure 3.2B), one can recognise the an almost flat phase over the first half a year at a value of 45%, before the CD4% drops by about 10 percent points to reach a nadir around the age of five years. Afterwards, the CD4% increases again to approach a plateau – at a level similar
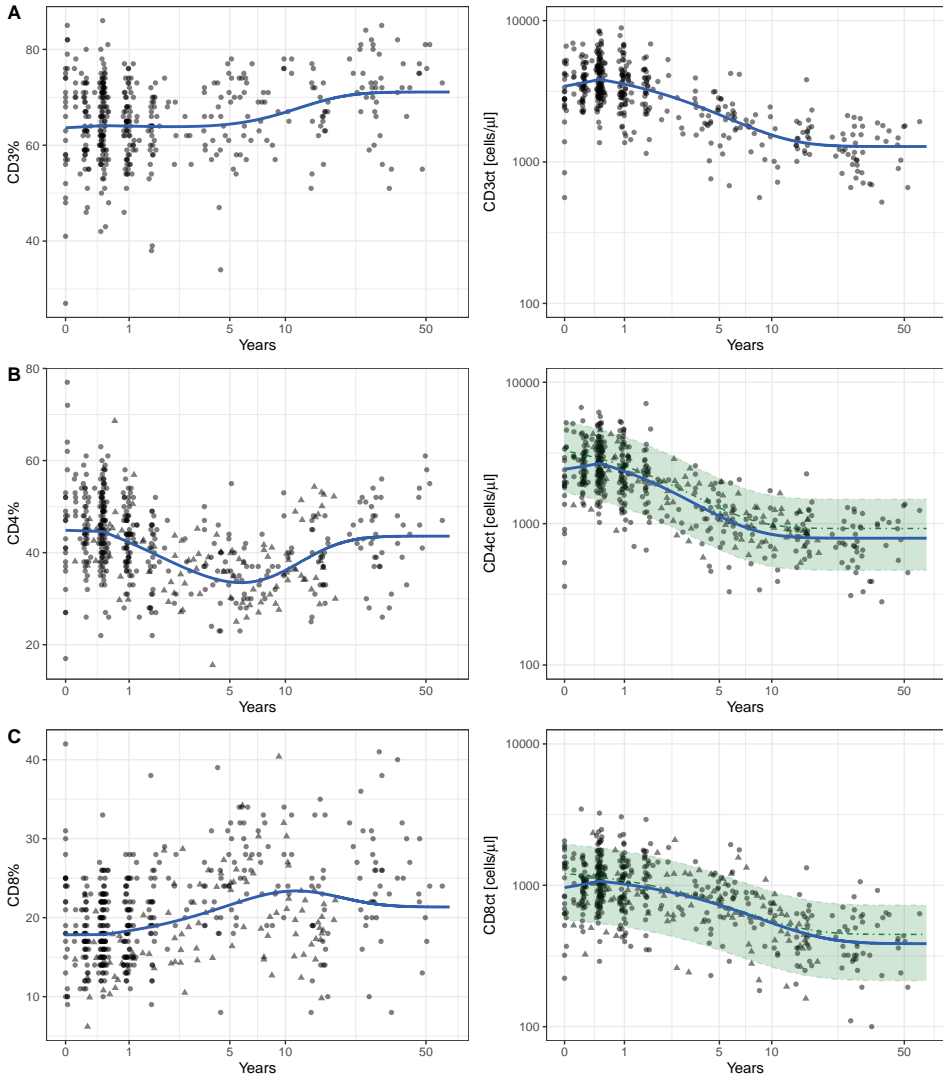
3

Figure 3.2: Trajectories of the T-lymphocyte subsets CD3+ (A), CD4+ (B), and CD8+ (C).
The left panels illustrate the measured percentages and the right panels the calculated
absolute counts. Data from Dutch I are represented by bullets (•), and data from Dutch
II by triangles (▲). In the left panels, the blue solid lines represent the best fit of model
(3.2). In the right panels, the blue solid lines represent the underlying trajectories for the
calculated absolute count according to model (3.1). The parameter estimates listed in
Table 3.1 are used. If available, the estimates from Huenecke et al. [2008] are presented
in green with their 95% confidence range.

Box 3.1 - Example calculations

Model (3.1) provides normalisation functions for count data with the parameters presented in Table 3.1. For example, for the reference population TLC and CD4 count (CD4ct) in cells per μL:

$$TLC(t) = \begin{cases} 5405.5 + 1165.1 \times t & \text{if } t \leq 0.5 \text{ years,} \\ (5988.1 - 1810.1) \times e^{-0.221(t-0.5)} + 1810.1 & \text{otherwise;} \end{cases}$$

$$CD4ct(t) = \begin{cases} 2424.7 + 490.1 \times t & \text{if } t \leq 0.5 \text{ years,} \\ (2670.0 - 788.9) \times e^{-0.380(t-0.5)} + 788.9 & \text{otherwise;} \end{cases}$$

Model (3.2) provides normalisation functions for the percentages. For example, for CD4%:

$$CD4\%(t) = \frac{CD4ct(t)}{TLC(t)} \times 100\,\%$$

$$= \begin{cases} \frac{2424.7 + 490.1 \times t}{5405.5 + 1165.1 \times t} \times 100\ \% & \text{if } t \leq 0.5 \text{ years,} \\ \frac{(2670.0 - 788.9) \times e^{-0.380(t-0.5)} + 788.9}{(5988.1 - 1810.1) \times e^{-0.221(t-0.5)} + 1810.1} \times 100\,\% & \text{otherwise.} \end{cases}$$

We first fit the function $TLC(t)$ to the TLC data, and subsequently fit the function $CD4\%(t)$ to the percentage data by estimating the four free parameters of the $CD4ct(t)$ function.

to the one observed at birth – in adulthood. Thus, a "wavy" CD4% trajectory is described, which confirms a previous observation [Valiathan et al., 2016]. The CD3% and CD8% both expand from birth onwards, and also approach a homeostatic level around the age of 30 (Figure 3.2A/C). Hence, by staying close to experimental procedures we model trajectories of the percentages that have more complicated dynamics than was previously appreciated.

Although our predictions for the calculated count data are based upon fitting the observed percentages, they are in good agreement with the calculated CD3+, CD4+, and CD8+ T-cell counts (Figure 3.2 right panels). Additionally, the trajectories predicted by our procedure of estimating observed data only, are in excellent

agreement with the trajectories that are obtained by estimating the calculated count directly with model (3.1) (Figure S3.1). Thus, the normalisation functions obtained with either method (Table 3.1 or Table S3.3 are very similar.

Fitting complementary T-cell subpopulations

Lastly, we provide estimates for the naive, effector and memory subpopulations of CD4+ and CD8+ T cells (Figure 3.3, Table 3.1). Those subpopulations are usually reported as fractions of either CD4+ or CD8+ T cells and sum up to almost 100%. Unfortunately, these reference populations are typically not truly counted, which precluded us from using model (3.2). We therefore fitted the calculated count data using model (3.1) (Figure 3.3 and Figure S3.2 left panels, Table 3.1). The three trajectories (naive, memory and effector subpopulations) are then considered to sum up to 100%, from which we calculated trajectories for the percentages of the subpopulations according to model (3.2) (Figure 3.3 and Figure S3.2 right panels).

Our results (in blue) fit the general trajectories of the data reasonably well (in grey). At birth the CD4+ and CD8+ T-cell pools are largely composed of naive T cells (80-90%; Figure 3.3). Naive T-cell counts decline about 4-fold over 50 years, i.e., from 1733 to 438 cells per μL for CD4+ and from 608 to 170 cells per μL for CD8+ T cells (Figure 3.3 and Table 3.1). The memory compartments show opposite dynamics and increase over time towards an asymptote (Figure 3.3). Overall our trajectories are in good agreement with those reported by Huenecke et al. [2008] (in green). Note that Huenecke et al. [2008] describe the memory CD4+ and naive CD8+ T-cell counts by a linear model, whereas we also consider the effect of homeostasis in the subpopulations.

Discussion

We present a new mathematical approach to describe the natural dynamics in lymphocyte numbers continuously. By providing parameters for various T-lymphocyte subsets (i.e., CD3+, CD4+, CD8+ T cells), and their subpopulations (naive and memory), reference functions for both their absolute counts and percentages can be formulated. Based on an extensive dataset, including age-matched cross-sectional lymphocyte measurements of 673 healthy Dutch individuals (covering particularly the dynamic first year of life), we are able to describe all trajectories phenomenologically with a bi-phasic model. We allowed for an initial phase of half a year in which lymphocyte subsets can
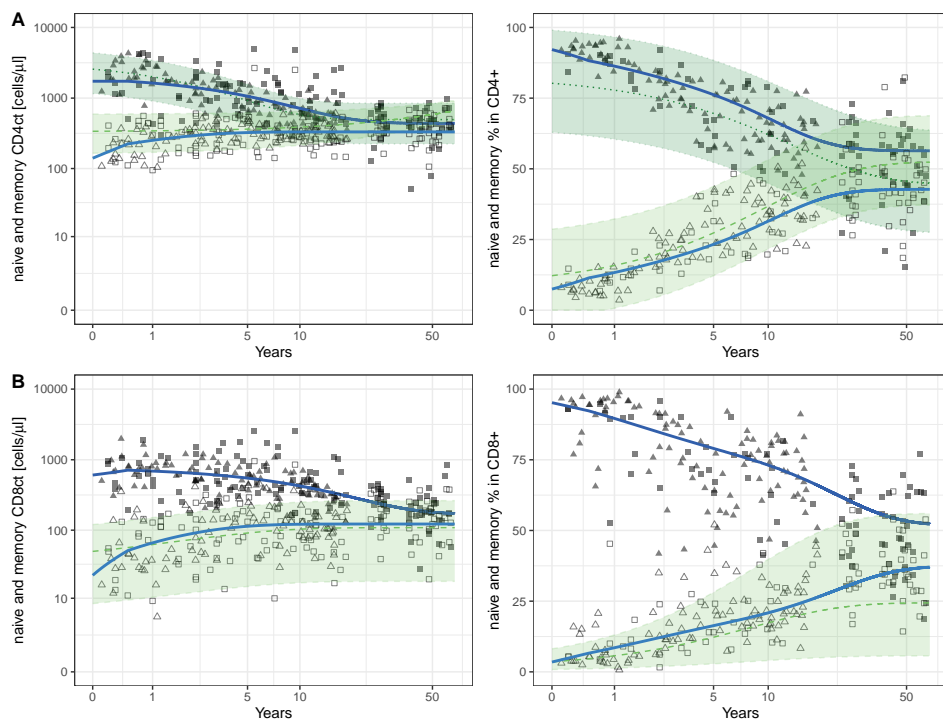
Figure 3.3: Trajectories of the naive and memory subpopulations of CD4+ (A) and CD8+ cells (B). The left panels give the absolute counts and the right panels the percentages. Data from Dutch II are represented by triangles (▲), and data from Dutch III by squares (■). The naive subpopulation is represented by filled symbols, the memory subpopulations by open symbols. In the left panels, the blue solid lines represent the best fit of model (3.1) and the parameters reported in Table 3.1. In the right panels, the blue solid lines represent the underlying trajectories for the percentages according to model (3.2) where the sum of naive, memory and effector cell counts add up to 100%. The dark blue colour refers to the naive subpopulation the lighter blue to the memory subpopulations. The green dotted (naive) and dashed (memory) lines represent the estimates from Huenecke et al. [2008] and their 95% confidence range (green area). We noticed that Huenecke et al. [2008] described the percentages of the naive CD8+ subpopulation by an increasing exponential function, while our data (and fit) follows a decline. We excluded this prediction from Huenecke et al. [2008] in panel (B) (i.e., the missing green range for naive CD8+ counts), because we assume this to be a mistake (since the percentage of naive T cells should decline to general immunological knowledge).

increase, followed by a second phase which describes an exponential that approaches an asymptote corresponding to the homeostatic adult level. Except for memory T cells, this homeostatic level is below the values at birth. Our

approach of fitting percentages to the ratio of two simple exponential models allowed us to simultaneously describe the counts and percentages of all populations of interest, delivering non-monotonic trajectories of the CD4+ and CD8+ T-cell percentages. We provide a consistent set of parameters describing both percentages and their dependent counts.

We extended the model of a similar previous publication [Huenecke et al., 2008] with an initial phase to relax the previous assumption that the TLC declines from birth onwards. Longitudinal data, as well as large cross-sectional studies, demonstrated that cell numbers per μL blood increase during the first half a year of life [de Vries et al., 1998; van den Heuvel et al., 2017; Li et al., 2020]. We checked for such an early increase in our own data by linear regression within selected early time windows (Table S3.2). As these slopes were positive, we allowed for a first phase that last for the minimum reported value of 0.5 years. The parameters of the first phase have been difficult to identify, as the initial value, C_0, and the slope parameter, α, are correlated. We are limited by the fact that the data are cross-sectional, and the data are variable between individuals. Accepting the strong external evidence for an initial increase, we decided to also accept the slopes estimated by the α parameter, even if these were not significantly different from zero.

We refrained from using the exponential initial phase proposed by Wade and Ades (1994), and Payne et al. (2020), because our linear model allowed us to easily define a fixed end-point of the initial phase, and even this simple linear slope during a fixed first phase was difficult to identify. Thus, the extension of previous models with a fixed initial linear phase kept the model simple, while nevertheless allowing it to capture the different initial dynamics. We think the introduction of an initial phase is important when normalising data from very young children.

Our method is novel in the way that it stays close to experimental measurement procedures and only fits truly measured data. In most cases, these are percentages that are received via flow cytometry analysis. The conventional procedure to obtain cell count data is to multiply these percentages with the counts of a reference population (like a total lymphocyte count). While count data tend to be variable, the calculated counts are even more variable because they combine the variation in the observed counts and the observed percentages. As a sanity check, we also fitted our model (3.1) to conventionally calculated count data (see Figure S3.1 and Table S3.3), and indeed obtain a

wider 95% confidence range of the estimated parameters (compare Table 3.1 with Table S3.3). Reassuringly, the average parameter estimates are in good agreement with each other, and as a consequence both methods provide very similar normalisation functions.

Since we are aiming for normalisation functions describing a population average, the main statistical question is what the best estimate is for the unobserved cell counts. The conventional calculated count has the advantage of using the count and percentage data from the same individual. This could be important if the counts and the percentages are dependent variables. Since the measurement of counts is difficult, and count data shows more inter-individual variability than percentages, we decided to only model what is really measured. Fortunately, both fitting procedures provide very similar normalisation functions. As techniques to count cell numbers are improving, one could in the future fit all of count data directly via model (3.1). Normalisation functions for the percentages would then be obtained by combining the model (3.1) parameters of the corresponding subpopulations using model (3.2), as we have done in gaining the trajectories for the percentages of the subpopulations. One could even think of fitting counts and percentages simultaneously to obtain the best population-based trajectories for counts and percentages.

In conclusion, we provide age-dependent continuous reference functions for lymphocyte data of both counts and percentages in the general Dutch population.Good agreement with a German reference [Huenecke et al., 2008] suggests that they might also serve as European references, and can be used to normalise data according to age. Our analysis does not replace the representation of lymphocyte data in contiguous age intervals, which is necessary to clinically determine the immunological health status of an individual, but rather provides an additional continuous presentation of the data. Age normalisation gains importance while quantitatively assessing changes in diseases associated with the immune system. Having a standard normalisation function at hand also simplifies the comparison of figures across different age categories by correcting for the confounding age effect.

Author Contributions

JS and RJdB conceived the study. JS performed the analysis and drafted the manuscript under supervision of RJdB. JAMB, WMB and JJMvD provided the data. JAMB and JJMvD read and edited the manuscript. All authors read and approved the manuscript.

Acknowledgement

Supplementary Tables and Figures

Table S3.1: Data composition of the different cohorts.

Study	Dutch I	Dutch II	Dutch III
Total	426	112	135
Children (< 18 years)	381	112	89
Adults	45	-	46
Age range [years]	0-60	0-18	0-62
Total lymphocyte counts	×	o	
CD3+ %	×		
CD3 counts	×		
CD3+CD4+ %	×	o	
CD3+CD4+ counts	×	o	×
CD27+ CD45RO- CD4+ %		o	×
CD27+ CD45RO- CD4+ counts		o	×
CD45RO+ CD4+ %		o	×
CD45RO+ CD4+ counts		o	×
CD27- CD45RO- CD4+ %		o	×
CD27- CD45RO- CD4+ counts		o	×
CD3+CD8+ %	×	o	
CD3+CD8+ counts	×	o	×
CD27+ CD45RO- CD8+ %		o	×
CD27+ CD45RO- CD8+ counts		o	×
CD45RO+ CD8+ %		o	×
CD45RO+ CD8+ counts		o	×
CD27- CD45RO- CD8+ %		o	×
CD27- CD45RO- CD8+ counts		o	×

x stands for full age range, and **o** for only children

Table S3.2: Linear regression analyses of subsets of the data selected according to the given time window in the early years of life. The intercept is in cells per μL and the slope has a dimension of cells per μL per year.

	Total lymphocyte count				CD3+ T-cell count				CD4+ T-cell count				CD8+ T-cell count			
	Intercept	p	Slope	p	Intercept	p	Slope	p	Intercept	p	Slope	p	Intercept	p	Slope	p
≤ 0.5 years	5729 (367)	***	1577 (1110)	NS.	3470 (252)	***	1614 (754)	*	2425 (191)	***	1142 (569)	*	1006 (87)	***	390 (261)	NS.
≤ 1 year	5984 (266)	***	428 (477)	NS.	3746 (192)	***	469 (344)	NS.	2670 (138)	***	199 (246)	NS.	1072 (62)	***	100 (111)	NS.
≤ 2 years	6228 (213)	***	-281 (263)	NS.	3967 (156)	***	-162 (195)	NS.	2863 (110)	***	-318 (135)	*	1084 (49)	***	45 (61)	NS.
≤ 5 years	6443 (147)	***	-655 (93)	***	4116 (111)	***	-420 (76)	***	2895 (74)	***	-392 (47)	***	1148 (35)	***	-66 (22)	**
All	5534 (102)	***	-138 (9)	***	3613 (79)	***	-78 (7)	***	2356 (53)	***	-60 (5)	***	1056 (23)	***	-22 (2)	***

Intercept and slope estimates with standard error (SE)
F-test p-value (p) to a significant level ≥ 0.05, NS.; < 0.05, *; < 0.01, **; < 0.001, ***

Table S3.3: Parameter estimates and their 95% confidence intervals obtained by fitting the calculated count data directly. Counts were calculated by multiplying the observed percentages with the observed TLC. The 95% confidence intervals for each parameter are received from bootstrapping the data 1000 times. The delay T was fixed to 0.5 years. The dimension of the parameters is the same as in Table 3.1.

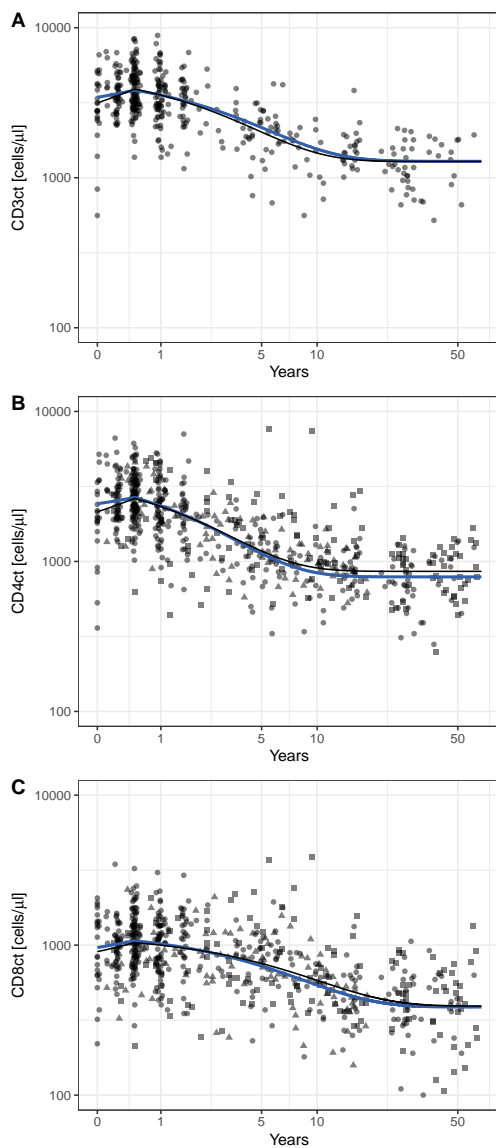| Subset		C_0	α	λ	A
CD3+ T-cell count	Estimate	3154.9	1493.8	0.289	1283.6
	95% CI	[2620.4 - 3727.2]	[115.1 - 2801.9]	[0.211 - 0.396]	[1164.5 - 1404.0]
CD4+ T-cell count	Estimate	2143.1	978.0	0.384	858.8
	95% CI	[1721.5 - 2527.3]	[0.0 - 2015.7]	[0.280 - 0.535]	[796.4 - 920.2]
CD8+ T-cell count	Estimate	904.7	269.0	0.129	392.3
	95% CI	[764.4 - 1025.4]	[0.0 - 585.9]	[0.095 - 0.173]	[338.6 - 439.0]

Figure S3.1: Direct fits of calculated count data are within confidence ranges of the predicted trajectories. The direct fits to the calculated CD3+ (A), CD4+ (B), CD8+ (C) cell counts are depicted by the black lines. In blue we depict our best predictions (Table 3.1). Bullets (•) represent data from Dutch I, triangles (▲) data from Dutch II, and squares (■) data from Dutch III.
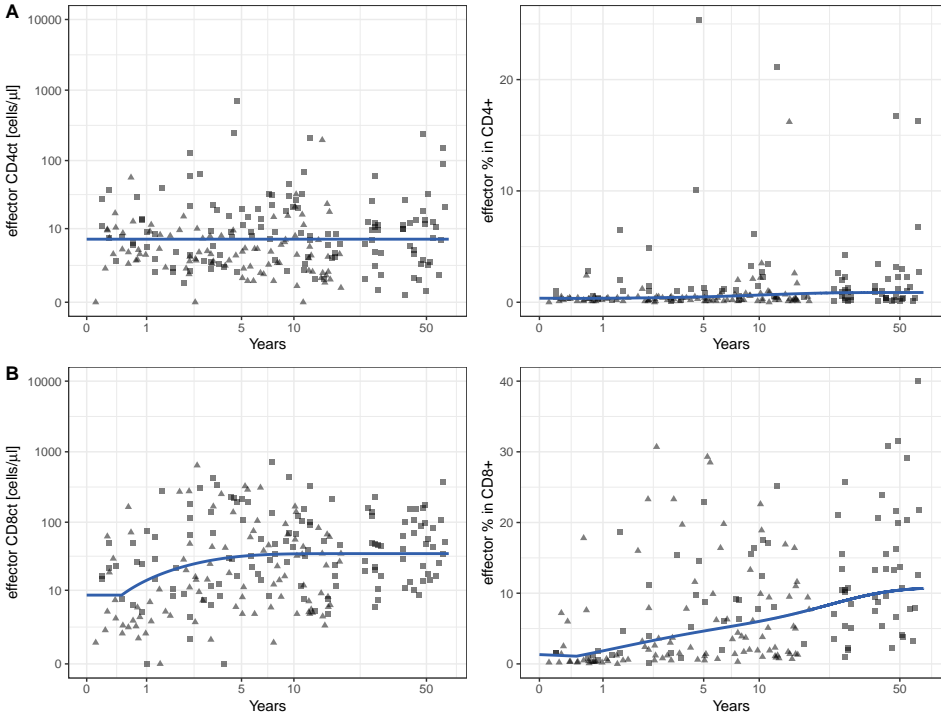
Figure S3.2: Trajectories of the effector subpopulation of CD4+ (A) and CD8+ cells (B) over age. The left panels give the absolute counts and and the right panels the percentages. Data from Dutch II are represented by triangles (▲), and data from Dutch III by squares (■). In the left panels, the blue solid lines represent the best fits via model (3.1) and with the parameters presented in Table 3.1. The predicted trajectories for the percentages are depicted by the blue solid lines in the right panels and calculated according to model (3.2) where the sum of naive, memory and effector cell counts add up to 100%.

4

Quantification of CD4 recovery in early-treated infants living with HIV

Juliane Schröter [1], Anet J.N. Anelone [1,2] & Rob J. de Boer [1]
on behalf of the EPIICAL Consortium

[1] Theoretical Biology & Bioinformatics, Utrecht University, The Netherlands
[2] School of Mathematics and Statistics, University of Sydney, Australia

Abstract

Background: Perinatally HIV-acquired infants benefit from an early antiretroviral treatment initiation. Thanks to a short viral exposure time, their immune system can be maintained or reconstituted, allowing a "normal" immune development. *Methods:* In this study, we mathematically modelled and quantified individual CD4+ T-cell reconstitution of a subset of 276 children who started treatment within 6 months of age and achieved sustained viral suppression. Considering natural age differences in CD4+ T-cell dynamics, we fitted distances to age-matched healthy reference values with a linear model approaching an asymptote. *Results:* Depleted CD4+ percentages (CD4%) and CD4+ counts (CD4ct) restored healthy levels during treatment. CD4ct recovered with a median rate of 4 cells/μL/day, and individual recovery rates were correlated negatively with their initial CD4ct. CD4 values at onset of treatment decrease with age, whereas recovery times and levels seem to be age-independent. CD4 recovery correlates positively with viral suppression, and the stabilisation of CD4 levels usually occurs after viral suppression. CD4 levels stabilise within 3-13 months after treatment initiation. The recovery dynamics of the CD4% is comparable to those of the CD4ct. *Conclusion:* In early-treated children with successful viral suppression, the CD4 depletion is typically mild and CD4+ T cells tend to "fully" recover in numbers.

Keywords: perinatal HIV, early antiretroviral therapy, lymphocytes, immune recovery, quantification, mathematical model

Introduction

Current WHO guidelines recommend starting antiretroviral treatment (ART) in perinatally HIV-acquired children as early as possible. Although in the past, critical CD4% levels, or a deteriorated health status, were used as criteria to initiate treatment, nowadays the presence of HIV is tested genetically, and a positive HIV diagnosis after birth usually leads to immediate treatment initiation. Early ART initiation not only reduces viral exposure time, and limits the establishment of latent HIV reservoirs, but probably also leads to either maintenance of the immune system or a better capacity for the regeneration of depleted CD4+ T cells [Palma et al., 2015]. Thus, early treatment initiation in perinatally HIV-acquired infants allows for a fairly normal development of their immune system.

Previous analyses have highlighted that children are better in regenerating their immune system than adults. This is probably due to increased thymic output and an increased CD4+ T-cell proliferation, which accelerate CD4+ T-cell count (CD4ct) recovery [Cohen Stuart et al., 1998; Douek et al., 1998; Simms et al., 2018]. Thus, the efficiency of T-cell reconstitution after treatment initiation is expected to depend on the age at which treatment is initiated. Furthermore, progressed HIV infections result in low CD4 levels at treatment initiation, which have been associated with poor CD4 reconstitution and reduced maintenance [Lewis et al., 2012; Picat et al., 2013; Simms et al., 2018]. Very early treatment initiation may therefore lead to rapid and durable immune reconstitution, which could open the opportunity for scheduled treatment interruptions and the possibility for a life without daily treatment for early-treated, perinatally HIV-acquired infants [Persaud et al., 2013; Sáez-Cirión et al., 2013; Klein et al., 2013; Cotton et al., 2013; Palma et al., 2015; Lewis et al., 2017; Palma et al., 2019].

In this study we aimed to quantify CD4 reconstitution in early-treated perinatally HIV-acquired infants who achieved successful viral suppression by using mathematical modelling. We correct for the natural CD4 decline in children by normalising CD4 levels to age-matched reference values from healthy children [Schröter et al., 2021]. This quantification showed that both depleted CD4ct and CD4% recover to healthy levels, and that stable CD4 levels are typically reached after viral suppression. As a consequence, late viral suppression, for example, because of poor adherence to ART, leads to late CD4 recovery.

Material & Methods

Data selection

We studied the reconstitution of CD4 levels (CD4ct and CD4% within total lymphocytes) in infants, from the database of the European Pregnancy and Paediatric Infections Cohort Collaboration (EPPICC), starting standard ART (bPI or NNRTI + 2-3 NRTI) within 6 months of age (N=469) [EPPICC, 2018; EPPICC and EPIICAL, 2019; Schröter et al., 2020]. We only considered children who successfully suppressed the virus (ie, achieved 2 consecutive viral loads (VLs) < 400 copies/mL, N=276) within the follow-up time of EPPICC [Schröter et al., 2020]. We defined a period of sustained viral suppression as the time having no VL measurements above 400 copies/mL once virally suppressed, and we neglected the fact that some infants achieved viral suppression a second time after a viral rebound, for example, because of treatment complications. We restricted our analyses to those observations obtained during the first period of sustained viral suppression. This period begins at ART initiation, although for some infants we use data from up to 10 days before ART initiation, to enrich baseline measurements. The period ends either at the end of follow-up, or at the last measurement before the VL rebounds above 400 copies/mL. For a subset of 58 infants belonging to the Collaborative HIV Paediatric Study (CHIPS) cohort [Collins et al., 2017], we also had data on total lymphocyte counts (TLCs). Their recovery was quantified in a similar fashion.

CD4 normalisation

TLC and CD4ct in healthy children follow a natural decline [Erkeller-Yuksel et al., 1992; Hulstaert et al., 1994]. To compare CD4 levels in infants at different ages, we used the normalisation functions provided by Schröter et al. [2021] as a reference for HIV unexposed ("healthy") infants. For each CD4+ T-cell measurement, we calculated the age-matched healthy median reference CD4 level ($CD4_{ref}$) and calculated the deviation of the measurement from this reference value:

$$\Delta CD4 = CD4 - CD4_{ref}.$$

We refer to this difference/distance as the $\Delta CD4$, which is negative if the CD4 measurement is below $CD4_{ref}$, positive if above, and zero if it is matching $CD4_{ref}$ (Figure 4.1). We define a $\Delta CD4$ for both the CD4ct and CD4%. The same normalisation procedure is applied to the TLC data.
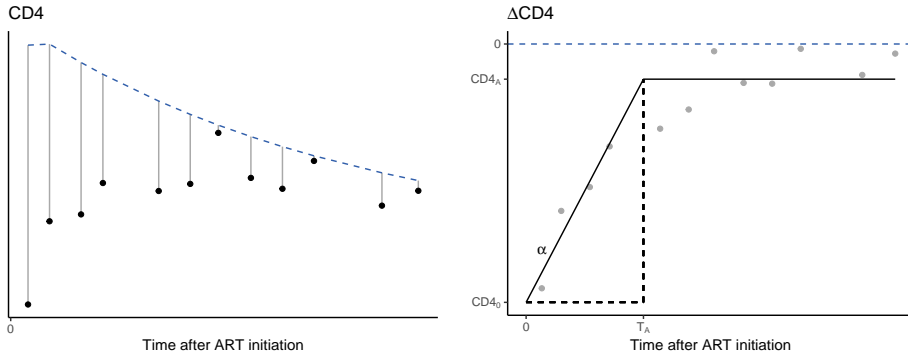
Figure 4.1: Schematic illustration of CD4 normalisation step and the recovery model. In the left panel, black bullets show the original CD4 measurements. In grey the distances to healthy CD4 reference values ($CD4_{ref}$) are depicted. In the right panel, these distances are presented by the grey bullets ($\Delta CD4$). The blue dashed lines represent the healthy median CD4 values retrieved from Schröter et al. [2021]. The median healthy CD4 values are used for the CD4 transformation and represent the horizontal blue dashed line at zero in the right part. The right part shows $\Delta CD4$, on which basis the fitting has been performed. An example model fit is illustrated by the black solid line. The model is fitted according to Equation (4.1), resulting in $CD4_0$, α, and T_A. The asymptote $CD4_A$ can be calculated from these 3 parameters. The dashed black lines highlight the CD4 recovery phase that ends at time T_A, when the asymptote $CD4_A$ is reached.

Mathematical model

Visual inspection of the data (see Figure S4.1) suggested that $\Delta CD4$ dynamics after ART initiation can be described empirically as a linear approach to a stable asymptote. Therefore, at a given time after ART initiation (t in days), we defined the $\Delta CD4$ by following recovery model:

$$\Delta CD4(t) = \begin{cases} \Delta CD4_0 + \alpha\, t\,, & \text{if } t \leq T_A, \\ \Delta CD4_0 + \alpha\, T_A = \Delta CD4_A\,, & \text{if } t > T_A, \end{cases} \quad (4.1)$$

where $\Delta CD4_0$ is the difference at start of treatment, α is the recovery rate in either cells per μL per day (for CD4 counts), or in percentages per day (for CD4%), and T_A is the time at which $\Delta CD4$ stabilised at the long-term asymptote $\Delta CD4_A$ (see Figure 4.1). We maximised $\Delta CD4$ to the negative reference value $CD4_{ref}$ to prevent negative CD4 levels, that is,

$$\Delta CD4(t) = \max(\Delta CD4_0 + \alpha\, t, \text{-}CD4_{ref}(t)).$$

This model Equation (4.1) is applied to both the CD4ct and CD4% data. We estimated $\Delta CD4_0$, α, T_A by minimising the sum of squared residuals between the model and the data for every individual child. We use therefore the R (version 4.0.5) package FME with its default Levenberg–Marquardt fitting algorithm [Soetaert and Petzoldt, 2010]. We determined lower and upper boundaries for parameter estimates: $\Delta CD4_0 \in [-CD4_{ref}(0), CD4_{ref}(0))]$, $\alpha_{ct} \in [-50, 50]$ for CD4ct, $\alpha_{\%} \in [-1, 1]$ for CD4%, and $T_A \in [0, t_{end}]$. Thus, these boundaries can vary per individual. For $\Delta CD4_0$, the boundaries were chosen to ensure that the initial values result in positive T-cell numbers, and do not exceed a doubling of the healthy reference value. The boundaries for the recovery rates, α, are arbitrarily chosen. Using the time of the last observation (t_{end}) as an upper bound for T_A may have shortened the actual time to reach an asymptote and lead to a lower $\Delta CD4_A$, but allowing for later estimates for T_A would have been arbitrary (as no later data are available). $\Delta CD4_A$ is not a free parameter and was derived from the model Equation (4.1).

To exclude children with treatment complications, we first only considered children with a monotonically declining VL to viral suppression (N=188). To be able to study the early CD4 dynamics after ART initiation, we required at least 5 measurements, of which at least 2 had to be collected within the first 120 days of ART for each child (N_{ct}=119, $N_{\%}$=117). If there was no baseline measurement available at time t_0, we extrapolated initiation from the closest measurements up to 10 days prior to ART initiation. We only considered those fits where the modFit function of the FME package was able to compute the Hessian matrix because standard errors for all 3 parameter estimates were provided for these fits. We considered parameters to be identifiable when all parameter estimates were significantly different from zero, to a significance level of 0.05 according to the t-statistic. Finally, we required at least the 2 first measurements before T_A because otherwise the recovery rate cannot be estimated.
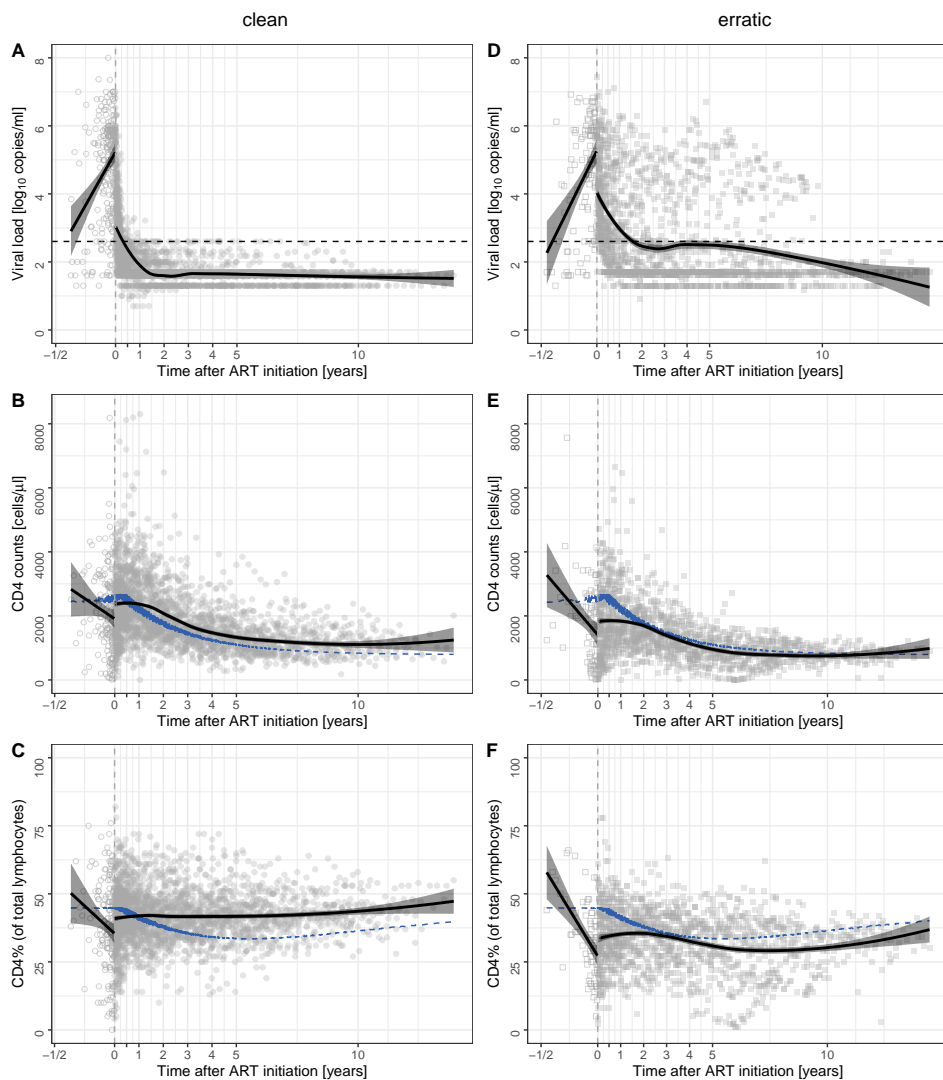
Figure 4.2: Reconstitution of CD4 levels after early ART initiation. Cross-sectional presentation of the trajectories of the VL (A, D), CD4+ T-cell count (B, E), and CD4+ T-cell percentage (C ,F) after ART initiation in 188 infants who suppressed their VL in a clean manner (left panels A-C, circles), and from 88 infants who suppressed their viral load erratically (right panels D-F, squares). Each symbol represents an individual measurement (with multiple measurements per individual). Open symbols are measurements before ART initiation, and filled symbols are measurements during treatment. The vertical grey dashed lines indicate the start of ART at time zero. Black solid lines present the regression lines with their 95% confidence intervals. For the measurements before ART initiation linear regression was performed; for the measurements after ART initiation, the locally estimated scatterplot smoothing (LOESS) regression lines are depicted. The horizontal black dashed lines in (A, D) present the VL threshold value of $\log_{10}(400 \text{ copies}/\text{mL})$. Blue dots in (B),(C), (E) and (F) represent median age-matched healthy reference values, retrieved from Schröter et al. [2021].

Results

Early ART initiation leads to CD4 reconstitution

We investigated CD4+ T-cell reconstitution in virally suppressed infants (N=276, Table S4.1), who acquired HIV-1 perinatally and started standard ART within median age of 82 days (IQR=[34, 121]). These infants achieved viral suppression after a median of 131 days (IQR=[63, 282]; 1 day earlier than described in Schröter et al. [2020] because we added 1 day to be able to plot time to viral suppression on a logarithmic scale, and previously did not correct for this in the summary statistics) and remained virally suppressed for a median of 836 days (IQR=[333, 2108], Figure 4.2A, D) while on treatment. Previously, we described that viral suppression can be achieved in a "clean" manner, with a VL declining monotonically (N=188, Figure 4.2A), or in an "erratic" manner, with VL measurements that also increase before viral suppression is attained (N=88, Figure 4.2D) [Schröter et al., 2020]. Because the latter might be resulting from treatment complications, we first focus on children with "clean" viral suppression patterns after treatment initiation.

First, we computed cross-sectional CD4 trajectories to depict the median trend of CD4+ T-cell reconstitution after ART initiation (Figure 4.2B, C, see Figure S4.1A, B). Before treatment initiation both the CD4ct and CD4% decline. After ART initiation, the CD4ct (Figure 4.2B and see Figure S4.1A) and CD4% (Figure 4.2C and see Figure S4.1B) stopped decreasing, stabilised, started increasing, and approach values

exceeding the median healthy reference value somewhat. Most children's CD4 levels (referring to both the CD4ct and CD4%, Figure 4.2B, C, see Figure S4.1A, B) subsequently followed the natural CD4 trajectory. These cross-sectional CD4 trajectories suggest that CD4 levels reach suprahealthy levels under ART. The CD4% (Figure 4.2C, see Figure S4.1B) takes somewhat longer to stabilise than the CD4ct (Figure 4.2B, see Figure S4.1A). In the following sections, we quantify CD4 recovery by modelling individual CD4 trajectories longitudinally.

Quantification of the CD4ct recovery

First, we constructed individual reconstitution trajectories of the CD4ct. To be able to compare CD4 trajectories between infants, we took the natural CD4 decline into account and computed CD4 measurements relative to their age-matched reference values (ΔCD4, Figure 4.1 and see Figure S4.1). Next, we fitted the ΔCD4ct data per infant using the mathematical model described in Equation (4.1) and obtained reliable CD4ct fits for 97 infants (for 32 fits all parameters, $CD4_0$, α and T_A, were identifiable) (Figure 4.3A-C, see Figure S4.2). At the start of treatment, the median CD4ct was below the median healthy age-matched level ($\Delta CD4_0$ = -965 cells/μL, IQR=[-1602, 71]), but a quarter of the infants maintained their CD4ct above median healthy age-matched values (25 out of 97 infants, Figure 4.3A)[Schröter et al., 2021]. During ART, the CD4ct increased by a median of 3.8 cells/μL/day (IQR=[0.5, 9.6], Figure 4.3A), and 64 infants acquired median healthy values (median $\Delta CD4_A$ = 182 cells/μL , IQR=[-98, 562]) Figure 4.3B). The reconstitution rate α_{ct} was negatively associated with the CD4ct at start of treatment (Spearman correlation: ρ=-0.67, p-value<0.001, Figure 4.3A), indicating that the recovery rate increases when cell numbers are low. Infants stabilised their CD4ct within a median of 222 days (IQR=[116, 403], Figure 4.3C). Note that the estimated time to stabilise CD4ct remains a lower bound because not every child reached a stable CD4ct by the end of the observation period. In the majority of cases (N=81) CD4ct recovery (T_A) took longer than viral suppression (time to viral suppression was defined as the time to the first of 2 consecutive viral load measurements of < 400 copies/mL [Schröter et al., 2020]), which took a median of 97 days (IQR=[58, 168], Figure 4.3C). The time to stabilise the CD4ct has a weak positive association with the time to viral suppression (Spearman correlation: ρ=0.21, p-value=0.04, Figure 4.3C). Previously, we showed that slower viral suppression is associated with high initial VL and low CD4 levels, both of which reflect HIV disease progression status [Schröter et al., 2020]. Thus, further progression of HIV infection results not only in a lower $\Delta CD4ct_0$ but also in a longer time to recover. We noticed that not all infants increased their ΔCD4ct and that 23
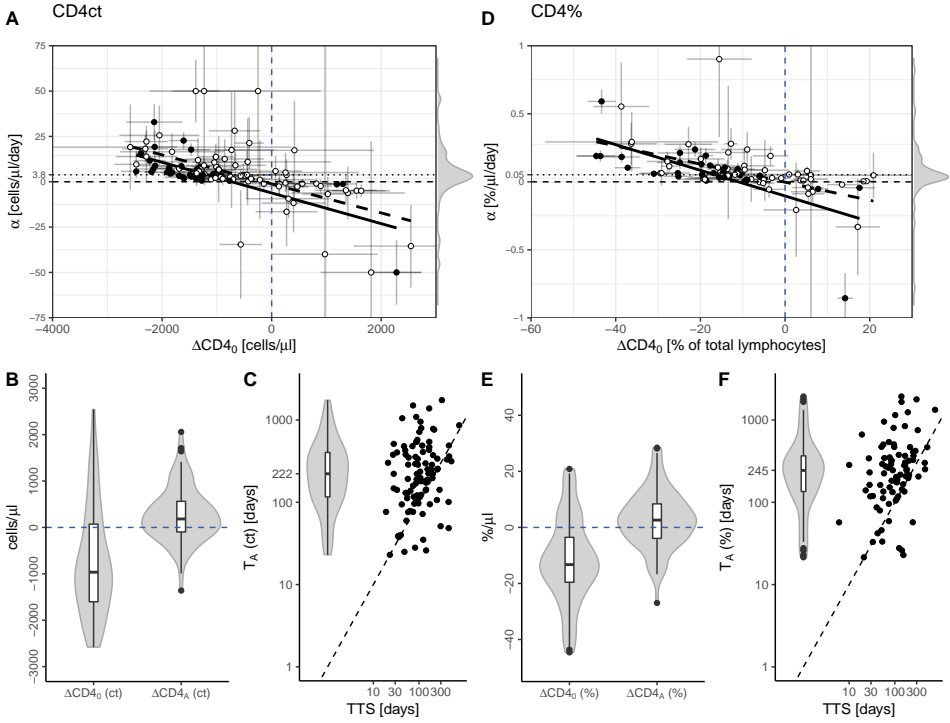
Figure 4.3: Similar CD4 recovery dynamics of the CD4ct and CD4%. Panels (A-F) summarise the model estimates. The results for the CD4ct are represented on the left side (A-C), and those for the CD4% are represented on the right side (D-F). In panels (A, D), the parameter estimates of $\Delta CD4_0$ are plotted against the parameter estimates of α. Each symbol shows the combination for 1 individual. Filled circles reflect that the estimates for all 3 parameters (CD4$_0$, α, T$_A$) were identifiable. The standard errors are depicted for both estimates by the error bars, for $\Delta CD4_0$ in horizontal and for α in vertical directions. The dashed lines represent the regression lines for all accepted estimates, the black regression lines are drawn only for fits where all 3 parameters were identifiable. A density plot of the parameter estimates for α is illustrated in the margin of the panels. The median recovery rate values are indicated by a horizontal dotted lines. In panels (B, E), the distributions of $\Delta CD4_0$ and $\Delta CD4_A$ are shown by a violin plots with integrated boxplots. The healthy reference CD4 levels are depicted by the blue dashed lines at zero. In (C, F) the distribution of T$_A$ (violin plot) and its correlations with time to viral suppression (TTS) are illustrated. The dashed black lines represent the identity lines.

experienced a further decline in their CD4ct despite being on ART (Figure 4.3A). However, the majority of these infants (N=21) had a supranormal CD4ct, that is, a positive ΔCD4ct, so it is unsurprising that their CD4ct decreased rather than increased. As the parameter estimates for infants with declining ΔCD4ct were mostly not significant (N=20, Figure 4.3A), we will not address them further. Summarising, after treatment initiation, the CD4ct recovers at a rate of 3.8 cells/μL/day and within approximately 200 days.

Quantification of the CD4% recovery

Second, we investigated the dynamics of CD4% within individuals after treatment initiation, again relative to the median age-matched healthy values. We obtained ΔCD4% fits for 86 infants, and for 34 children, all parameters were identifiable (Figure 4.3D, see Figure S4.2). Infants started ART with a median ΔCD4% of -13.27% (IQR=[-19.56, -3.53], Figure 4.3D), and reconstitution occurred at a median rate of 0.05%/day (IQR=[0.02, 0.12], Figure 4.3D). CD4% reconstitution rates and the initial $\Delta CD4_0\%$ were negatively correlated (Spearman ρ=-0.67, p<0.001, Figure 4.3D), suggesting a density dependence in CD4 reconstitution, such that more profound depletion in CD4+ T cells induces more rapid rebound. The CD4% stabilised at a median of 245 days (IQR=[135, 375], Figure 4.3F). A stable CD4% is again reached after viral suppression occurred after a median of 106 days (IQR=[57, 168], Figure 4.3F). The correlation between the time to CD4% stabilisation and the time to viral suppression were comparable to those of the CD4ct (Spearman ρ=0.36, p<0.001, Figure 4.3C, F). The ΔCD4% asymptote levels differed by a median of 2.61% (IQR=[-3.91, 8.40], Figure 4.3E), implying that the majority of infants (N=55) exceeded median healthy values. Thus, the CD4% recovery is comparable to the CD4ct recovery.

The TLC also increase with treatment initiation

TLC data were available for 58 infants belonging to the CHIPS cohort within EPPICC. We investigated the TLC dynamics of 33 infants fulfilling the criteria of "clean" viral suppression (Figure 4.4, see Figure S4.3, S4.4). Cross-sectional trajectories suggest that TLC and CD4ct exhibit similar patterns of reconstitution after ART initiation (Figure 4.4A). We quantified TLC reconstitution by fitting individual ΔTLC trajectories using our model Equation (4.1) and obtained 26 fits (Figure 4.4B, C, see Figure S4.3, S4.4). The TLC increased initially by a median of 8.5 cells/μL/day (IQR=[-0.1, 18.9], see Figure S4.4), which overlaps with the rate at which the CD4ct recover. The times to stabilisation (T_A(TLC)=193 days, IQR=[90, 316], Figure 4.4C) are
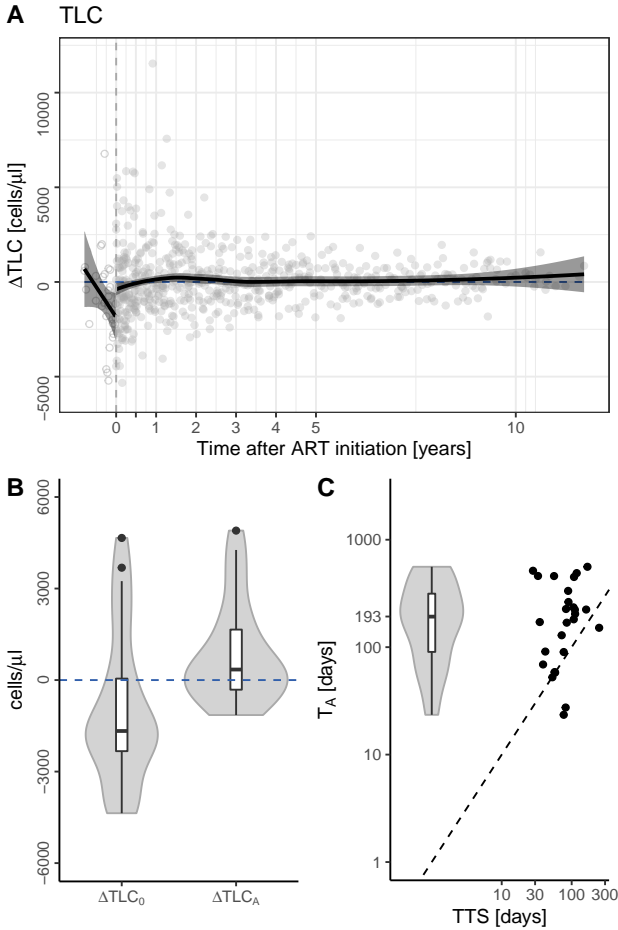
Figure 4.4: Dynamics of total lymphocyte count (TLC). Panel (A) depicts cross-sectional trajectories of age-matched ΔTLC trajectories of a subset of 57 infants from the CHIPS cohort (an EPPICC subset). Each symbol represents the difference of a measurement to age-matched median healthy reference value (ΔTLC). Open symbols are measurements before the initiation of ART, and filled symbols are measurements after ART initiation. The vertical grey dashed lines indicate the start of ART at time zero. The solid black lines present regression lines with their 95% confidence intervals. For the measurements before ART initiation a linear regression is performed; for the measurements after ART initiation the LOESS regression line is depicted. The horizontal blue dashed lines at zero represent the median healthy reference values, retrieved from Schröter et al. [2021]. In panel (B) the distributions of the initial differences and the differences of the asymptote levels are shown by a violin plots with integrated boxplots, ΔTLC_0 and ΔTLC_A. The healthy reference TLC levels are depicted by the blue dashed lines at zero. Panel (C) depicts the distribution of T_A (violin plot) and its correlation with time to viral suppression (TTS). The dashed black lines represent the identity lines.

in the same range as those of the CD4ct, and although the initial TLC (ΔTLC_0=-1670, IQR=[-2330, 48], see Figure S4.4) is markedly reduced, the range overlaps with that of the CD4ct. The median stable level (ΔTLC_A) with 345 cells/μL (IQR=[-315, 1655]) is also somewhat above healthy TLC levels (Figure 4.4B). Thus, the TLC and CD4ct recovery show comparable recovery dynamics, which is not unexpected because the depletion of the TLC during HIV infection should largely be due to a depletion of the CD4+ T-cell counts.

CD4 recovery is density-dependent rather than age-dependent

According to current literature, the timing and the levels of CD4 reconstitution depend on age at start of treatment, and on the initial CD4 levels [Lewis et al., 2012; Picat et al., 2013; Simms et al., 2018]. We found evidence for an increase in the rate of CD4ct recovery when the CD4+ T-cell density is low. Because CD4 levels decline before treatment (Figure 4.2B-F), we then expect age to be positively associated with the recovery rate. We confirmed this by studying the impact of the age at start of treatment on the dynamics of CD4 reconstitution. The individual initial CD4ct ($\Delta CD4ct_0$, Spearman ρ=-0.35, p<0.001, see Figure S4.5A), and CD4 recovery rate (Spearman ρ=0.30, p=0.002, see Figure S4.5B) was weakly correlated with age at start of treatment. The time to stabilise and the CD4 recovery levels ($CD4_A$), however, do not show any significant correlations with age at start of treatment (see Figure S4.5C, D). Thus, we find no evidence for an age-dependent CD4ct reconstitution in these individuals. We find similar results for the reconstitution of the CD4%. Although the initial $\Delta CD4\%$ declines with age (Spearman ρ= -0.45, p<10^{-4}; see Figure S4.5E), and the CD4% recovery rate (Spearman correlation: ρ=0.37, p-value<0.001; see Figure S4.5F) correlates with age, the asymptote level and time to stabilise are independent of the age at start of treatment. The positive effect of age on the recovery rate could therefore be indirect and because of a density-dependent recovery of the CD4%. Summarising, we find no evidence for a direct effect of age on CD4+ T-cell reconstitution in these early-treated children.

CD4 recovery is delayed in infants with erratic viral suppression patterns

Finally, we return to the children with an erratic viral suppression pattern (N=88, Figure 4.2D-F). Given that CD4 recovery occurs in children experiencing a monotonic decline of VL on ART, it is interesting to explore whether perinatally HIV-acquired children with treatment complications, and/or erratic viral suppression

patterns, also experience a "full" recovery of their immune system. Because CD4 trajectories of "erratic" children are difficult to model, we interpreted their cross-sectional data visually (Figure 4.2D-F and see Figure S4.1C, D). Infants with erratic viral suppression patterns seem to exhibit a slower CD4 recovery than infants in the "clean" subset (Figure 4.2, see Figure S4.1). Treatment halts the decline of CD4+ T-cell levels, and reconstitution tends to stabilise only after the VL is fully suppressed. Ultimately, the CD4ct and CD4% do approach median healthy levels (Figure 4.2E, F, see Figure S4.1C, D). Infants with erratic viral suppression patterns experience significantly longer times to viral suppression than infants with clean viral suppression patterns (clean: 90 days, IQR=[48, 166]; erratic: 375 days, IQR=[204, 855]) [Schröter et al., 2020], which might explain the delay in CD4 recovery. The asymptotic CD4 levels tend to be lower in "erratic" infants than in "clean" ones (Figure 4.2C, F, see Figure S4.1B, D). The lower initial CD4 levels in the erratic subset suggests that the infection has progressed further in the pretreatment phase. The slower recovery in the erratic subset is probably also because of a longer viral exposure during treatment, since prolonged immune activation may delay the reconstitution of CD4 T cells. Thus, early initiation of ART in infants reduces HIV disease progression, and enables reconstitution of CD4+ T cells despite erratic viral suppression.

Discussion

Early initiation of ART in individuals living with HIV has been proven to be very effective in stabilising and reconstituting CD4 levels, and to prevent progression to AIDS, and this is particularly true in children [Violari et al., 2008; Beaudrap et al., 2008; EPPICC, 2011; Lewis et al., 2012; Cotton et al., 2013; Palma et al., 2015]. Here we quantified the trajectories of CD4+ T-cell recovery in very-early treated, perinatally HIV-acquired infants using mathematical modelling. Depleted CD4ct generally increase by approximately 4 cells/μL/day in infants, and recover to healthy age-matched levels in about 3-13 months. These estimates are in line with other paediatric studies [Cohen Stuart et al., 1998; Van Rossum et al., 2001]. The estimated recovery rate in infants is about 3-fold faster than those reported values for adults [Pakker et al., 1998; Cohen Stuart et al., 1998; Bucy et al., 1999; Van Rossum et al., 2001; Hardy et al., 2003; Bains et al., 2009a]. For example, Hardy et al. [2003] report an increase of 147 cells/μL within 16 weeks in adults on ART, corresponding to a recovery rate of 1.3 cells/μL/day.

The CD4+ T-cell reconstitution process can be divided into 2 phases: (i) early

redistribution of T cells from lymphoid tissue and (ii) *de novo* production of T cells by peripheral cell division and/or the thymus [Pakker et al., 1998; Kaufmann et al., 1999; Carcelain et al., 2001]. Our model Equation (4.1) unifies the 2 phases into a single linear increase because we typically have no data to capture the early redistribution of T cells (the second data point is typically after 1 month). In adults, redistribution generally occurs within the first month of treatment [Mosier et al., 1995; Dimitrov and Martin, 1995; Bucy et al., 1999], which is much shorter than our times of follow-up and our estimated times to recover. Thus, the linear recovery that we model largely captures the second phase. If the true recovery were nonlinear due to an additional early redistribution, our model with a single linear recovery phase would have overestimated the initial $CD4_0$ values and have averaged the recovery rates. However, we expect these effects to be minor and conclude that a model with a linear increase is an appropriate conservative choice.

Our estimated recovery rate of 4 cells/μL/day in young children is fairly slow. The daily production of naive T cells by the thymus in children has been estimated in 2 articles [Bains et al., 2009b,a]. For a 2-year old child, which is a midpoint of most of our recovery phases, the estimates for the total body production vary from 0.3×10^9 [Bains et al., 2009a] to 1.3×10^9 [Bains et al., 2009b] cells per day. In the same articles, the blood volume of a 2-year old child is estimates to be about a 1000 mL. Assuming that 2% of the T cells reside in the blood, and recalculating into microliters, these published estimates vary from 6 to 26 cells/μL/day, which is the same range, but somewhat higher than our median estimate. Because our estimated recovery rate of 4 cells/μL/day should also include production of memory CD4+ T cells, this suggest the CD4 recovery in children living with HIV is slower than the normal daily production would allow for.

A monophasic model of reconstitution, in combination with a normalisation of CD4+ T-cell levels to age-matched reference values, is commonly used for modelling paediatric CD4 recovery [Van Rossum et al., 2001; Lewis et al., 2012; Picat et al., 2013; Simms et al., 2018]. We nevertheless introduced few improvements. First, for the normalisation we do not use the conventional z-scores [Wade and Ades, 1994], but we express our data as the distance from the age-matched reference value (ie, zero is the normal value). This choice allows for a more intuitive graphical representation of the data and for a more intuitive interpretation of the estimated parameters. For instance, the units of the recovery rate are given in cells per microliter per day. Second, we use a linear model approaching an asymptote rather than an exponential

model with an asymptote [Lewis et al., 2012; Picat et al., 2013]. The number of estimated parameters is the same, but we prefer the linear model of our Equation (4.1) because it (i) is less sensitive to a potential initial increase because of redistribution; and (ii) it naturally identifies the time at which CD4 levels stabilise. Finally, in contrast to the two-knot linear spline model used by Simms et al. [2018], we do not fix the time at which CD4 levels stabilise, but estimate it. Although Simms et al. [2018] considered the first 3 months after ART initiation as the main window for CD4 reconstitution in children and fixed the time of CD4 stabilisation to 84 days, we find in our data that CD4 reconstitution is considerably slower with both CD4ct and CD4% stabilising around 200 days after ART initiation. We find that the time to CD4 recovery is at least 100 days later than the time to viral suppression, which is in agreement with previous studies associating CD4 recovery with viral exposure time [Walker et al., 2004; Adland et al., 2018]. For a few patients with a short follow-up, our time to stabilisation should be taken as a lower bound because the long-term asymptote may not be reached within the observation window. Summarising, we present here a new quantitative framework for describing CD4 recovery dynamics in infants.

Our analyses suggest that the rate of CD4+ T-cell recovery increases when cell densities are low, which is in good agreement with previous studies showing that CD4 recovery is density-dependent [Walker et al., 2004; Lewis et al., 2012; Picat et al., 2013]. However, these results should be interpreted with care because they could be because of a regression to the mean effect, that is, a too low or too high estimate of the initial CD4 level will lead to a too high or too low estimate of the recovery rate at the next time point. In addition, we show that the asymptote levels and the time to stabilise are all independent of age in these very-early treated infants. Van Rossum et al. [2001] and Vrisekoop et al. [2008] also argue that CD4+ T-cell recovery is age-independent. The contribution of age on CD4+ T-cell recovery is extensively discussed in the literature and might play a role in older-treated children [Hainaut et al., 2003; Walker et al., 2004; Beaudrap et al., 2008]. In this cohort of very young children, the most rapid recovery of the immune system is achieved with early and successful viral suppression, which can be achieved by early treatment initiation.

In the field of immunology, it is often debated whether the CD4ct or CD4% should be used [Goicoechea and Haubrich, 2005]. Because the CD4ct are much more sensitive to measurement errors, the CD4% was generally recommended as a biomarker for HIV disease progression and as an indicator to initiate treatment in infants [O'Gorman and Zijenah, 2008]. However, the majority of CD4

recovery models are based on CD4ct data. We have modelled both, and have shown similar general recovery dynamics for age-normalised CD4ct and CD4%. Summarising, considering CD4ct and CD4% data together is most informative, as the CD4ct is more noisy but better reflects reconstitution levels, and the CD4% is less variable but is also influenced by other components of the cellular immune system.

In conclusion, early-treated children achieving sustained viral suppression typically attain "healthy" CD4 levels. This is the remarkable achievement of ART, allowing HIV-infected people to live a long and "almost healthy" life [Kaufmann et al., 1999; Klein et al., 2013]. However, perinatally HIV-acquired infants carry the high burden of being on life-long treatment, affecting their general (immuno-, neuro-)development and might lead to yet unknown side effects [Palma et al., 2015; Puthanakit et al., 2013; Laughton et al., 2018]. Moreover, long-term drug use and stigmatisation can result in psychological difficulties once these children enter adolescence [Giannattasio et al., 2011]. Current paediatric HIV research therefore focusses on providing simpler, more tolerable regimens, faster, and novel strategies such as weekends off, which makes ART easier to take [Palma et al., 2015, 2019; Penazzato et al., 2019; Kuhn et al., 2020]. Controlled treatment interruptions is sometimes successful in children, and has resulted in the maintenance of viral suppression off-treatment [Persaud et al., 2013; Sáez-Cirión et al., 2013; Violari et al., 2019]. However, the optimal timing and medical conditions for scheduled treatment interruptions or additional immunotherapies next to ART remain elusive. Quantification of the CD4 recovery and the viral suppression, such as we provide here, can inform the timing of such an intervention.

Author Contributions

JS and AJNA contributed equally to this work. JS and AJNA performed the mathematical analysis and drafted the manuscript under the supervision of RJdB. All co-authors contributed to the concept and the design of this work, participated in discussions about interpretation of findings, and contributed to the final version of this manuscript.

Acknowledgements

Supplementary Tables and Figures

Table S4.1: Baseline study characteristics and sociodemographics. This table is an extended version of the one in Schröter et al. [2020].

	All (N=276)		**Clean** (N=188)		**Erratic** (N=88)	
Variables	N	%	N	%	N	%
Gender						
Female	164	59.4	112	59.6	52	59.1
Male	112	40.6	76	40.4	36	40.9
Ethnicity						
White	79	28.6	58	30.9	21	23.9
Black	100	36.2	63	33.5	37	42
Other (including Asian)	8	2.9	4	2.1	4	4.5
Unknown (Prohibited)	89	32.2	63	33.5	26	29.5
Geographical region						
Central and Western Europe	166	60.1	123	65.4	43	48.9
UK/Ireland [*]	94	34.1	56	29.8	38	43.2
Eastern Europe (Russia/Ukraine)	12	4.3	8	4.3	4	4.5
Thailand	4	1.4	1	0.5	3	3.4
ART regime						
bPI + ≥ 2 NRTI	105	38	79	42	26	29.5
NNRTI + 2 NRTI	109	39.5	66	35.1	43	48.9
NNRTI + 3 NRTI	62	22.5	43	22.9	19	21.6
Age at ART start (in days)						
median [IQR]	82	[34, 121]	79	[31, 120]	90	[42, 131][1]
Baseline $\log_{10}$(VL) (copies/ml) [ab]	128	46.4	87	46.3	41	46.6
median [IQR]	5.3	[4.2, 5.9]	5.4	[4.4, 5.9]	5.0	[4.2, 5.9]
Baseline CD4 counts (cells/µl) [ab]	104	37.7	72	38.3	32	36.4
median [IQR]	1600	[868, 2429]	1648	[1016, 2465]	1530	[529, 2163]
Baseline CD4% [abc]	99	35.9	69	36.7	30	34.1
median [IQR]	33	[22.5, 42.5]	35	[26.0, 46.0]	29.5	[20.3, 34.0]
Time to viral suppression (TTS) (days) [d]						
median [IQR]	131	[63, 282]	89.5	[48, 166]	374.5	[204, 855]

bPI, boosted protease inhibitor; NRTI, nucleoside reverse transcriptase inhibitor; NNRTI, non-nucleoside reverse transcriptase inhibitor

[a] baseline measurements at start of ART including 10 days apriori

[b] Number of available data is shown

[c] CD4% of total lymphocytes

[d] TTS is defined as the first observed measruemnt of 2 consecutive VL meaaurments < 400 copies/ml

[*] Data included in CHIP cohort

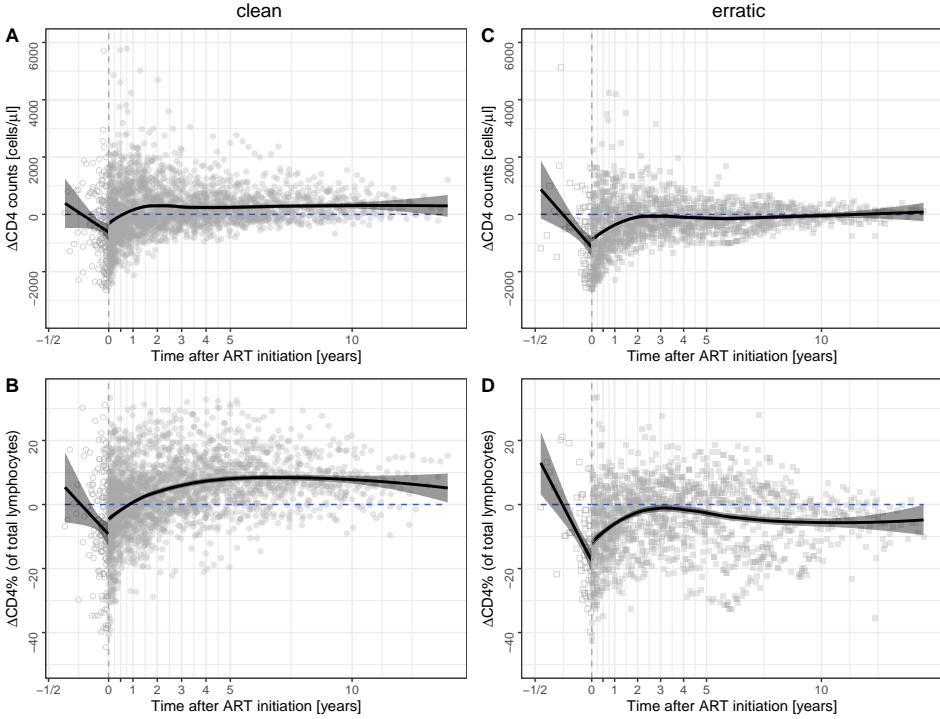[1] Figures differ from Schröter et al. [2020] , and are corrected here

Figure S4.1: Reconstitution of △CD4 after early ART initiation. The figure depicts △CD4ct (panels A ,C), and △CD4% (B, D) trajectories after ART initiation from 188 infants who suppressed their viral load in a clean manner (panels A/B, circles) and from 88 infants who suppressed their viral load erratically (panels C, D, squares). Each symbol presents the difference of a measurement to age-matched median healthy reference value (△CD4). Open symbols are measurements before ART initiation, filled symbols are measurements after ART initiation. The vertical grey dashed lines indicate the start of ART at time zero. The solid black lines present regression lines with their 95% confidence intervals. For the measurements before ART initiation a linear regression is performed; for the measurements after ART initiation a LOESS regression line is depicted. The horizontal blue dashed lines at zero represent the median healthy reference values, retrieved from Schröter et al. [2021].

ΔCD4% (of total lymphocytes)

Figure S4.2: Continued.

Time after ART initiation [years]

ΔCD4ct [cells/μl]
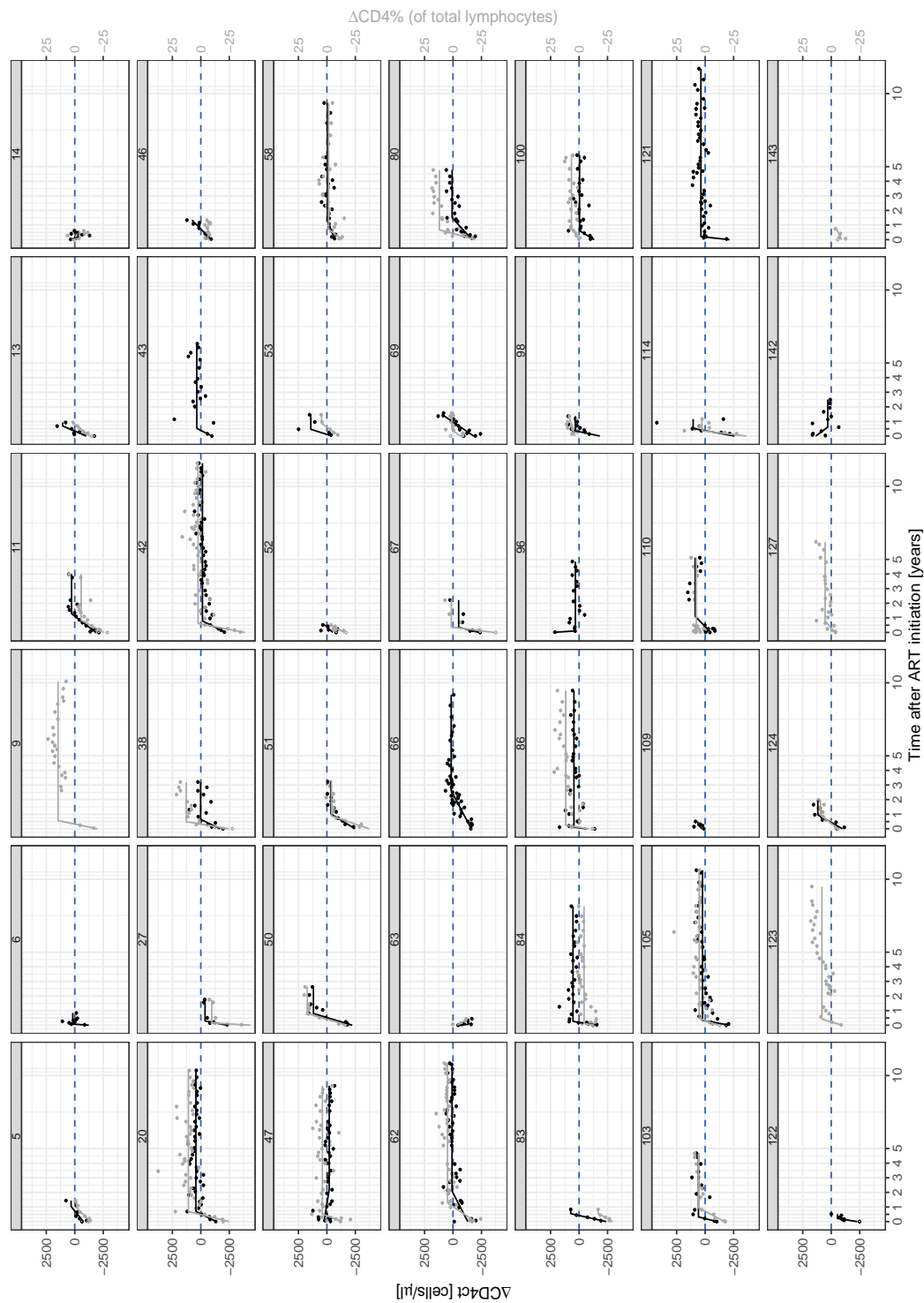
Figure S4.2: Continued.
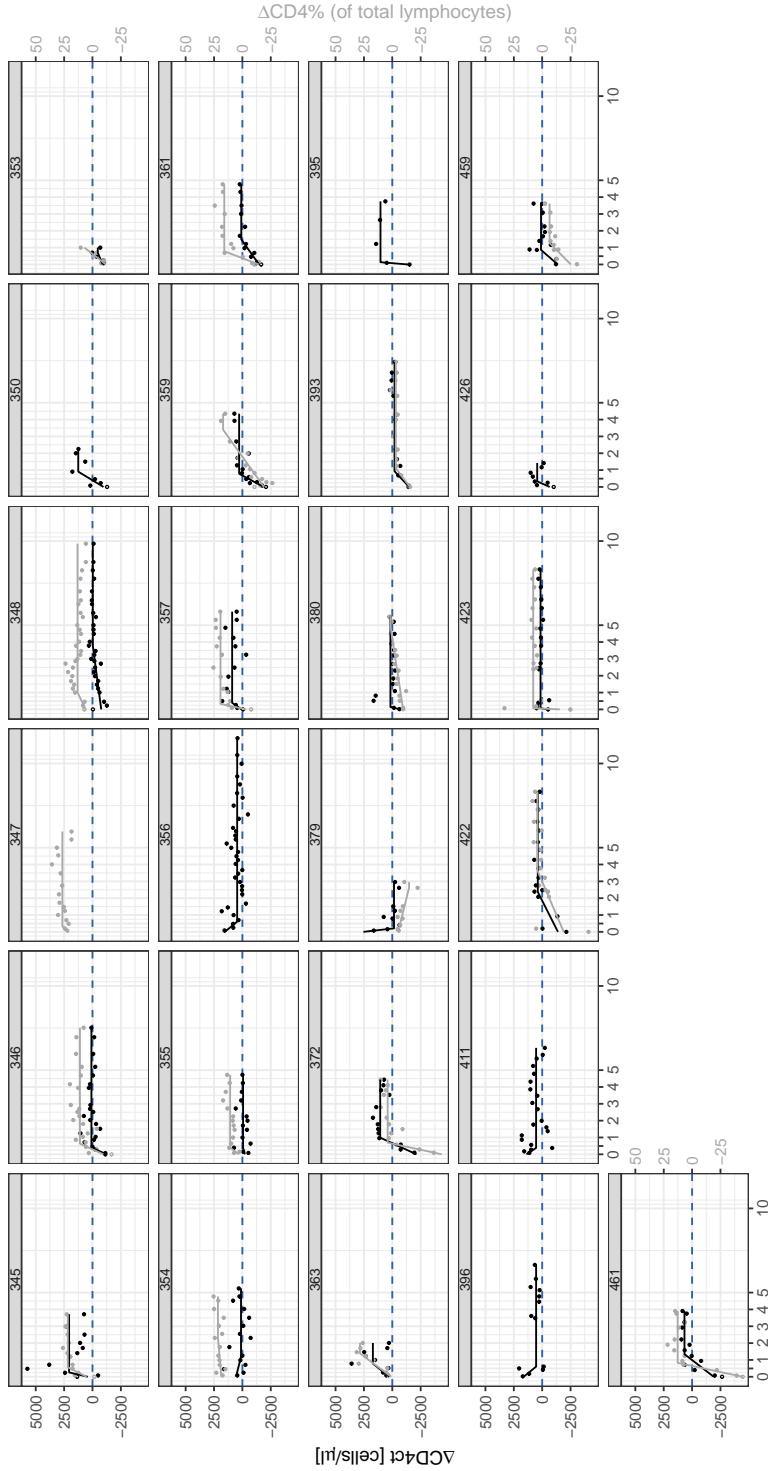
Figure S4.2: Time courses and fits of ΔCD4 trajectories after ART initiation. Each panel represents one infant labelled with an anonymous ID. The bullets represent ΔCD4 measurements and solid lines the model fits. Black bullets and lines depict the ΔCD4ct (left y-axis), while grey bullets and lines depict the ΔCD4% (right y-axis). Open circles present extrapolated baseline measurements from the closest measurement 10 days prior to ART initiation. The horizontal dashed blue lines represent CD4ref, which are at zero in the ΔCD4 transformation.

4

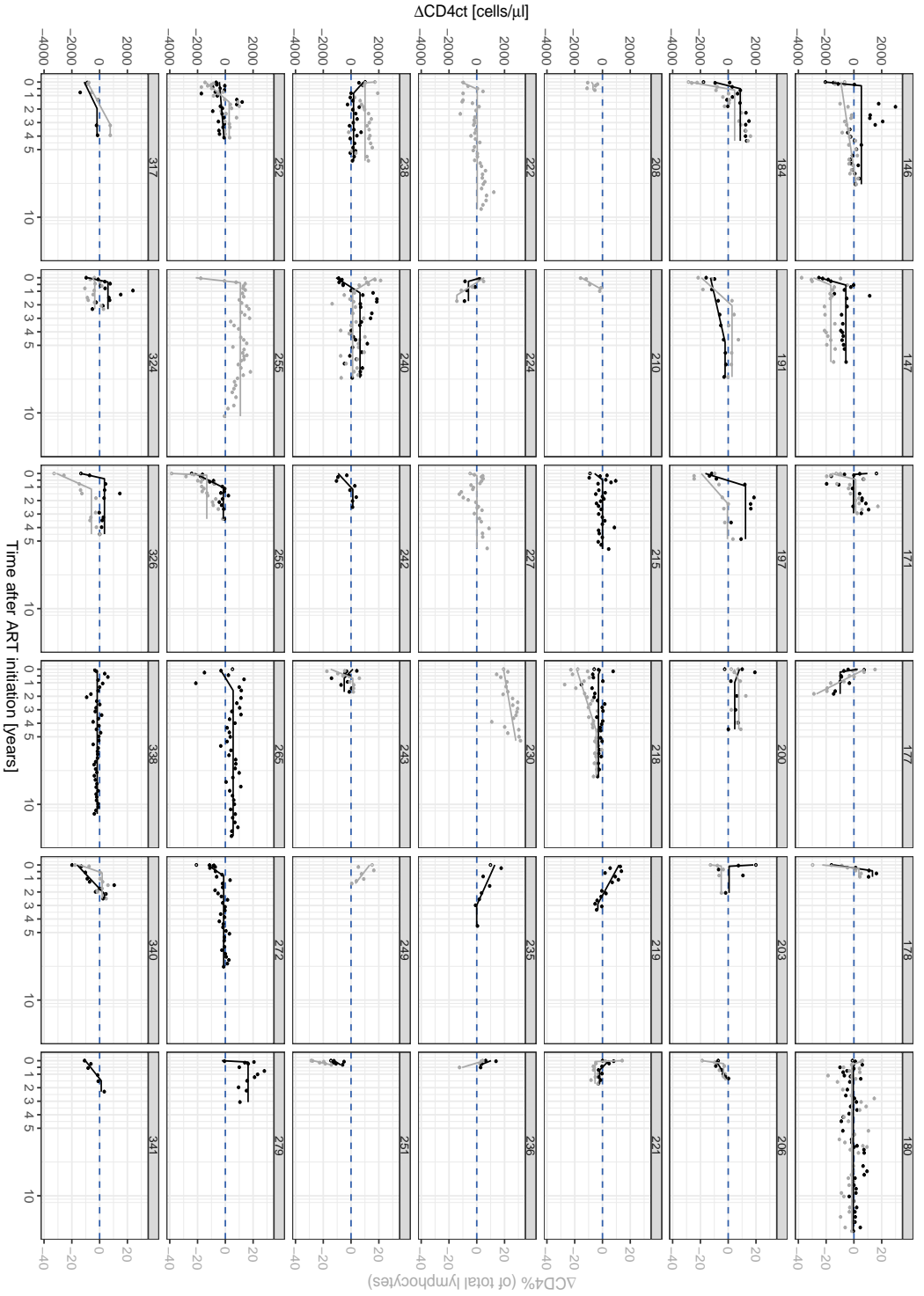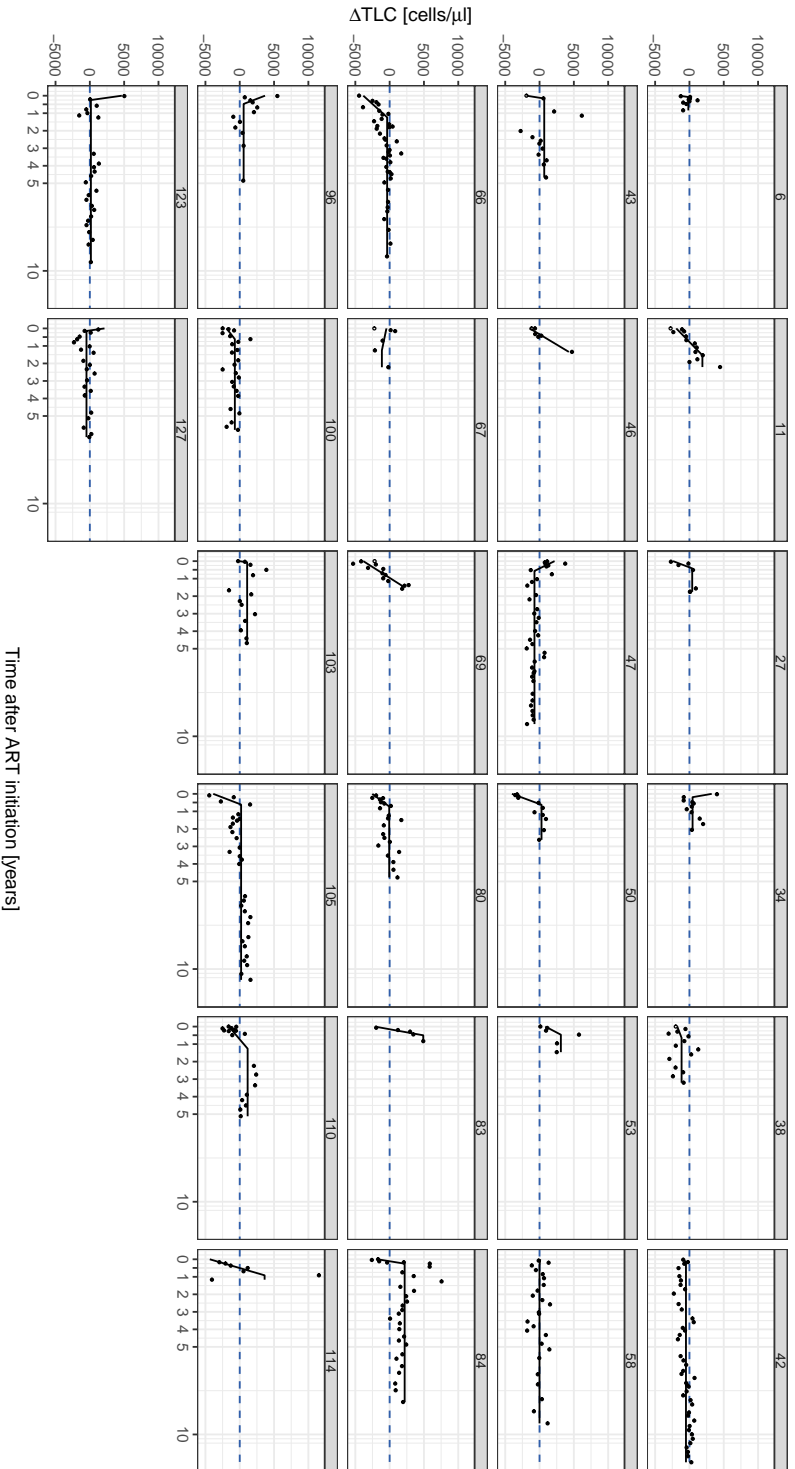**Figure S4.3: Time courses and fits of ΔTLC trajectories after ART initiation.**
Each panel represents one infant labelled with an anonymous ID. The bullets represent measurements and solid lines the model fits. Black bullets and lines refer to ΔTLC. Open circles present extrapolated baseline measurements from the closest measurement 10 days prior to ART initiation. The horizontal dashed blue lines at zero represents the median healthy reference.

TLC
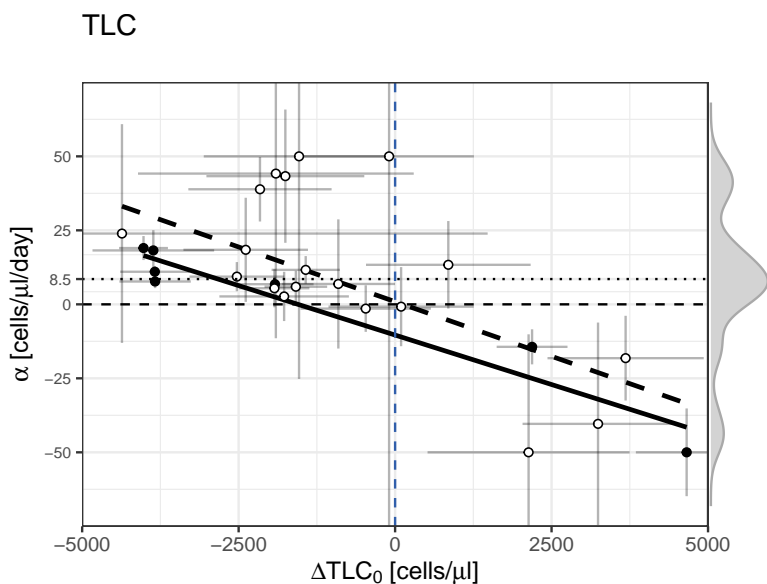
Figure S4.4: Summary of the parameter estimates from modelling ΔTLC. The parameter estimates of the initial values are plotted against the parameter estimates of the recovery rates α. Each symbol shows the combination for one individual. Filled circles reflect that the estimates for all 3 parameters (TLC_0, α, T_A) were identifiable. The standard errors are depicted for both estimates by the error bars, for the initial values in horizontal and for α in vertical directions. The dashed lines represent the regression lines for all reasonable estimates, the black regression lines are drawn only for fits where all 3 parameters were identifiable. A density plot of the parameter estimates for α is illustrated in the margin of the panels. The median recovery rate values are indicated by horizontal dotted lines.

CD4ct

CD4%

A $\rho = -0.35, ***$

E $\rho = -0.45, ***$

B $\rho = 0.31, **$

F $\rho = 0.37, ***$

C $\rho = 0.13, NS.$

G $\rho = 0.18, NS.$

D $\rho = 0.03, NS.$

H $\rho = 0.12, NS.$
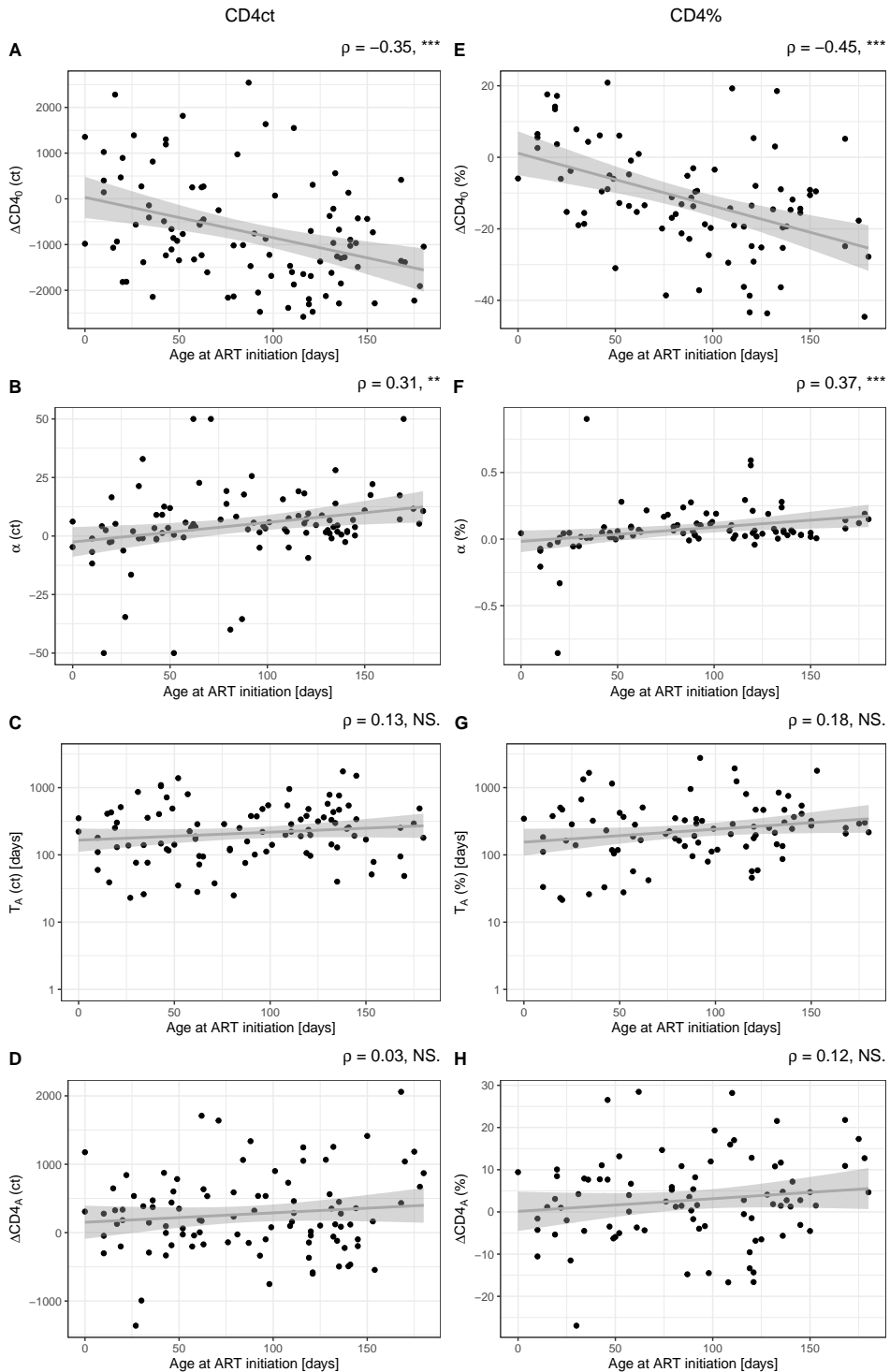
Figure S4.5: CD4 recovery appears to be age-independent. Correlation plots with age at ART initiation on the horizontal axis are drawn on the left side for the CD4ct (A-D), and on the right side for the CD4% (E-H). The correlation with the initial $\Delta CD4_0$ are depicted in panels (A) and (E), with the recovery rates α in panels (B) and (F), with time to stabilise T_A in panels (C) and (G), and with the asymptote level $CD4_A$ in panels (D) and (H). The linear regression lines and their 95% confidence intervals are given in grey. Spearman's correlation coefficients, ρ, are given above each panel (p-value < 0.001: ***, p-value $\geq$ 0.05: NS.).

What explains the poor contraction of the viral load during paediatric HIV infection?

Juliane Schröter & Rob J. de Boer

Theoretical Biology & Bioinformatics, Utrecht University, Utrecht, The Netherlands

Abstract

An acute HIV infection in young children differs markedly from that in adults: Children have higher viral loads (VL), and a poor contraction to a setpoint VL that is not much lower than the peak VL. As a result, children progress faster towards AIDS in the absence of treatment. We used a classical ordinary differential equation model for viral infection dynamics to study why children have a lower viral contraction ratio than adults. We performed parameter sweeps to identify factors explaining the observed difference between children and adults. We grouped parameters associated with the host, the infection, or the immune response. Based on paediatric data available from datasets within the EPIICAL project (https://www.epiical.org/), we refuted that viral replication rates differ between young children and adults, and therefore these cannot be responsible for the low VL contraction ratios seen in children. The major differences in lowering VL contraction ratio resulted from sweeping the parameters linked to the immune response. Thus, we postulate that an "ineffective" (late and/or weak) immune response is the most parsimonious explanation for the higher setpoint VL in young children, and hence the reason for their fast disease progression.

5

Introduction

Several mathematical models describe the course of an acute HIV infection in adults by very similar mechanisms, i.e., by classical within-host viral kinetics [Ho et al., 1995; Wei et al., 1995; Perelson et al., 1996; Kirschner and Webb, 1996; Nowak et al., 1997; de Boer and Perelson, 1998; Nowak and May, 2000; Stafford et al., 2000; Perelson, 2002; Canini and Perelson, 2014; van Dorp et al., 2020]. HIV infects CD4+ T-cells and replicates rapidly, as indicated by a steep initial increase of the viral load (VL), peaking around 10^6 RNA copies/mL within a few weeks, and is accompanied by a progressive loss of CD4+ T-cells [Kaufmann et al., 1998; Little et al., 1999]. Once the target cells decline and the immune response is mobilised, the viral load declines several orders of magnitude (10-100 fold) to a setpoint VL within a few months [Kaufmann1998, Richardson2003]. The CD4+ T-cell population recovers and a "quasi" steady state is attained, that is maintained for years to decades until acquired immunodeficiency syndrome (AIDS) develops [Babiker et al., 2000].

An acute paediatric HIV infection course looks very different from the one in adults. Children can acquire HIV before birth (during pregnancy) or at birth [Tobin and Aldrovandi, 2013]. In the first case they are typically born with a high viral load. In the second case, the initial phase during which the VL increases is often not observed because this phase is short and data is sparse [De Rossi et al., 1996]. Some data sets suggest that peak VL levels in infants can be up to 10 fold higher compared to adults during an acute HIV infection [Shearer et al., 1997; Biggar et al., 2001; Richardson et al., 2003]. After reaching the peak, the VL hardly contracts in young children, and high VLs are typically maintained [McIntosh et al., 1996; Richardson et al., 2003; Goulder et al., 2016]. As a consequence, an untreated paediatric HIV infection typically progresses fast, AIDS develops within 1 year, and children often do not survive their second birthday without treatment [Goulder et al., 2016].

In the literature several reasons can be found to explain these observed differences in VLs between adult and paediatric acute HIV infections. (i) A high VL peak may result from fast viral replication [De Rossi et al., 1996; Bonhoeffer et al., 2003]. (ii) HIV-targeted CD4+ T-cell densities might be higher in children compared to adults [Bonhoeffer et al., 2003]. Due to a shift in the T-cell compartment from naive towards memory T-cells, (iii) the virus tropism in a primary paediatric HIV infection might be different [Davenport et al., 2002;

Ribeiro et al., 2006], or (iv) different target cell subpopulations might be infected [Essunger and Perelson, 1994]. (v) A poor viral contraction might be explained by the immature state of immune system of children, which makes them more susceptible to infections in general [De Rossi et al., 1996; Tobin and Aldrovandi, 2013; Goulder et al., 2016].

The aim of this study is to find mechanistic explanations of why children have a lower viral contraction compared to adults. Using a conventional mathematical model for viral infection, we performed parameter sweeps to test which parameter differences between adults and children account for the observed differences in the course of an acute HIV infection. We thereby identify parameter settings accounting for the low contraction observed in children. Whenever possible, we incorporate paediatric data from the EPIICAL project (https://www.epiical.org/) to validate parameters.

Methods

Data

Longitudinal measurements from untreated HIV-positive infants are rare, particularly during the initial phase of the infection, which only last a few weeks. We were able to select 7 HIV positive children from European Pregnancy and Paediatric Infections Cohort Collaboration (EPPICC), who had at least 2 valid HIV RNA measurements available within 14 days after birth and before treatment initiation. A valid measurement was defined as detectable HIV RNA with an explicit VL. We excluded measurements at the detection limits. These measurements are considered to be taken at early time points during an acute HIV infection.

Viral replication rate

For each of these 7 children, the initial viral growth rate, ρ, has been calculated by using linear regression on the natural logarithmic-transformed VL measurements, i.e.:

$$\rho = \frac{In[V(t_2)] - In[V(t_1)]}{t_2 - t_1},$$

(5.1)

where $V(t_1)$ and $V(t_2)$ are two measurements at the two early time points t_1 and t_2. Similar to Ribeiro et al. [2010], who reported a viral replication rate around

ρ=1/day for adults, we estimated the viral replication rate in children (Equation (5.1)).

Acute HIV infection model

This study is based on a conventional model for an acute HIV infection with a target population T, early infected cells I_1, late infected cells I_2, and immune effector cells E (like cytotoxic T cells or NK cells) [Gadhamsetty et al., 2016; van Dorp et al., 2020]. As the dynamics of the virus V are much faster than those of the infected cells, a (conventional) quasi steady state assumption applies for the viral population, implying that V is proportional to I_2, i.e., $V = cI_2$. The remainder of the model is defined in terms of ordinary differential equations (ODE), i.e.:

$$\frac{dT}{dt} = \sigma - d_T T - \beta\, T\, I_2, \tag{5.2}$$

$$\frac{dI_1}{dt} = f\beta\, T\, I_2 - (d_T + \gamma)I_1 - k_1 I_1 nE, \tag{5.3}$$

$$\frac{dI_2}{dt} = \gamma I_1 - (d_T + \alpha)I_2 - k_2 I_2 nE, \tag{5.4}$$

$$\frac{dE}{dt} = p_E \frac{E\, I_2}{h + E + I_2} - d_E E. \tag{5.5}$$

Target cells, T, which can consist of CD4+ T-cells and other CD4+ cell types like macrophages, are produced at a constant rate σ, and have a death rate d_T. They are infected by virus produced by infected cells, I_2, with an infection rate β. Following Gadhamsetty et al. [2016], β is estimated from the viral replication rate ρ,

$$\beta = \frac{(d_T + \gamma + \rho)(d_T + \alpha + \rho)}{f\gamma\, \overline{T}}\ \text{, with}\ \overline{T} = \frac{\sigma}{d_T}.$$

If not otherwise stated we fixed β to 4.2×10^{-5}, which corresponds to a replication rate of ρ=1/day.

Only a fraction f of T cells infected by HIV turns into successfully infected cells I_1 [Doitsh et al., 2014]. After some time, called the eclipse-phase, here with an average length of $1/\gamma$ days, these cells turn into virus producing cells I_2 [Dixit et al., 2004]. I_1 and I_2 die at their natural death rate d_T, while productively infected cells I_2 are also affected by the virus-induced cytopathic effects, α [Markowitz et al., 2003]. Several clones of cytotoxic effector cells (n) kill I_1 cells at a rate k_1, and I_2 cells at a rate k_2 respectively. Note that the n and k parameters cannot be separated in this model and are treated as a single parameter combination. The

5

Table 5.1: Default parameter values for acute HIV infection in adults. The parameters correspond mainly to those of van Dorp et al. [2020].

Parameter	Value	Units	Explanation
σ	10^5	cells mL^{-1} day^{-1}	source of target cells
d_T	0.1	day^{-1}	death rate of target cells
β	4.2×10^{-5}	cells^{-1} mL day^{-1}	infection rate
f	0.1	-	fraction of successfully infected cells
$1/\gamma$	1.0	day	eclipse time
α	0.9	day^{-1}	virus-induced cytopathic effect
$n \times k_1$	0	cells^{-1} mL day^{-1}	killing rate of virus-producing cells
$n \times k_2$	10^{-4}	cells^{-1} mL day^{-1}	killing rate of virus-producing cells
p_E	1.1	day^{-1}	maximal division rate of effector cells
d_E	0.1	day^{-1}	death rate of effector cells
h	10^4	cells mL^{-1}	saturation constant
c	45	-	scaling parameter for viral load
ρ	1	day^{-1}	viral replication rate

division rate of immune effector cells E increases as a function of the viral load. This is implemented using a competitive saturation term defining a maximum division rate, p_E, and a saturation constant h. Effector cells E have a death rate d_E.

Models like this (5.2)-(5.5) have three steady states [de Boer and Perelson, 1998]: (1) in the absence of infection $T = \frac{\sigma}{d_T}$ and $I_1 = I_2 = E = 0$; (2) in the absence of an immune response, $E = 0$, there is a 'target cell limited' steady state of the infection; and (3) in the presence of an immune response, $E > 0$, there exists an 'immune-controlled' steady state of the infection.

The implementation of the model and the analyses were performed in R. We make use of a wrapper grind.R around the FME package for simulations of the infection course [Soetaert and Petzoldt, 2010].

Results

Acute adult HIV dynamics as default

With the parameters presented in Table 5.1, the mathematical model (5.2)-(5.5) describes a typical acute HIV infection course in adults (Figure 5.1). We initiated

the model with $T(0) = 10^6$ target cells/mL, which refers to the homeostatic level, $\overline{T}$, in the infection-free state. An infection was introduced by one infected cell ($I_1(0) = 1$). The initial value for the effector cells was set to $E(0) = 0.1$ cells/mL to allow for the expected delay of a few weeks in immune responses to a viral infection. The model was simulated for 365 days which is longer than the typical time taken to reach the setpoint VL after an acute HIV infection in adults. The viral load increases steeply, peaks and then declines towards a plateau. The decline is stepwise towards the setpoint VL. The first drop in the VL is due to target cell limitation and the second is induced by the onset of the immune response [de Boer and Perelson, 1998], which here occurs after the VL peak. The setpoint VL plateau is established by 3 months and is, in our example, around 10-fold lower than the peak value. The actual fold difference between peak and setpoint VL depends on various parameters, including the killing rate $n \times k_2$, which illustrates that adults with a broader set of cellular immune responses ($n > 1$) are expected to have a lower setpoint VL [Edwards et al., 2002; Kiepiela et al., 2007]. The here described dynamics of an acute HIV infection in adults (Figure 5.1) serve as a default and the 10 fold change between peak and setpoint VL as a benchmark to evaluate differences in the ratio of VL contraction.
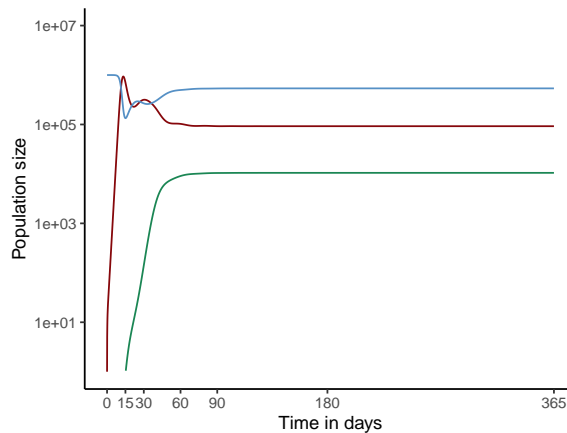
Figure 5.1: Trajectory of an acute HIV infection in adults. The course of the target cell population T (blue), the virus population V (red) and the effector population E (green) are presented. At the start of infection the target cell population is at its homeostatic level ($T(0) = 10^6$ cells mL^{-1}). Infection is introduced with 1 infected cell ($I_1(0) = 1$, $I_2(0) = 0$). Effector cells are delayed by setting the initial effector population to $E(0) = 0.1$.

Paediatric viral replication rate comparable to adults

The high VLs in children have been attributed to faster viral replication rates than observed in adults [Bonhoeffer et al., 2003]. We estimated the viral replication rate by calculating the initial growth rate from VL measurements taken from 7 untreated children (Figure 5.2). Estimating the replication rate from Equation (5.1), we find a median viral growth rate of 0.17/day (IQR=[0.01, 0.48]). In these children, paediatric viral replications rates appear to be slower than those of adults which are reported to be between 1 and 1.5 per day [Little et al., 1999; Ribeiro et al., 2010]. Although, we have only included measurements taken within the first 2 weeks after birth, we may have missed (part of) the initial growth phase since HIV infection can have occurred in utero. However, in most children the VL increases, suggesting that peak VL has not been reached and that we do capture (most of) the initial expansion phase (Figure 5.2). Hence, we have no evidence that paediatric viral replication rates are faster compared to those in adults.
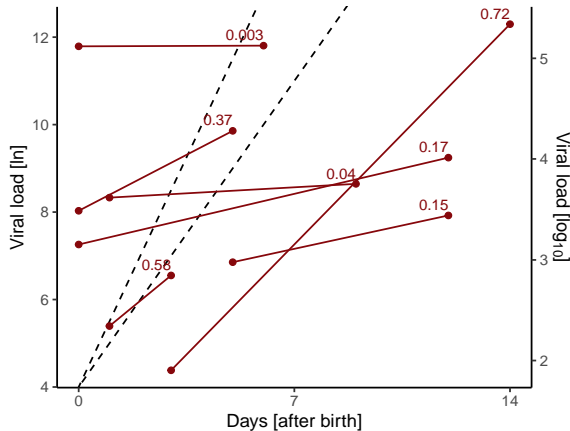
Figure 5.2: Viral replication rates in children. For 7 children untreated viral loads measured within the first 2 weeks after birth are shown, and compared to the viral replication rates of adults. Measurements (red bullets) per child are connected by a solid line. The second measurement is labelled with the estimated initial growth rate estimated by Equation (1). Adult replication rates of 1 and 1.5 per day are illustrated by the slopes of the dashed black lines [Little et al., 1999; Ribeiro et al., 2010].

Parameter sweeps to understand poor VL contraction ratio in children

Based on the "adult" acute HIV infection model (5.2)-(5.5), we took a "non-supervised" approach to investigate how different parameter settings in children could explain their poor contraction from peak to setpoint VL. We refer to this from now on as the contraction ratio, i.e., the ratio of the peak over the setpoint VL (peak/setpoint VL), which is typically high in adults and low in infants. By grouping the parameters into host-, infection- and immune-associated, we searched for parameters that markedly affect the contraction ratio. Changing one parameter at a time, we keep the remaining ones at their default values as listed in Table 5.1. The contraction ratio can change because either the peak VL and/or the setpoint VL change. We are mostly interested in explaining heightened setpoint VLs, i.e., low viral contraction ratios, even if peak VL are similar to those in adults. The setpoint viral load is reported for both the target cell limited (dashed lines) and the immune controlled steady state (solid lines in Figures 5.3-5.5).

Turnover rate of target cells results in lower VL contraction ratio

First we investigated the host-associated parameters (Figure 5.3). An adult acute HIV infection typically starts at the homeostatic state, $T(0) = \sigma/d_T$, of the CD4+ target cells. The immune system of children is immature and developing, i.e. the target cell numbers need not be in steady state. By perturbing the number of initial target cells, we mimic an immune system that is not yet in homeostasis. An increased initial $T(0)$ resulted in an increased peak VL but (obviously) had no effect on the setpoint VL. Thus, changes in ratio between the peak and setpoint VL are mainly caused by changes in peak VL (Figure 5.3A).

Assuming a homeostatic state of the target cell population before infection, and decreasing the source term σ (Figure 5.3B), or increasing the death rate d_T (Figure 5.3C) decreases the contraction ratio. However, this was also mainly due to changes in the peak VLs. Interestingly, by increasing the turnover rate of the target cell population (i.e. changing the source and death rate simultaneously, Figure 5.3D) a slightly smaller contraction ratio can be achieved, that is mainly due to an increase in the setpoint VL, while peak VL remains constant. This was mostly visible in the target cell regulated steady state, i.e., in the absence of an immune response, however.
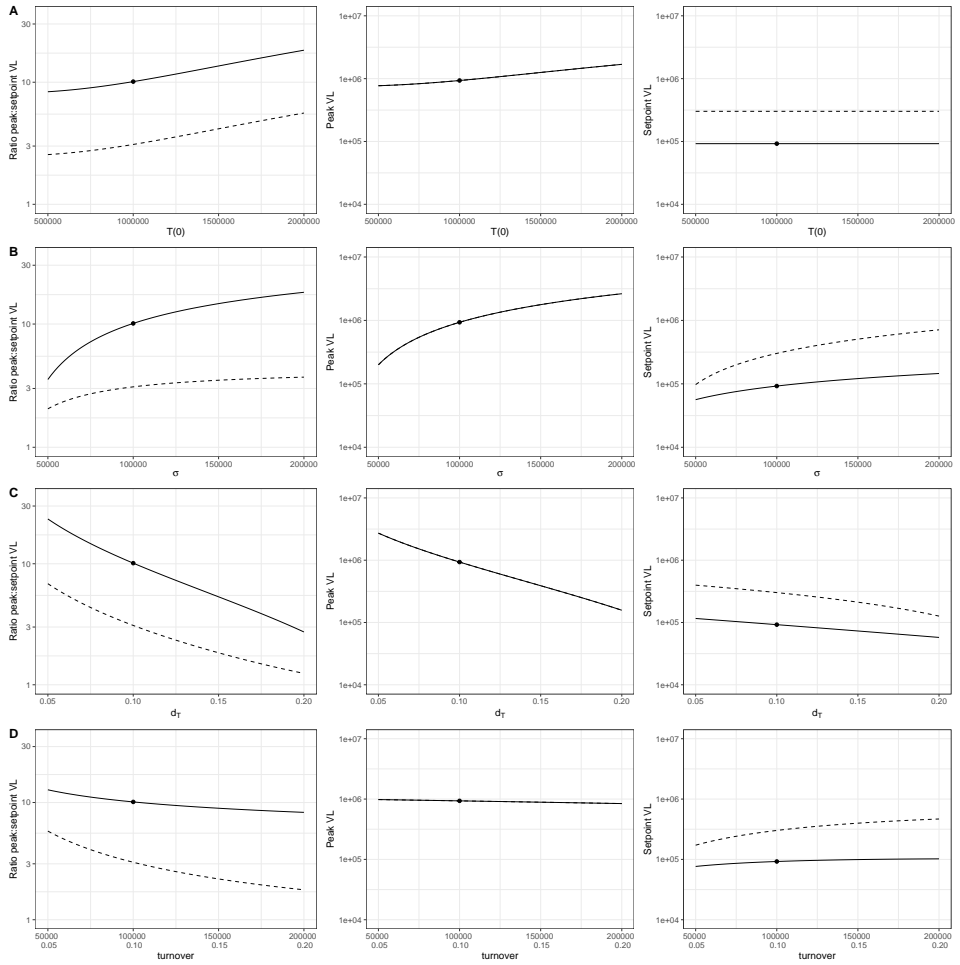
Figure 5.3: Effect of host-associated parameters. (A) Changes in initial target cell population, $T(0)$, (B) source of target cells, σ, (C) death rate of the target cell population, d_T, and (D) turnover of target cell population, $\frac{\sigma}{d_T}$, while keeping the same steady state, $\overline{T}(0) = 10^6$. Parameters are changed individually and the remaining parameters are kept at the default values in Table 5.1. The effect of the parameter sweep on the ratio peak:setpoint VL (left panels), the peak VL (middle panels) and the setpoint value taken at day 365 (right panels) are illustrated. Bullets represent the default values. The solid lines represent the immune-controlled state and the dashed lines the target cell limited steady state. Since the peak VL is largely determined by target cell availability in our model, both lines overlap in the middle panels.
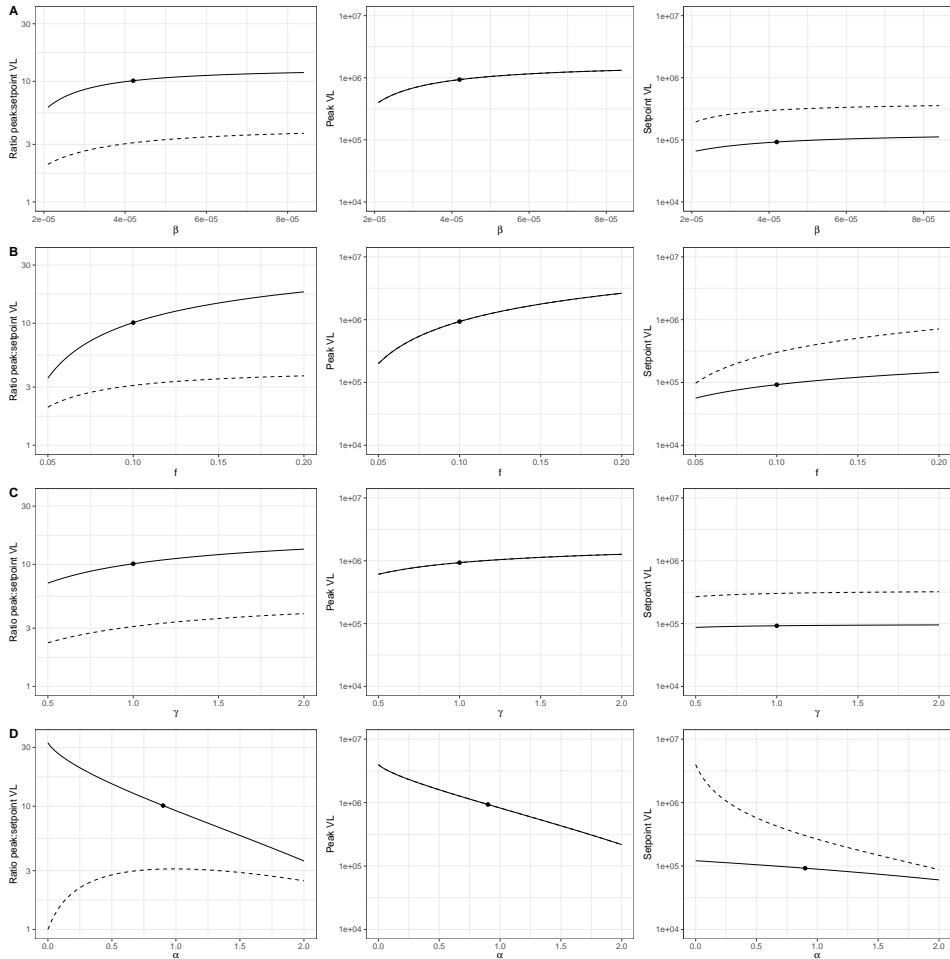
Figure 5.4: Effect of infection-associated parameters. (A) Changes in infection rate (β), (B) fraction of successfully infected cells (f), (C) duration of eclipse phase (γ), and (D) virus-induced cytopathic effect (α). Parameters are changed individually and the remaining parameters are set to the default values in Table (1). The effect of the parameter sweep on the ratio peak:setpoint VL (left panels), the peak VL (middle panels) and the setpoint value taken at day 365 (right panels) are illustrated. The bullets represent the default values. The solid lines represent the immune-controlled state and the dashed lines the target cell limited steady state. Since the peak VL is largely determined by target cell availability in our model, both lines overlap in the middle panels.

Non-cytopathic virus can damp the VL contraction ratio

Second, we investigated the infection-associated parameters (Figure 5.4). We perturbed the infection rate (β, Figure 5.4A), the fraction of successfully infected cells (f, Figure 5.4B), duration of eclipse phase (γ, Figure 5.4C), and the virus-induced cytopathic effect (α, Figure 5.4D). Decreasing the parameters β and γ reduces the VL contraction ratio, but this was once again mainly caused by a decline in the peak VL. The setpoint level itself hardly changed (Figure 5.4A/C). The setpoint VL slightly increases by increasing the fraction of cells becoming infected (f), but this had almost no effect on the VL contraction ratio - at least not in the target limited scenario - as peak values increased simultaneously (Figure 5.4B). Decreasing the cytopathicity α resulted in increased setpoint viral loads. While in the immune-controlled scenario the contraction ratio increased, the target cell limited scenario showed the opposite effect, and the VL contraction ratio decreased, despite the same peak VLs (Figure 5.4D). A virus with almost no cytopathic effect of the virus dampens the contraction ratio towards one in the absence of an immune response.

Immune response is the most parsimonious explanation for poor VL contraction

Finally, we investigated the parameters associated with the immune response (Figure 5.5). As already seen in Figure 5.3 and 5.4, the absence of immune responses (target cell limited scenario, $E = 0$) had a dominant influence on the contraction ratio. Changes in the parameters associated with the immune response confirmed these observations. A lower division rate (p_E, Figure 5.5A), a higher sensitivity to recognise antigens (h, Figure 5.5B), a reduced killing rate or fewer numbers of effector cells ($n \times k_2$, Figure 5.5C), as well as a shorter expected life time of the effector cells (d_E, Figure 5.5D) led all to a reduced ratio between peak and setpoint VL. As peak values remained similar, the lower contraction ratio was mainly due to the increase in setpoint VLs. Thus, reduced immune responses in children appear to be the most parsimonious explanation for a low contraction ratio in VL.

Discussion and Conclusion

An acute HIV infection in children is known to be very different from that in adults, as children tend to have a high VL and do not show the typical contraction towards a markedly lower setpoint VL [Richardson et al., 2003; Goulder et al., 2016]. Via parameter sweeps in an viral infection model, we here showed
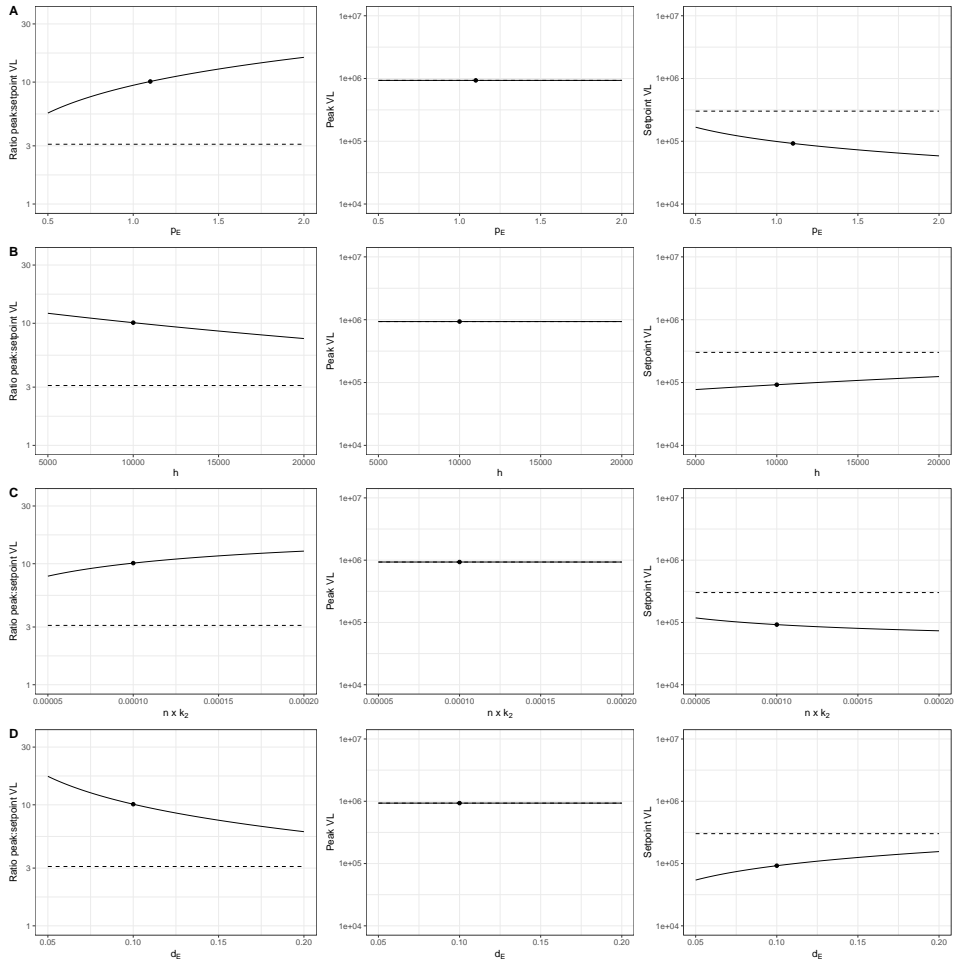
Figure 5.5: Effect of immune-associated parameters. (A) Changes in division rate of effector cells (p_E), (B) Michaelis Menten constant (h), (C) killing rate ($n \times k_2$), and (D) death rate of effector cells (d_E). Parameters are changed individually and the remaining parameters are set to the default values in Table (1). The effect of the parameter sweep on the ratio peak:setpoint VL (left panels), the peak VL (middle panels) and the setpoint value taken at day 365 (right panels) are illustrated. The bullets represent the default values. The solid lines represent the immune-controlled state and the dashed lines the target cell controlled steady state. Since the peak VL is largely determined by target cell availability in our model, both lines overlap in the middle panels.

that the low contraction ratio in children is readily explained by an immature state of their cellular immune response, and not easily by any other factors. A higher turnover rate of the target cell population, as well as lower cytopathic effects of the virus, also reduce the contraction ratio without increasing peak VLs, but only in the absence of an immune response. We therefore identify a poor early immune response as the most parsimonious factor explaining the poor contraction that is typically observed in paediatric HIV infection.

High setpoint VLs have been postulated to be due to high viral replication rates [De Rossi et al., 1996; Bonhoeffer et al., 2003]. We were unable to confirm that the viral replication rate is faster in children compared to adults. The initial HIV viral growth rate in adults has been estimated to be 1-1.5 per day [Little et al., 1999; Ribeiro et al., 2010], which is similar to that during an SIV infection in macaques [Nowak et al., 1997]. By calculating the initial viral growth rate of 7 untreated children, we could not find any evidence for higher viral replication rates compared to adults. We are limited to only a few infants in our dataset, and that maternal HIV treatment might affect our results (explaining the slow viral replication rates), but none of the 7 children would support a replication rate higher than 1 per day as observed in adults [Ribeiro et al., 2010]. Since pre-ART measurements in children are sparse, it is difficult to improve upon this analysis, and the data provide at least no evidence for the hypothesis that HIV replicates faster in young children. Interestingly, Nagaraja et al. [2021] reports that the reproductive ratio R_0 increases with age in children of 0 to 17 years old. Since this calculation is mainly based on the ratio of CD4+ T-cell counts in healthy and HIV-infected children, which is somewhat indirect, we find it difficult to compare this to our more direct measure of viral replication rate. Measurements taken during untreated paediatric HIV infection course will remain rare because most infants who are sampled are also treated. Hence, further insights into natural acute paediatric HIV infections can only be obtained from existing experimental material, or by mathematical modelling. Using the latter, we provide a mechanistic understanding for the poor viral contraction seen in most paediatric HIV infection.

There is ample experimental evidence that the CD8+ cellular immune response plays an important role in controlling HIV infections in adults, and in controlling SIV infections in macaques [McBrien et al., 2018]. For instance, a recent study showed that HIV-specific CD8+ T cells become functionally impaired in HIV infected individuals who spontaneously controlled the virus but then show an aborted viral control [Collins et al., 2021]. The depletion of CD8+ T cells during

acute and chronic SIV infection has a major effect on the viral load [Schmitz et al., 1999; Cardozo et al., 2018]. Importantly, there is hardly any contraction of the SIV VL when CD8+ T cells are depleted in the initial phase of the infection [Schmitz et al., 1999], which mimics the poor contraction of the HIV VL that is typically observed in children. Moreover, it is typically hard to find HIV-specific immune responses in young children living with HIV [Palma et al., 2015]. Also for other viruses like CMV, influenza, and RSV, it is known that very young children show poor immune responses. Indeed, the VL contraction ratio is increased in somewhat older children that become infected with HIV [Richardson et al., 2003]. These observations are in good agreement with our postulate that the poor VL contraction ratio in paediatric HIV infection is due to a late and/or poor immune response.

In conclusion, an immature cellular immune response in infants readily explains their poor control of an early HIV infection. As a high setpoint VL is a strong predictor for fast disease progression, this also explains why untreated infants progress fast towards AIDS, and why it is important to control the virus as fast as possible.

Author Contributions

JS performed the mathematical analysis and drafted the manuscript. RJdB supervised this project and contributed to the final version of this manuscript. JS and RJdB conceptualised the study, discussed and interpreted the findings together.

Acknowledgements

6

General Discussion

At this point of time, children born with HIV rely lifelong on antiretroviral drugs to control their HIV infection and to prevent further progression towards AIDS. As part of the EPIICAL project, which is concerned with the improvement of the life of children with HIV, the research presented in this thesis has aimed to quantify paediatric HIV infection courses and response kinetics to early treatment initiations. The presented results could help with the selection of potential candidates for alternative treatment strategies, as a replacement or an addition to conventional ART. Mathematical models have been developed that describe VL and CD4+ T-cell dynamics for every child individually to gain more insight into the differences among children.

In **Chapter 2**, we have focused on the viral decay dynamics of children who perinatally acquired HIV and started early treatment within 6 months after birth. We have characterised their viral decay patterns and quantified time to viral suppression individually. Based on the VL and the percentages of CD4+ T cells of every individual child at start of treatment, we have been able to predict their TTS, provided these children have not experienced any treatment complications. Unexpectedly, we could exclude age as an additional factor associated with TTS. As we studied a very young population of children who all acquired HIV around birth, an independent contribution of age has been difficult to verify. Age is hardly different from the time since infection in these children.

To further study CD4+ T-cell reconstitution in response to early-initiated treatment, we have developed normalisation functions for the natural dynamics of T-lymphocytes over age in **Chapter 3**. Based on cross-sectional studies of healthy individuals, both T-cell counts and percentages of the same lymphocyte subsets have been described by a consistent set of parameters. We have considered the experimental procedures of how the measurements were gained in the fitting procedure. A special focus has been dedicated to the dynamics during the first year of life, in which the maturation of the immune system shows the major developmental progresses in the different lymphocyte compartments, which has not been mathematically captured in such a large extent beforehand. For example, CD4+ T cells do not follow the known natural decline during the first half a year but rather initially increase. Thus, we have provided new normalisation function for T-lymphocytes and their subsets for the purpose of quantification.

Chapter 4 refers back to the same population as already studied in Chapter 2, and has investigates the CD4 recovery dynamics of successfully early-

treated children with viral suppression. CD4+ T-cell measurements have been normalised to the functions provided in Chapter 3. We have showed that CD4+ T cells recovered "fully" towards healthy levels during treatment. The recovery levels and the time to reach these levels appear once more to be age-independent. The recovery rates correlate negatively with the CD4+ T-cell levels at start of treatment, thus we have concluded that the CD4 recovery process is partly density-dependent. The recovery of both CD4+ T-cell counts and percentages occur in parallel. An inconsistent VL suppression results in a delayed CD4 recovery, but very early treated children with HIV seem to still achieve "healthy" CD4+ T-cell levels once the VL is in control.

The results of Chapter 2 and 4 together have indicated that VL and CD4+ T-cell levels at start of treatment have a major influence on the viral and immunological response kinetics in very young perinatally HIV-infected children. As both values, VL and CD4+ T-cell levels, are associated with the progression of the disease, the untreated paediatric HIV infection course is further investigated in the hypothesis driven **Chapter 5**. As children show a fast disease progression towards AIDS, and additionally have high VLs in the absence of treatment, we have questioned which mechanisms best explain these high VLs and the connected poor contraction between peak and setpoint VLs. We have identified a weak infant immune response to be the most parsimonious explanation for the observed phenomena in a paediatric HIV infection course, indicating that early treatment is essential to support the infant immune system and for the child's survival.

Throughout this thesis, we have focused on a very specific study population: early treated perinatally HIV-infected children with successful treatment. In the following discussion, we highlight the special features of this population, and zoom out to discuss in which way the knowledge gained from this special target population may help paediatric HIV research in general, especially in consideration towards a functional HIV cure. We assess how the knowledge gained in the context of this thesis can be transferred and further developed.

Study population defined by three "earlies"

In contrast to previous studies of paediatric HIV data (on the same cohorts) [Lewis et al., 2012; Picat et al., 2013; Lewis et al., 2017; EPPICC and EPIICAL, 2019], we were very selective with the choice of our study population. This was necessary as we

tried to get a better insight into the viral and immunological kinetics of very young children, starting treatment early after a perinatally acquired HIV infection and achieving a successful control. While epidemiological and statistical studies provide population-based averages to describe responses to treatment and focus on special events in time, like time to viral suppression or CD4+ T-cell levels after 5 years on treatment, mathematical modelling focuses on (individual) longitudinal measurements and their dynamics explaining these special events in time [Nowak and May, 2000; Hill et al., 2018]. This also validates the subtitle of this thesis: Taking care of every child. To be able to quantify these individual dynamics with a simple mathematical model, we require a well defined study population. Co-founding effects, such as transiently poor adherence of treatment, are not captured by these models, and would lead to incorrect parameter estimates. Thus, trajectories of children who are not suppressing the virus, are excluded. Consequently, we can define our study population by three "earlies": early in age, early in treatment, and early in controlling the virus. Let us discuss these three "earlies", considered throughout this thesis, in somewhat more detail.

Early age - Studying an infant's immune system

Infant studies are required to account for immunological differences compared to adults

A healthy infant's immune system is very different from that of an adult, it is immature and under development. The maturation itself is not yet well understood. An infant immune system is functional but in a different way than in adults [Thapa et al., 2021]. Children show good immune responses to vaccination, and have the potential to develop better long-term immunity, while an acute viral infection is more difficult to fight compared to adults, which might explain their fast progression to AIDS. The knowledge about the developmental processes of the immune system is still in its early stage. An infant immune system is very dynamic, components change, and compensations between subsets occur [Ygberg and Nilsson, 2012]. These natural immune processes are much more prominent in childhood than in adulthood. We get a glance of this in Chapter 3, when we provide normalisation functions for T-lymphocytes through age in healthy individuals. Next to the natural decline in cell numbers over age, we find an increase in T-cell numbers, while zooming into the the first 6 months of life. These characteristics of an infant immune system have to be considered while studying disease dynamics.

An immature immune system provides a different environment and sets different conditions than an adult immune system, which influences the courses of an infection. Consequently, disease progression and recovery rates might differ. In terms of a paediatric HIV infection, the route of transmission differs, for example. Thus, the virus is not only confronted with an infant immune system but also enters a totally different immunological environment. Very young children are known to tend towards immune tolerance [Ygberg and Nilsson, 2012]. On the one hand, immunological tolerance is required to prevent an over-reactivity of the immune system in newborns, as they are born from an almost sterile uterus into a pathogenic environment. A sudden large response to multiple pathogens at once would overstimulate the infant system and may lead to death, as an infant immune system cannot yet resort memory responses [Levy, 2007]. On the other hand, immunological tolerance facilitates the fast establishment of an infection, as specific immune responses are missing and require time to be built up [Tobin and Aldrovandi, 2013]. This explains why infants are highly susceptible to infection in general (e.g. RSV, influenza, and CMV infection have often a more severe course in infants than seen in adults or somewhat older children), and why children with acquired HIV infection barely show any HIV-specific immune responses [Payne et al., 2015; Liu et al., 2016]. The results drawn in Chapter 5 are in line with a poor or delayed onset of an HIV-specific immune response, and might explain fast disease progression in paediatric HIV.

Additionally, the major target cell populations in infant's remain ill defined. In children naive CD4+ T cells may be better targets than in adults [Davenport et al., 2002; Ribeiro et al., 2006]. Infants are known to have a higher thymic output, their T-cell compartments exist mainly of naive cells (see Chapter 3) with higher turnover rates, which would be beneficial for viral reproduction [Davenport et al., 2002; Fraser et al., 2014]. Also, macrophages are potential target cells, as they also express the CCR5 receptors which HIV requires to enter cells [Koppensteiner et al., 2012; Davenport et al., 2002]. We touch on this in Chapter 5 by keeping the definition of the target cell population broad. However, in terms of early treatment initiation, the faster turnover of CD4+ T cells might enable an infant immune system to more rapidly recover from the damage caused by an HIV infection. Additionally, a developing immune system also might have the potential to establish long-term immunity, for example, induced by vaccinations administered at a proper age. We will come back to this when considering potential ways towards a cure. Thus, infants who receive treatment early are typically considered as a unique target

6

population with the ability to recover (see Chapter 4) from an HIV infection "fully" .

There are, however, large differences between children, and the dynamics underlying these observations remain elusive. The maternal immune system might influence and help to shape an infant's immune system during pregnancy and breastfeeding. Its contribution is, however, beyond the scope of this thesis. In future studies, it might be of interest to also include the maternal HIV status and immunological conditions. Many assumptions and conditions based on an adult immune system, such as the homeostasis of cell numbers, are not yet valid and therefore not applicable for an infant immune system. Hence, we are dealing with a highly dynamical system, which seems to be very diverse when breaking it down to the individual child. This makes infants a very interesting but also challenging study population in general, particularly in the context of a disease. Consequently, results drawn from adult HIV research are not always transferable to infants. Separate studies focused on infants, like those represented in this thesis, are required.

Accessing infant data for modelling purposes is not straight forward

In general, immunological insights in infants are lacking behind the information obtained from adults. This has been just recently seen during the *Coronavirus SARS-CoV-2* (COVID-19) pandemic, during which children first were not considered as transmitters of the virus, as they often show an asymptomatic infection course, and a vaccination for infants has still not been released 1 1/2 years after the authorisations for vaccination for adults [European Medicines Agency, 2022]; similar is true for HIV infection, even though HIV is already around for more than 40 years. General paediatric HIV infection courses are known, but detailed quantitative information has been missing. This thesis tries to fill the gap.

Newborns are a vulnerable, and very rare study population. Immunological studies on infants are mainly conducted in the case of a disease. Thus, there is barely any information available about the "healthy" development of an infant immune system, which would provide a norm in studying disease. Additionally, biological specimens for laboratory measurements are quantitatively limited. For example, less amount of blood can be taken from infants than from an adult per individual blood extraction, which also have to occur in greater time intervals. Furthermore, the setting up of infant studies often faces greater ethical obstacles, because they are more vulnerable than adults and the fear to cause lifelong damage is greater. The set up of a new study requires years of planning, ethical agreements and approvals. For these reasons, it is difficult to gather

immunological infant data and in general it is even more complicated to gain access to longitudinal data for the purpose of mathematical modelling. We have been lucky to be part of the international and interdisciplinary EPIICAL consortium, in which data sharing and mathematical analysis has been simplified.

Handling sparse clinical and immunological data

Nevertheless, the data we have worked with bears its limitations. The data we have analysed in Chapters 2, 3 and 5 are from observational cohort studies. The available longitudinal data was not explicitly collected for the purpose of mathematical modelling, and is rather a collection of data from children whenever they have visited the care units. Consequently, regular measurements were not available and the time intervals between the measurements varied. Often informative and important measurements at birth and/or baseline measurements at start of treatment initiation were missing, and had to be extrapolated. Additionally, CD4+ T-cell and VL measurements are not necessarily available at the same time point. While CD4+ T-cell measurements belong to standard measures in the field of HIV, VL data is often costly, and are not always obtained. VL measurements are often only acquired at points of interest, such as the time of immunological failure. Furthermore, VL measurements are not always given in absolute numbers as they are constrained to the upper and lower detection limits of the assays. As assays have become better over the years, their limits of detections varies, and we had to deal with different limits of detections in the cohort data reaching from 400 copies/mL to 20 copies/mL at the lower bound. These constraints had to be considered during modelling, aggravating the modelling process and introducing a certain inaccuracy in the results. New diagnostic tools dealing with small amount of blood are in development, which might help to gain more accurate and reliable infant data in the future [Tuaillon et al., 2020]. To be able to obtain appropriated parameter estimates, we had to ensure that sufficient qualitative and quantitative measurements were available per individual child, leading to a drastic re-duction of the number of children in the cohorts suitable for modelling purposes.

We are using a second dataset in Chapter 4 including cross-sectional data from healthy individuals. Our analysis would have benefited from longitudinal data, but who would prick someone's newborn every week for several months, if there is not really a need for. Moreover, even though T-lymphocyte counts and percentages were given in the dataset, we had to carefully track how these numbers have been generated, because typically only percentages have been

truly measured. In immunology the obvious reference cell populations are often not indicated, which makes it difficult to follow the generation process to obtain the counted data. As counts and percentages depend on each other, it was important for us to also reflect this in the normalisation function given in Chapter 4. Summarising, we have tried our best to "squeeze" the available datasets as much as possible to make them usable for modelling purposes, and to gain new biological insights.

Early treatment - How much harm has been done by the virus?

Benefits of early treatment initiation

In Chapter 2 and 4, we showed that children who started treatment within their first 6 months of life are mostly able to suppress the virus, and also seem to be able to regenerate their immune system fully (at least in numbers). So what are the actual benefits of early treatment initiation in terms of the HIV infection? At an early stage of an HIV infection, HIV has had only limited time to infect target cells, to reproduce, and to mutate. Thus, the latent reservoir, which is already seeded within the first few days of an HIV infection – and is therefore the major hurdle to an HIV cure – can remain relatively small and uniform [Palma et al., 2015; Millar et al., 2021]. Furthermore, the damage caused to the immune system may still be limited. Hence, early initiated treatment stops the HIV infection at a very early stage, which sets the optimal conditions for further treatment interventions, as seen in non-human primates benefiting from early interventions [Terrade et al., 2021].

Early treatment initiation requires early diagnosis

Treatment can, however, only be initiated early, when HIV infection has been detected very early. In contrast to adults, the time of infection can be determined more easily in infants. As HIV testing belongs nowadays to the standard of care for pregnant women, newborns born to an HIV-positive mother are rigorously tested for HIV, and once diagnosed are treated immediately. Antiretroviral prophylaxis is sometimes administered to infants born to HIV-positive mothers with undetectable VL, meaning that an infant receives antiretroviral drugs during the first weeks after birth, even though HIV has not yet been documented [National Institutes of Health, 2022]. This, nevertheless, bears the risk that an HIV infection of a child remains undetectable, and cost intensive deep sequencing

techniques to detect viral genetic material would be required to take an infant safely off the prophylaxis again. Consequently, some HIV negative children are kept on antiretroviral drugs while there is no need for treatment. Thus, an early diagnosis is essential to allow for early treatment initiation.

In the EPPICC cohort studies we selected children who started ART within 6 months after birth, which is in principle already quite late for early treatment initiation, considering that HIV reservoir builds up within few days after infection. We were faced with the constraint that the data was collected before the era of early treatment initiation, which has its start in 2008 with the first publication of the CHER study [Violari et al., 2008]. Hence, those children receiving ART early within EPPICC might have suffered from a progressed stage of the disease, and/or might have had very low CD4+ T-cell numbers, justifying early medical intervention. Although we could show that children were not been biased towards low CD4+ T-cell levels in our study of Chapter 2, we cannot completely exclude medical necessities and health complications for the initiation of ART in this selected subpopulation we have studied. Our results are, however, in line with the study of Morris et al. [2020], in which the viral decay dynamics of infants who started ART within 2 days after birth have been analysed. This data originated from a more recently collected study (LEOPARD) which follows the most recent guidelines for early ART initiation in infants [Kuhn et al., 2020]. Both our studies [Schröter et al., 2020; Morris et al., 2020] are following comparable analysis and modelling procedures. Thus, we have little concern that our results are strongly biased by children with fast progressing HIV infection.

Is age by itself a mechanism?

The age at treatment initiation is often highlighted as a predictor for fast VL suppression [EPPICC and EPIICAL, 2019] and for better CD4+ T-cell reconstitution [Lewis et al., 2012]. An independent contribution of age is, however, difficult to verify in our subset of infants starting ART below 6 months of age (Chapter 2 and 4), as our age range of only 6 months is very narrow. In Chapter 3, we showed how difficult it is to get good estimates for T-cell counts during the first 6 months. The overall initially increasing dynamics could also be described by a flat phase, as the observed trajectories may vary per individual, and considerably for children younger than 6 months. The VL and CD4+ T-cell dynamics also vary with age while the HIV infection further progresses (Chapter 2). As age is highly linked to time of infection, which occurs around birth, an independent age effect is difficult to disentangle from normal disease progression. Thus, even if there is a

correlation, age by itself does not need to influence VL suppression and CD4+ T-cell reconstitution mechanistically.

Nevertheless, some children may have been infected before birth. Accordingly, they would have a longer time of infection than their actual age. Unfortunately, we do not have any information about the time of infection. VL and CD4+ T-cell measurements at birth are often the only indication informing us about the stage of disease progression. Similar to Equation (2.2) predicting when viral suppression is expected after treatment initiation (Chapter 2), a formula predicting time of infection would be needed. Studies particularly focused on time of infection at birth, such as distinguishing in utero from intrapartum infections, and substantial collection of baseline measurement and information, such as those of Kuhn et al. [2020] or Millar et al. [2021], might be more appropriate to establish whether or not age provides an independent contribution to HIV progression. In our dataset age and time of infection remain difficult to disentangle.

Future studies factor in mathematical modelling of data

Within the EPIICAL consortium we have been able to highlight the necessity of regular and precise measurements for the purpose of mathematical modelling, and have reached consensus on the importance of mathematical modelling to gain further knowledge about the viral and immunological response dynamics to early initiated ART in infants living with HIV. Particularly, we have acknowledged the requirement of measurements in regular time intervals directly after treatment initiation, as these measurements hold valuable and informative insights about VL multiphasic decay dynamics. We are aware that this kind of data is difficult to gather from a clinical and ethical point of view, but assays are becoming better and better, which may make it more feasible to gain more informative immunological data from an infant study population. We also advocate a close collaboration and interdisciplinary communication to advance progress and outcomes towards an HIV cure in the field of paediatric HIV.

Over the last 5 years, we have witnessed the planning and setting up of a new study – Cohort of **E**arly **A**nti-**R**etroviral **T**reatment in **H**IV-infected Children (EARTH) – by the EPIICAL project [EPIICAL, 2022]. A well established interdisciplinary collaborations has led the way to this study, where we contributed from a mathematical modelling perspective. EARTH is a prospective multi-centre cohort study expected to involve 300 newly diagnosed HIV-positive perinatally infected children who start early ART early in life and are following the local standard of care. These children will be followed until they reach the age of 4, and clinical,

virological and immunological features are regularly monitored and collected. These observations should help to identify and characterise a proportion of early-treated children having excellent viral and immunological HIV control, and may become potential participants in proof-of-concept trials directed towards an HIV cure. Since 2018, 150 children have been enrolled at 5 sites in South Africa and Mozambique, and regular measurements from birth onwards are taken (birth, 2 weeks, 2 month, ...). The data collection is still ongoing, and data analysis and allocation are centralised; a platform is created to allow data access for researchers of different disciplines.

Early control - Keep the viral exposure time to a minimum

Characterising "ideal" responders to ART

Treatment should not only start early, it should also be effective. With effective, we mean that an early control of the virus is achieved. Throughout this thesis we, therefore, mainly consider children with a "clean" VL decay pattern, and only investigate the period of successful control. However, clean viral decay patterns are not the norm. We have marginally discussed erratic VL decay patterns, and have excluded periods of rebounds completely. One could criticise that we were too selective with the choice of our study population. For instance, a one time detectable viral load after achieved viral suppression, a so called VL blip, need not be a reason of concern. However, in this thesis we aimed to describe the viral and immunological dynamics in response to successful treatment on an individual basis to characterise the good responders. For this reason, a clearly defined study population was required. Other studies might ask more population based questions like, do children respond to treatment, and what are the predictors for fast viral suppression or recovery. These kind of studies consider a broader population and should not be as selective as we were. In Chapters 2 and 4, we could clearly identify two categories, clean and erratic children, with different properties in suppressing the virus and in recruiting the immune system. The erratic subset is characterised, at least partly, by poor treatment adherence, which is a co-founder effect that we do not aim to model. Thus, we tried to exclude the obvious cases of children with treatment complications, to receive a clearer picture of the dynamics in a well-defined study subset.

Sustained viral suppression before interruption

Planned treatment interruption is a highly debated topic. Currently, treatment interruption is the only way to judge whether or not a child will show treatment-free HIV control. However, only a few children experienced successful treatment interruption and remained untreated since then [Persaud et al., 2013; Sáez-Cirión et al., 2013; Luzuriaga et al., 2015; Frange et al., 2016; Violari et al., 2019]. Thus, the success of such interventions remain disappointing. In the CHER trial, interruption was introduced even before children fully controlled the virus while on ART [Violari et al., 2008; Cotton et al., 2013]. Although the context between successful viral suppression, and its impact on interruption is still unclear and not well studied, we would favour a reliable viral suppression before considering ART interruption. We would advise against a "blind" ART interruption at a given time after ART initiation, as was done in the CHER study. Rather, virological and immunological dynamics should be considered to determine possible interruptions and to coordinate its timing. The CHER dataset would allow one to conduct further studies of early treated children in combination with ART interruption. The timing of such interruptions needs to be addressed in future studies, as every child is different and at the current stage the timing of ART interruption was predefined.

Unsuccessful treatment interruption defeats gained benefits

Unsuccessful treatment interruptions may ruin the advantages gained from an early intervention, such as a less impacted immune system and a reduced reservoir. Instead, the virus gains the opportunity to prevail again. Ensuring that children on ART are able to successfully suppress the virus, and to also maintain viral suppression during ART, should remain our primary aim before thinking about treatment interruptions. A study by Morris et al. [2022] investigated HIV resurgence dynamics in perinatally-infected infants on antiretroviral therapy. Our function describing T-cell recovery dynamics (see Chapter 4) have been used in their model to successfully predict resurgences of VL during treatment. Taking this together favours a continuous ART, which is currently also advocated in paediatric HIV research [National Institutes of Health, 2022]. However, long term effects of ART on the development of infants seem to be harmful. Hence, we need safe methods to allow children, for example, medical controlled ART holidays, and to be able to identify those children, in which ART may have become unnecessary.

Outlook - the next steps towards a potential HIV cure in early treated infants

Early recovery - maintaining long-term viral control off ART?

While an early age of infection is a given, an early treatment initiation can be influenced, and the question remains how one achieves an early recovery from HIV infection in infants. Enabling this "fourth early" for children living with perinatally acquired HIV would reflect the ideal scenario hoped for by the research community and by the EPIICAL project (aiming to improve the actual life for children living with HIV). Complete elimination of HIV will remain difficult, as the seeding of the viral reservoir occurs already very early on in the HIV infection course [Frenkel et al., 2003; Joos et al., 2008]. In this thesis, we have not considered the viral reservoir. Because the HIV reservoir is the major obstacle in HIV cure research, novel treatment strategies should aim at controlling the reservoir. The main strongpoint of early treated infants is that their latent reservoir is relatively small and limited [Okoye et al., 2018; Tagarro et al., 2018a; Garcia-Broncano et al., 2019; Millar et al., 2021]. The analysis of reservoir data has gained more and more importance over the last years, and it has been suggested that an established reservoir declines during continuous and longterm ART [Luzuriaga et al., 2014; Veldsman et al., 2019]. Part of the reservoir consists of non-functional virus [Jiang et al., 2020]. Longitudinal reservoir data is still rare, but further reservoir studies are currently being undertaken by several cohorts of infants with early initiated ART [Violari et al., 2008; Ibrahim et al., 2018; Violari et al., 2019]. Thus, in the coming years mathematical modelling of reservoir data combined with traditional viral and immunological data may provide new insights in their interactions and dynamics over time.

To understand, we have to be even more selective

A small group of children are successfully controlling HIV. These children were exposed to HIV during pregnancy, but were either not infected (HEU children), or were able to sustain the virus at undetectable levels by staying ART-naive (elite controllers) or after ART interruption (non-progressors), and do not show any further progression towards AIDS [Vieira et al., 2022]. This subset of children is of special interest, as they would fulfil the criteria for a functional HIV cure. Similar to the original host of HIV - sooty mangabeys - this selective subset of children either has a high VL but their immune system seems to ignore the

presence of the virus, such as in the case of non-progressors, or the immune system effectively keeps the virus at bay, as in the case of elite controllers. It would be of importance to properly profile the viral and immunological dynamics of these children, as well as the functionality of their T-cells, to learn about the underlying mechanisms, and to learn what would be required for achieving prolonged viral control, or immunological ignorance towards HIV, in early-treated children.

Helping the immune system of infants

Perinatally HIV-infected children treated with suppressive ART from early infancy face, the best conditions for achieving a potential HIV cure with little consequential damages. Their immune system is barely impacted and normal neurodevelopment seems to be possible [Laughton et al., 2019]. The critical point remains the taking off of the ART. An early onset of ART clearly has its benefits but may also prevent the immune system to get activated and to develop long-term immunity against HIV. A CHER analysis has shown that HIV-specific antibodies are reduced, or cannot be detected in early treated children [Payne et al., 2015]. On the downside of perinatally acquired HIV infection, an infant immune system is less equipped to fight the infection during the acute phase (see Chapter 5), nor well prepared to fight rebounding virus after an early onset of ART. Thus, the infant immune system requires help.

Novel treatment strategies may help the infant immune system to recognise and fight HIV. Childhood vaccinations are a promising avenue to establish long lasting immunity, that in HIV-infected children would be "therapeutic vaccinations". Additionally, in non-human primates, broadly neutralising antibodies (bNAb) have shown success in keeping the virus in control when ART is discontinued [Terrade et al., 2021]. Further research into this alternative treatment strategy is required, particularly the effect on supporting the immune system should be considered.

Taking the results presented in this thesis together, early-treated perinatally HIV-infected children who have not yet progressed in their disease, and successfully responded to their treatment, might be candidates for future novel medical implementations. The hope for an HIV cure is on the horizon, but at this stage it is too early to say that it is indeed achievable.

Concluding remarks

This thesis provides new measures to characterise viral and immunological response kinetics in infants with HIV starting successful early ART. Disease progression at start of treatment results in differences in the response kinetics towards HIV suppression, and impacts the reconstitution of the affected immune system. As an infant immune system is immature and highly dynamic, it seems to have the potential to "fully" recover from an early HIV infection with the help of treatment. Since the immune system typically fails to control HIV by itself, we need to control the viral reservoir, and early treatment initiation is essential and required. To enable an HIV cure, the immune system probably requires support in the form of novel strategies, which have to be timed precisely.

With studying a paediatric population we have chosen a tricky population to model. Data is often sparse and we have little knowledge about the development of the immune system. More information about the early state of life and the maturation of the immune system is required. This becomes even more complicated when studying the immunological kinetics of diseased children. Hence, the quantification of the early development of the human immune system remains an important area of research.

Quantification using mathematical models relies on experimental data, however. The more data becomes available, the better we can identify the parameters of the system, and the better the underlying biological process can be described. As we were working with infants, we were faced with a population, for which accessing data is connected with considerable ethical constraints. Thus, experiments cannot be easily designed and conducted. This may explain why there is little mathematical modelling on data of infants with perinatally acquired HIV. Therefore, it is important to have consortia like the EPIICAL, in which research communication occurs between different disciplines and interdisciplinary collaborations emerge. There is often more in collected data than one discipline can make use of, and next to the general summary statistics, it is worth looking at the data from a mathematical perspective, as modelling every individual child mechanistically allows us to better understand heterogeneity of their dynamics, and hence their future treatment options.

6

Appendix

The EPPICC cohorts:

Belgium: Hospital St Pierre Cohort, Brussels: Tessa Goetghebuer, MD, PhD; Marc Hainaut, MD PhD; Evelyne Van der Kelen, Research nurse; Marc Delforge, data manager.

France: French Perinatal Cohort Study/Enquête Périnatale Française, ANRS EPF-CO10. Coordinating center, INSERM U1018, team 4: Josiane Warszawski, Jerome Le Chenadec, Elisa Ramos, Olivia Dialla, Thierry Wack, Corine Laurent, Lamya Ait si Selmi, Isabelle Leymarie, Fazia Ait Benali, Maud Brossard, Leila Boufassa.
Participating sites (hospital name, city, main investigator): Hôpital Louis Mourier, Colombes, Dr Corinne Floch-Tudal; Groupe Hospitalier Cochin Tarnier Port-Royal, PARIS, Dr Ghislaine Firtion; Centre Hospitalier Intercommunal, Creteil, Dr Isabelle Hau; Centre Hospitalier Général, Villeneuve Saint Georges, Dr Anne Chace; Centre Hospitalier Général-Hôpital Delafontaine, Saint-Denis, Dr Pascal Bolot; Groupe Hospitalier Necker, Paris, Pr Stéphane Blanche; Centre hospitalier Francilien Sud, Corbeil Essonne, Dr Michèle Granier; Hôpital Antoine Béclère, Clamart, Pr Philippe Labrune; Hôpital Jean Verdier, Bondy, Dr Eric Lachassine; Hôpital Trousseau, Paris, Dr Catherine Dollfus; Hôpital Robert Debёr, Paris, Dr Martine Levine; Hôpital Bicêtre, Le Kremlin Bicêtre, Dr Corinne Fourcade; Centre Hospitalier Intercommunal, Montreuil, Dr Brigitte Heller- Roussin; Centre Hospitalier Pellegrin, Bordeaux, Dr Camille Runel-Belliard; CHU Paule de Viguier, Toulouse, Dr Joëlle Tricoire; CHU Hôpital de l'Archet II, Nice, Dr Fabrice Monpoux; Groupe Hospitalier de la Timone, Marseille; CHU Hôpital Jean Minjoz, Besancon, Dr Catherine Chirouze; CHU Nantes Hotel Dieu, Nantes, Dr Véronique Reliquet; CHU Caen, Caen, Pr Jacques Brouard; Institut d'Hématologie et Oncologie Pédiatrique, Lyon, Dr Kamila Kebaili; CHU Angers, Angers, Dr Pascale Fialaire; CHR Arnaud de Villeneuve, Montpellier, Dr Muriel Lalande; CHR Jeanne de Flandres, Lille, Dr Françoise Mazingue; Hôpital Civil, Strasbourg, Dr Maria Luisa Partisani.

A

Germany: German Paediatric & Adolescent HIV Cohort (GEPIC): Dr Christoph Königs, Dr Stephan Schultze-Strasser. *German clinical centers:* Hannover Medical School, Dr. U. Baumann; Pediatric Hospital Krefeld, Dr. T. Niehues; University Hospital Düsseldorf, Dr. J. Neubert; University Hospital Hamburg, Dr. R. Kobbe; Charite Berlin, Dr. C. Feiterna-Sperling; University Hospital Frankfurt, Dr. C. Königs; University Hospital Mannheim, Dr. B. Buchholz; Munich University Hospital, Dr. G. Notheis.

Greece: Greek cohort: Vana Spoulou.

Italy: Italian Register for HIV infection in Children. Coordinators: Maurizio de Martino (Florence), Pier Angelo Tovo (Turin). Participants: Osimani Patrizia (Ancona), Domenico Larovere (Bari), Maurizio Ruggeri (Bergamo), Giacomo Faldella, Francesco Baldi (Bologna) Raffaele Badolato (Brescia), Carlotta Montagnani, Elisabetta Venturini, Catiuscia Lisi (Florence), Antonio Di Biagio, Lucia Taramasso (Genua), Vania Giacomet, Paola Erba, Susanna Esposito, Rita Lipreri, Filippo Salvini, Claudia Tagliabue (Milan), Monica Cellini (Modena), Eugenia Bruzzese, Andrea Lo Vecchio (Naples), Osvalda Rampon, Daniele Donà (Padua), Amelia Romano (Palermo), Icilio Dodi (Parma), Anna Maccabruni (Pavia), Rita Consolini (Pisa), Stefania Bernardi, Hyppolite Tchidjou Kuekou, Orazio Genovese (Rome), Paolina Olmeo (Sassari), Letizia Cristiano (Taranto), Antonio Mazza (Trento), Clara Gabiano, Silvia Garazzino (Turin), Antonio Pellegatta (Varese).

Netherlands: The ATHENA database is maintained by Stichting HIV Monitoring and supported by a grant from the Dutch Ministry of Health, Welfare and Sport through the Centre for Infectious Disease Control of the National Institute for Public Health and the Environment.
Clinical centres (Paediatric care): Emma Kinderziekenhuis, Amsterdam Universitair Medische Centra: HIV treating physicians: D. Pajkrt, H.J. Scherpbier; HIV nurse consultants: C. de Boer, A.M. Weijsenfeld; HIV clinical virologists/chemists: S. Jurriaans, N.K.T. Back, H.L. Zaaijer, B. Berkhout, M.T.E. Cornelissen, C.J. Schinkel, K.C. Wolthers. Erasmus MC–Sophia, Rotterdam: HIV treating physicians: P.L.A. Fraaij, A.M.C. van Rossum, C.L. Vermont; HIV nurse consultants: L.C. van der Knaap, E.G. Visser; HIV clinical virologists/chemists: C.A.B. Boucher, M.P.G Koopmans, J.J.A van Kampen, S.D. Pas. Radboudumc, Nijmegen: HIV treating physicians: S.S.V. Henriet, M. van de Flier, K. van Aerde; HIV nurse consultants: R. Strik-Albers; HIV clinical virologists/chemists: J. Rahamat-Langendoen, F.F. Stelma. Universitair Medisch Centrum Groningen, Groningen: HIV treating physicians: E.H. Schölvinck; HIV nurse consultants: H. de Groot-de Jonge; HIV clinical virologists/chemists:

H.G.M. Niesters, C.C. van Leer-Buter, M. Knoester. Wilhelmina Kinderziekenhuis, UMC Utrecht, Utrecht: HIV treating physicians: L.J. Bont, S.P.M. Geelen, T.F.W. Wolfs; HIV nurse consultants: N. Nauta; HIV clinical virologists/chemists: R. Schuurman, F. Verduyn-Lunel, A.M.J. Wensing.

Coordinating Centre: Director: P. Reiss; Data analysis: D.O. Bezemer, A.I. van Sighem, C. Smit, F.W.M.N. Wit, T.S. Boender; Data management and quality control: S. Zaheri, M. Hillebregt, A. de Jong; Data monitoring: D. Bergsma, S. Grivell, A. Jansen, M. Raethke, R. Meijering; Data collection: L. de Groot, M. van den Akker, Y. Bakker, E. Claessen, A. El Berkaoui, J. Koops, E. Kruijne, C. Lodewijk, L. Munjishvili, B. Peeck, C. Ree, R. Regtop, Y. Ruijs, T. Rutkens, M. Schoorl, A. Timmerman, E. Tuijn, L. Veenenberg, S. van der Vliet, A. Wisse, T. Woudstra; Patient registration: B. Tuk.

Poland: Polish paediatric cohort: Head of the team: Prof Magdalena Marczyńska, MD, PhD. Members of the team: Jolanta Popielska, MD, PhD; Maria Pokorska-Śpiewak, MD, PhD; Agnieszka Ołdakowska, MD, PhD; Konrad Zawadka, MD, PhD; Urszula Coupland, MD, PhD. Administration assistant: Małgorzata Doroba. Affiliation: Medical University of Warsaw, Poland, Department of Children's Infectious Diseases; Hospital of Infectious Diseases in Warsaw, Poland.

Portugal: Centro Hospitalar do Porto: Laura Marques, Carla Teixeira, Alexandre Fernandes. Departamento de Pediatria/Hospital de Santa Maria/CHULN: Filipa Prata.

Romania: "Victor Babes" Hospital Cohort, Bucharest: Dr Luminita Ene.

Russia: Federal State-owned Institution "Republican Clinical Infectious Diseases Hospital" of the Ministry of Health of the Russian Federation, St Petersburg: Liubov Okhonskaia, Evgeny Voronin, Milana Miloenko, Svetlana Labutina.

Spain: CoRISPE-cat, Catalonia: Financial support for CoRISPE-cat was provided by the Instituto de Salud Carlos III through the Red Temática de Investigación Co-operativa en Sida. Members: Hospital Universitari Vall d'Hebron, Barcelona (Pere Soler-Palacín, Maria Antoinette Frick and Santiago Pérez-Hoyos (statistician)), Hospital Universitari del Mar, Barcelona (Antonio Mur, Núria López), Hospital Universitari Germans Trias i Pujol, Badalona (María Méndez), Hospital Universitari JosepTrueta, Girona (Lluís Mayol), Hospital Universitari Arnau de Vilanova, Lleida (Teresa Vallmanya), Hospital Universitari Joan XXIII, Tarragona (Olga Calavia), Consorci Sanitari del Maresme, Mataró (Lourdes García), Hospital General de Granollers (Maite Coll), Corporació Sanitària Parc Taulí, Sabadell (Valentí Pineda),

A

Hospital Universitari Sant Joan, Reus (Neus Rius), Fundació Althaia, Manresa (Núria Rovira), Hospital Son Espases, Mallorca (Joaquín Dueñas) and Hospital Sant Joan de Déu, Esplugues (Clàudia Fortuny, Antoni Noguera-Julian).

CoRISPE and Madrid Cohort Working Group: María José Mellado, Luis Escosa, Milagros García Hortelano, Talía Sainz (Hospital Universitario La Paz, Madrid); Pablo Rojo, Daniel Blázquez, Luis Prieto-Tato, Cristina Epalza (Hospital Universitario Doce de Octubre, Madrid); José Tomás Ramos (Hospital Clínico San Carlos, Madrid); Sara Guillén (Hospital Universitario de Getafe, Madrid); María Luisa Navarro, Jesús Saavedra, Mar Santos, Begoña Santiago, Santiago Jimenez de Ory, Itzíar Carrasco, Mª Angeles Muñoz-Fernández (Hospital Universitario Gregorio Marañón, Madrid); Miguel Ángel Roa (Hospital Universitario de Móstoles, Madrid); María Penín (Hospital Universitario Príncipe de Asturias de Alcalá de Henares, Madrid); Jorge Martínez (Hospital Infantil Universitario Niño Jesús, Madrid); Katie Badillo (Hospital Universitario de Torrejón, Madrid); Eider Oñate (Hospital Universitario Donostia, Guipúzcoa); Itziar Pocheville (Hospital Universitario Cruces, Vizcaya); Elisa Garrote (Hospital Universitario Basurto, Vizcaya); Elena Colino (Hospital Insular Materno Infantil, Gran Canaria); Jorge Gómez Sirvent (Hospital Universitario Virgen de la Candelaria, Tenerife); Mónica Garzón, Vicente Román (Hospital General, Lanzarote); Raquel Angulo (Hospital de Poniente de El Ejido, Almería); Olaf Neth, Lola Falcón (Hospital Universitario Virgen del Rocío, Sevilla); Pedro Terol (Hospital Universitario Virgen de la Macarena, Sevilla); Juan Luis Santos (Hospital Universitario Virgen de las Nieves, Granada); David Moreno (Hospital Regional Universitario Carlos Haya, Málaga); Francisco Lendínez (Complejo Hospitalario Torrecárdenas, Almería); Estrella Peromingo (Hospital Universitario Puerta del Mar, Cádiz); José Uberos (Hospital Clínico San Cecilio, Granada); Beatriz Ruiz (Hospital Universitario Reina Sofía de Córdoba); Ana Grande (Complejo Hospitalario Universitario Infanta Cristina, Badajoz); Francisco José Romero (Complejo Hospitalario, Cáceres); Carlos Pérez (Hospital de Cabueñes, Asturias); Miguel Lillo (Complejo Hospitalario Universitario, Albacete); Begoña Losada (Hospital Virgen de la Salud, Toledo); Mercedes Herranz (Hospital Virgen del Camino, Navarra); Matilde Bustillo (Hospital Universitario Miguel Servet, Zaragoza); Pilar Collado (Hospital Clínico Universitario Lozano Blesa, Zaragoza); José Antonio Couceiro (Complejo Hospitalario Universitario, Pontevedra); Leticia Vila (Complejo Hospitalario Universitario, La Coruña); Consuelo Calviño (Hospital Universitario Lucus Augusti, Lugo); Ana Isabel Piqueras, Manuel Oltra (Hospital Universitario La Fe, Valencia); César Gavilán (Hospital Universitario de San Juan de Alicante, Alicante); Elena Montesinos (Hospital General Universitario, Valencia); Marta Dapena (Hospital General, Castellón); Cristina Álvarez, Beatriz Jiménez (Hospital Universitario

Marqués de Valdecilla, Cantabria); Ana Gloria Andrés (Complejo Hospitalario, León); Víctor Marugán, Carlos Ochoa (Complejo Hospitalario, Zamora); Santiago Alfayate, Ana Isabel Menasalvas (Hospital Universitario Virgen de la Arrixaca, Murcia); Yolanda Ruiz del Prado (Complejo Hospitalario San Millán-San Pedro, la Rioja) and Paediatric HIV-BioBank integrated in the Spanish AIDS Research Network and collaborating Centers.

Sweden: Karolinska Institutet and University Hospital, Stockholm (Lars Naver, Sandra Soeria-Atmadja, Vendela Hagås).

Switzerland: Members of the Swiss HIV Cohort Study (SHCS) and the Swiss Mother and Child HIV Cohort Study: Aebi-Popp K, Anagnostopoulos A, Battegay M, Baumann M, Bernasconi E, Böni J, Braun DL, Bucher HC, Calmy A, Cavassini M, Ciuffi A, Crisinel PA, Duppenthaler A, Dollenmaier G, Egger M, Elzi L, Fehr J, Fellay J, Francini K, Furrer H, Fux CA, Günthard HF (President of the SHCS), Haerry D (deputy of "Positive Council"), Hasse B, Hirsch HH, Hoffmann M, Hösli I, Huber M, Kahlert CR (Chairman of the Mother & Child Substudy), Kaiser L, Keiser O, Klimkait T, Kottanattu L, Kouyos RD, Kovari H, Ledergerber B, Martinetti G, Martinez de Tejada B, Marzolini C, Metzner KJ, Müller N, Nicca D, Paioni P, Pantaleo G, Perreau M, Polli Ch, Rauch A (Chairman of the Scientific Board), Rudin C, Scherrer AU (Head of Data Centre), Schmid P, Speck R, Stöckle M (Chairman of the Clinical and Laboratory Committee), Sultan-Beyer L, Tarr P, Thanh Lecompte M, Trkola A, Vernazza P, Wagner N, Wandeler G, Weber R, Yerly S.

Thailand: Program for HIV Prevention & Treatment (PHPT).
Participating hospitals: Lamphun: Pornpun Wannarit; Phayao Provincial Hospital: Pornchai Techakunakorn; Chiangrai Prachanukroh: Rawiwan Hansudewechakul; Chiang Kham: Vanichaya Wanchaitanawong; Phan: Sookchai Theansavettrakul; Mae Sai: Sirisak Nanta; Prapokklao: Chaiwat Ngampiyaskul; Banglamung: Siriluk Phanomcheong; Chonburi: Suchat Hongsiriwon; Rayong: Warit Karn-chanamayul; Bhuddasothorn Chacheongsao: Ratchanee Kwanchaipanich; Nakornping: Suparat Kanjanavanit; Somdej Prapinklao: Nareerat Kamonpakorn,

Maneeratn Nantarukchaikul; Bhumibol Adulyadej: Prapaisri Layangool, Jutarat Mekmullica; Pranangklao: Paiboon Lucksanapisitkul, Sudarat Watanayothin; Buddhachinaraj: Narong Lertpienthum; Hat Yai: Boonyarat Warachit; Regional Health Promotion Center 6, Khon Kaen: Sansanee Hanpinitsak; Nong Khai: Sathit Potchalongsin; Samutsakhon: Pimpraphai Thanasiri, Sawitree Krikajornkitti; Phaholpolphayuhasena: Pornsawan Attavinijtrakarn; Kalasin: Sakulrat Srirojana; Nakhonpathom: Suthunya Bunjongpak; Samutprakarn: Achara Puangsombat; Mahasarakam: Sathaporn Na-Rajsima; Roi-et: Pornchai Ananpatharachai; Sanpatong: Noppadon Akarathum; Vachira Phuket: Weerasak Lawtongkum; Chiangdao: Prapawan Kheunjan, Thitiporn Suriyaboon, Airada Saipanya.
Data management team: Kanchana Than-in-at, Nirattiya Jaisieng, Rapeepan Suaysod, Sanuphong Chailoet, Naritsara Naratee, and Suttipong Kawilapat.

Ukraine: Paediatric HIV Cohort: Dr T. Kaleeva, Dr Y. Baryshnikova (Odessa Regional Centre for HIV/AIDS), Ruslan Malyuta (Perinatal Prevention of AIDS Initiative, Odessa), Dr S. Soloha (Donetsk Regional Centre for HIV/AIDS), Dr N. Bashkatova (Mariupol AIDS Center), Dr I. Raus (Kiev City Centre for HIV/AIDS), Alla Volokha (Shupyk National Medical Academy of Postgraduate Education, Kiev), Dr O. Glutshenko, Dr Z. Ruban (Mykolaiv Regional Centre for HIV/AIDS), Dr N. Prymak (Kryvyi Rih), Dr G. Kiseleva (Simferopol), Dr H. Bailey (UCL, London, UK).
Funding acknowledgement: PENTA Foundation.

UK & Ireland: Collaborative HIV Paediatric Study (CHIPS): CHIPS is funded by the NHS (London Specialised Commissioning Group) and has received additional support from Bristol-Myers Squibb, Boehringer Ingelheim, GlaxoSmithKline, Roche, Abbott, and Gilead Sciences. The MRC Clinical Trials Unit at UCL is supported by the Medical Research Council (https://www.mrc.ac.uk) programme number MC_UU_12023/26. CHIPS Steering Committee: Hermione Lyall, Alasdair Bamford, Karina Butler, Katja Doerholt, Caroline Foster, Nigel Klein, Paddy McMaster, Katia Prime, Andrew Riordan, Fiona Shackley, Delane Shingadia, Sharon Storey, Gareth Tudor-Williams, Anna Turkova, Steve Welch. MRC Clinical Trials Unit: Intira Jeannie Collins, Claire Cook, Siobhan Crichton, Donna Dobson, Keith Fairbrother, Diana M. Gibb, Lynda Harper, Ali Judd, Marthe Le Prevost, Nadine Van Looy.
National Study of HIV in Pregnancy and Childhood, UCL: Helen Peters, Claire Thorne.
Participating hospitals: Republic of Ireland: Our Lady's Children's Hospital Crumlin, Dublin: K Butler, A Walsh. UK: Birmingham Heartlands Hospital, Birmingham: L Thrasyvoulou , S Welch; Bristol Royal Hospital for Children, Bristol: J Bernatoniene, F Manyika ; Calderdale Royal Hospital, Halifax: G Sharpe; Derby: B

A

Subramaniam; Middlesex: K Sloper; Eastbourne District General Hospital, Eastbourne: K Fidler, Glasgow Royal Hospital for Sick Children, Glasgow: R Hague, V Price; Great Ormond St Hospital for Children, London: M Clapson, J Flynn, A Cardoso M Abou–Rayyah, N Klein, D Shingadia; Homerton University Hospital, London: D Gurtin, John Radcliffe Hospital, Oxford: S Yeadon, S Segal; King's College Hospital, London: C Ball, S Hawkins; Leeds General Infirmary, Leeds: M Dowie; Leicester Royal Infirmary, Leicester: S Bandi, E Percival; Luton and Dunstable Hospital, Luton: M Eisenhut; K Duncan, S Clough; Milton Keynes General Hospital, Milton Keynes: Dr L Anguvaa, S Conway, Newcastle General, Newcastle: T Flood, A Pickering; North Manchester General, Manchester: P McMaster C Murphy; North Middlesex Hospital, London: J Daniels, Y Lees; Northampton General Hospital, Northampton: F Thompson; Northwick Park Hospital Middlesex; , B Williams, S Pope; Nottingham QMC , Nottingham: L Cliffe, A Smyth, S Southall; Queen Alexandra Hospital, Portsmouth: A Freeman; Raigmore Hospital, Inverness: H Freeman; Royal Belfast Hospital for Sick Children, Belfast: S Christie; Royal Berkshire Hospital, Reading: A Gordon; Royal Children's Hospital, Aberdeen: D Rogahn L Clarke; Royal Edinburgh Hospital for Sick Children, Edinburgh: L Jones, B Offerman; Royal Free Hospital, London: M Greenberg ; Royal Liverpool Children's Hospital, Liverpool: C Benson, A Riordan; Sheffield Children's Hospital, Sheffield: L Ibberson, F Shackley; Southampton General Hospital, Southampton: SN Faust, J Hancock; St George's Hospital, London: K Doerholt, K Prime, M Sharland, S Storey; St Mary's Hospital, London: H Lyall, C Monrose, P Seery, G Tudor-Williams; St Thomas' Hospital (Evelina Children's Hospital), London: E Menson, A Callaghan; Royal Stoke University Hospital, Stoke On Trent: A Bridgwood, P McMaster; University Hospital of Wales, Cardiff: J Evans, E Blake; Wexham Park, Slough: A Yannoulias.

A

Abbreviations

AIDS acquired immune deficiency syndrome
ART antiretroviral therapy/treatment
bPI boosted protease inhibitor
bNAb broadly neutralising antibody
CCR5 co-receptor
CD4% percentages of CD4$^+$ T cells in total lymphocyte counts
CD4ct CD4$^+$ T cells counts in a μL of blood
cDNA circular deoxyribonucleic acid
CHER children with HIV early antiretroviral therapy
COVID-19 *coronavirus* disease
CXCR4 co-receptor
DNA deoxyribonucleic acid
e.g. exempli gratia, for example
EPIICAL early-treated perinatally HIV-infected individuals: improving children's actual life with novel immunotherapeutic strategies
EPPICC European pregnancy and paediatric HIV cohort collaboration
EARTH cohort of early antiretroviral treatment in HIV-perinatally infected children
HIV *human immunodeficiency virus*
i.e. id est, that is
LEOPARD latency and early neonatal provision of antiretroviral drugs clinical trial
μL microlitre
mL millilitre
MTCT mother-to-child-ransmission
NNRTI non-nucleoside reverse-transcriptase inhibitor
NRTI nucleoside reverse-transcriptase inhibitor
ODE ordinary differential equation
QSS quasi steady state

A

RNA	ribonucleic acid
SHIV	*simian-human immunodeficiency virus*
SIV	*simian immunodeficiency virus*
TLC	total lymphocyte count
TTS	time to (viral) suppression
VL	viral load
WHO	World Health Organisation

A

References

Adland, E., Mori, L., Laker, L., Csala, A., Muenchhoff, M., Swordy, A., Mori, M., Matthews, P., Tudor-Williams, G., Jooste, P., and Goulder, P. (2018). Recovery of effective HIV-specific CD4 + T-cell activity following antiretroviral therapy in paediatric infection requires sustained suppression of viraemia. *Aids*, 32(11):1413–1422.

Ásbjörnsdóttir, K. H., Hughes, J. P., Wamalwa, D., Langat, A., Slyker, J. A., Okinyi, H. M., Overbaugh, J., Benki-Nugent, S., Tapia, K., Maleche-Obimbo, E., Rowhani-Rahbar, A., and John-Stewart, G. (2016). Differences in virologic and immunologic response to antiretroviral therapy among HIV-1-infected infants and children. *Aids*, 30(18):2835–2843.

Babiker, A., Darby, S., De Angelis, D., Ewart, D., Porter, K., Beral, V., Darbyshire, J., Day, N., and Gill, N. (2000). Time from HIV-1 seroconversion to AIDS and death before widespread use of highly-active antiretroviral therapy: a collaborative re-analysis. *The Lancet*, 355(9210):1131–1137.

Bains, I., Antia, R., Callard, R., and Yates, A. J. (2009a). Quantifying the development of the peripheral naive CD4+ T-cell pool in humans. *Blood*, 113(22):5480–5487.

Bains, I., Thiébaut, R., Yates, A. J., and Callard, R. (2009b). Quantifying Thymic Export: Combining Models of Naive T Cell Proliferation and TCR Excision Circle Dynamics Gives an Explicit Measure of Thymic Output 1.

Barré-Sinoussi, F., Chermann, J. C., Rey, F., Nugeyre, M. T., Chamaret, S., Gruest, J., Dauguet, C., Rouzioux, C., Rozenbaum, W., Montagnier, L., Series, N., and May, N. (1983). Isolation of a T-Lymphotropic Retrovirus from a Patient at Risk for Acquired Immune Deficiency Syndrome (AIDS). *Science*, 220(4599):868–871.

Beaudrap, P. D., Rouet, F., Fassinou, P., Kouakoussui, A., Mercier, S., Ecochard, R., and Msellati, P. (2008). CD4 cell response before and after HAART initiation according to viral load and growth indicators in HIV-1-infected children in abidjan, côte d'ivoire. *Journal of Acquired Immune Deficiency Syndromes*, 49(1):70–76.

R

Biggar, R. J., Broadhead, R., Janes, M., Kumwenda, N., Taha, T. E. T., and Cassol, S. (2001). Viral levels in newborn African infants undergoing primary HIV-1 infection. *AIDS*, 15(10):1311–1313.

Blanco, E., Pérez-Andrés, M., Arriba-Méndez, S., Contreras-Sanfeliciano, T., Criado, I., Pelak, O., Serra-Caetano, A., Romero, A., Puig, N., Remesal, A., Torres Canizales, J., López-Granados, E., Kalina, T., Sousa, A. E., van Zelm, M., van der Burg, M., van Dongen, J. J., and Orfao, A. (2018). Age-associated distribution of normal B-cell and plasma cell subsets in peripheral blood. *Journal of Allergy and Clinical Immunology*, 141(6):2208–2219.e16.

Bonhoeffer, S., Funk, G. A., Günthard, H. F., Fischer, M., and Müller, V. (2003). Glancing behind virus load variation in HIV-1 infection. *Trends in Microbiology*, 11(11):499–504.

Bonhoeffer, S., May, R. M., Shaw, G. M., and Nowak, M. A. (1997). Virus dynamics and drug therapy. *Proceedings of the National Academy of Sciences of the United States of America*, 94(13):6971–6976.

Bucy, R. P., Hockett, R. D., Derdeyn, C. A., Saag, M. S., Squires, K., Sillers, M., Mitsuyasu, R. T., and Kilby, J. M. (1999). Initial increase in blood CD4+ lymphocytes after HIV antiretroviral therapy reflects redistribution from lymphoid tissues. *Journal of Clinical Investigation*, 103(10):1391–1398.

Byrareddy, S. N., Arthos, J., Cicala, C., Villinger, F., Ortiz, K. T., Little, D., Sidell, N., Kane, M. A., Yu, J., Jones, J. W., Santangelo, P. J., Zurla, C., McKinnon, L. R., Arnold, K. B., Woody, C. E., Walter, L., Roos, C., Noll, A., Van Ryk, D., Jelicic, K., Cimbro, R., Gumber, S., Reid, M. D., Adsay, V., Amancha, P. K., Mayne, A. E., Parslow, T. G., Fauci, A. S., and Ansari, A. A. (2016). Sustained virologic control in SIV+ macaques after antiretroviral and $\alpha_4\beta_7$ antibody therapy. *Science*, 354(6309):197–202.

Canini, L. and Perelson, A. S. (2014). Viral Kinetic Modeling: State of the Art. *Journal of pharmacokinetics and pharmacodynamics*, 41(5):431.

Carcelain, G., Debré, P., and Autran, B. (2001). Reconstitution of CD4+ T lymphocytes in HIV-infected individuals following antiretroviral therapy. *Current Opinion in Immunology*, 13(4):483–488.

Cardozo, E. F., Apetrei, C., Pandrea, I., and Ribeiro, R. M. (2018). The dynamics of simian immunodeficiency virus (SIV) after depletion of CD8+ cells. *Immunological reviews*, 285(1):26.

R

Chun, T.-W., Engel, D., Berrey, M. M., Shea, T., Corey, L., and Fauci, A. S. (1998). Early establishment of a pool of latently infected, resting CD4+ T cells during primary HIV-1 infection. *Proceedings of the National Academy of Sciences*, 95(15):8869–8873.

Cohen Stuart, J. W., Slieker, W. A., Rijkers, G. T., Noest, A., Boucher, C. A., Suur, M. H., de Boer, R., Geelen, S. P., Scherpbier, H. J., Hartwig, N. G., Hooijkaas, H., Roos, M. T., de Graeff-Meeder, B., and de Groot, R. (1998). Early recovery of CD4+ T lymphocytes in children on highly active antiretroviral therapy. Dutch study group for children with HIV infections. *AIDS*, 12(16):2155–219.

Collins, D. R., Urbach, J. M., Racenet, Z. J., Arshad, U., Power, K. A., Newman, R. M., Mylvaganam, G. H., Ly, N. L., Lian, X., Rull, A., Rassadkina, Y., Yanez, A. G., Peluso, M. J., Deeks, S. G., Vidal, F., Lichterfeld, M., Yu, X. G., Gaiha, G. D., Allen, T. M., and Walker, B. D. (2021). Functional impairment of HIV-specific CD8 + T cells precedes aborted spontaneous control of viremia. *Immunity*, 54(10):2372–2384.e7.

Collins, I. J., Foster, C., Tostevin, A., Tookey, P., Riordan, A., Dunn, D., Gibb, D. M., Judd, A., Hiv, C., and Study, P. (2017). Europe PMC Funders Group Europe PMC Funders Author Manuscripts Europe PMC Funders Author Manuscripts Clinical status of adolescents with perinatal HIV at transfer to adult care in the UK / Ireland. 64(8):1105–1112.

Comans-Bitter, W. M., De Groot, R., Van den Beemd, R., Neijens, H. J., Hop, W. C., Groeneveld, K., Hooijkaas, H., and Van Dongen, J. J. (1997). Immunophenotyping of blood lymphocytes in childhood: Reference values for lymphocyte subpopulations. *Journal of Pediatrics*, 130(3):388–393.

Cotton, M. F., Violari, A., Otwombe, K., Panchia, R., Dobbels, E., Rabie, H., Josipovic, D., Liberty, A., Lazarus, E., Innes, S., Janse van Rensburg, A., Pelser, W., Truter, H., Madhi, S. A., Handelsman, E., Jean-Philippe, P., McIntyre, J. A., Gibb, D. M., and Babiker, A. G. (2013). Early limited antiretroviral therapy is superior to deferred therapy in HIV-infected South African infants: results from the CHER (Children with HIV Early antiRetroviral) Randomized Trial. *Lancet*, 382(9904):1555–1563.

Davenport, M. P., Zaunders, J. J., Hazenberg, M. D., Schuitemaker, H., and Van Rij, R. P. (2002). Cell turnover and cell tropism in HIV-1 infection. *Trends in Microbiology*, 10(6):275–278.

de Boer, R. J. and Perelson, A. S. (1998). Target cell limited and immune control models of HIV infection: A comparison. *Journal of Theoretical Biology*, 190(3):201–214.

De Rossi, A., Masiero, S., Giaquinto, C., Ruga, E., Comar, M., Giacca, M., and Chieco-Bianchi, L. (1996). Dynamics of viral replication in infants with vertically acquired human immunodeficiency virus type 1 infection. *The Journal of clinical investigation*, 97(2):323–30.

de Vries, E., de Bruin-Versteeg, S., Comans-Bitter, M. W., and van Dongen, J. J. M. (1998). Longitudinal follow-up of blood lymphocyte subpopu- lations from birth to 1 year of age. (October):586–588.

Dimitrov, D. S. and Martin, M. A. (1995). HIV results in the frame. CD4+ cell turnover.

Dixit, N. M., Markowitz, M., Ho, D. D., and Perelson, A. S. (2004). Estimates of intracellular delay and average drug efficacy from viral load data of HIV-infected individuals under antiretroviral therapy. *Antiviral Therapy*, 9(2):237–246.

Doitsh, G., Galloway, N. L., Geng, X., Yang, Z., Monroe, K. M., Zepeda, O., Hunt, P. W., Hatano, H., Sowinski, S., Muñoz-Arias, I., and Greene, W. C. (2014). Cell death by pyroptosis drives CD4 T-cell depletion in HIV-1 infection. *Nature*, 505(7484):509–514.

Douek, D. C., McFarland, R. D., Keiser, P. H., Gage, E. A., Massey, J. M., Haynes, B. F., Polis, M. A., Haase, A. T., Feinberg, M. B., Sullivan, J. L., Jamieson, B. D., Zack, J. A., Picker, L. J., and Koup, R. A. (1998). Changes in thymic function with age and during the treatment of HIV infection. *Nature*, 396(6712):690–695.

Edwards, B. H., Bansal, A., Sabbaj, S., Bakari, J., Mulligan, M. J., and Goepfert, P. A. (2002). Magnitude of functional CD8+ T-cell responses to the gag protein of human immunodeficiency virus type 1 correlates inversely with viral load in plasma. *Journal of virology*, 76(5):2298–2305.

EPIICAL (2022). EARTH.

EPPICC (2011). Response to early antiretroviral therapy in HIV-1 infected infants in Europe , 1996-2008. *Aids*, 25(18):2279–2287.

EPPICC (2018). Time to switch to second-line antiretroviral therapy in children with HIV in Europe and Thailand. *Clinical Infectious Diseases*, 66(4):594–603.

EPPICC and EPIICAL (2019). Predictors of faster virological suppression in early treated infants with perinatal HIV from Europe and Thailand. *AIDS*, 33(7):1155–1165.

Erkeller-Yuksel, F. M., Deneys, V., Yuksel, B., Hannet, I., Hulstaert, F., Hamilton, C., Mackinnon, H., Stokes, L. T., Munhyeshuli, V., Vanlangendonck, F., De Bruyère, M., Bach, B. A., and Lydyard, P. M. (1992). Age-related changes in human blood lymphocyte subpopulations. *The Journal of Pediatrics*, 120(2 PART 1):216–222.

Essunger, P. and Perelson, A. S. (1994). Modeling HIV infection of CD4+ T-cell subpopulations. *Journal of Theoretical Biology*, 170(4):367–391.

European Medicines Agency (2022). COVID-19 vaccines: authorised.

Finzi, D., Blankson, J., Siliciano, J. D., Margolick, J. B., Chadwick, K., Pierson, T., Smith, K., Lisziewicz, J., Lori, F., Flexner, C., Quinn, T. C., Chaisson, R. E., Rosenberg, E., Walker, B., Gange, S., Gallant, J., and Siliciano, R. F. (1999). Latent infection of CD4+ T cells provides a mechanism for lifelong persistence of HIV-1, even in patients on effective combination therapy. *Nature Medicine*, 5(5):512–517.

Frange, P., Faye, A., Avettand-Fenoël, V., Bellaton, E., Descamps, D., Angin, M., David, A., Caillat-Zucman, S., Peytavin, G., Dollfus, C., Le Chenadec, J., Warszawski, J., Rouzioux, C., and Sáez-Cirión, A. (2016). HIV-1 virological remission lasting more than 12 years after interruption of early antiretroviral therapy in a perinatally infected teenager enrolled in the French ANRS EPF-CO10 paediatric cohort: a case report. *The Lancet HIV*, 3(1):e49–e54.

Fraser, C., Hollingsworth, T. D., Chapman, R., De Wolf, F., and Hanage, W. P. (2007). Variation in HIV-1 set-point viral load: epidemiological analysis and an evolutionary hypothesis. *Proceedings of the National Academy of Sciences of the United States of America*, 104(44):17441–17446.

Fraser, C., Lythgoe, K., Leventhal, G. E., Shirreff, G., Hollingsworth, T. D., Alizon, S., and Bonhoeffer, S. (2014). Virulence and pathogenesis of HIV-1 infection: an evolutionary perspective. *Science*, 343(6177):1243727.

Frenkel, L. M., Wang, Y., Learn, G. H., McKernan, J. L., Ellis, G. M., Mohan, K. M., Holte, S. E., De Vange, S. M., Pawluk, D. M., Melvin, A. J., Lewis, P. F., Heath, L. M., Beck, I. A., Mahalanabis, M., Naugler, W. E., Tobin, N. H., and Mullins, J. I. (2003). Multiple viral genetic analyses detect low-level human immunodeficiency virus type 1 replication during effective highly active antiretroviral therapy. *Journal of virology*, 77(10):5721–5730.

R

Gadhamsetty, S., Coorens, T., and de Boer, R. J. (2016). Notwithstanding Circumstantial Alibis, Cytotoxic T Cells Can Be Major Killers of HIV-1-Infected Cells. *Journal of Virology*, 90(16):7066–7083.

Garcia-Broncano, P., Maddali, S., Einkauf, K. B., Jiang, C., Gao, C., Chevalier, J., Chowdhury, F. Z., Maswabi, K., Ajibola, G., Moyo, S., Mohammed, T., Ncube, T., Makhema, J., Jean-Philippe, P., Yu, X. G., Powis, K. M., Lockman, S., Kuritzkes, D. R., Shapiro, R., and Lichterfeld, M. (2019). Early antiretroviral therapy in neonates with HIV-1 infection restricts viral reservoir size and induces a distinct innate immune profile. *Science translational medicine*, 11(520).

Giannattasio, A., Officioso, A., Continisio, G. I., Griso, G., Storace, C., Coppini, S., Longhi, D., Mango, C., Guarino, A., Badolato, R., and Pisacane, A. (2011). Psychosocial issues in children and adolescents with HIV infection evaluated with a world health organization age-specific descriptor system. *Journal of Developmental and Behavioral Pediatrics*, 32(1):52–55.

Goicoechea, M. and Haubrich, R. (2005). CD4 lymphoctye percentage versus absolute CD4 lymphocyte count in predicting HIV disease progression: An old debate revisited. *Journal of Infectious Diseases*, 192(6):945–947.

Goulder, P. J., Lewin, S. R., and Leitman, E. M. (2016). Paediatric HIV infection: the potential for cure. *Nature Reviews Immunology*, 16(4):259–271.

Hainaut, M., Ducarme, M., Schandené, L., Peltier, C. A., Marissens, D., Zissis, G., Mascart, F., and Levy, J. (2003). Age-related immune reconstitution during highly active antiretroviral therapy in human immunodeficiency virus type 1-infected children: IN REPLY. *Pediatric Infectious Disease Journal*, 22(10):935.

Hardy, G. A., Imami, N., Sullivan, A. K., Pires, A., Burton, C. T., Nelson, M. R., Gazzard, B. G., and Gotch, F. M. (2003). Reconstitution of CD4+ T cell responses in HIV-1 infected individuals initiating highly active antiretroviral therapy (HAART) is associated with renewed interleukin-2 production and responsiveness. *Clinical and Experimental Immunology*, 134(1):98–106.

Hecht, F. M., Wang, L., Collier, A., Little, S., Markowitz, M., Margolick, J., Kilby, J. M., Daar, E., Conway, B., and Holte, S. (2006). A multicenter observational study of the potential benefits of initiating combination antiretroviral therapy during acute HIV infection. *The Journal of infectious diseases*, 194(6):725–733.

Hill, A. L., Rosenbloom, D. I., Nowak, M. A., and Siliciano, R. F. (2018). Insight into treatment of HIV infection from viral dynamics models. *Immunological Reviews*, 285(1):9–25.

R

Ho, D. D., Neumann, A. U., Perelson, A. S., Chen, W., Leonard, J. M., and Markowitz, M. (1995). Rapid turnover of plasma virions and CD4 lymphocytes in HIV-1 infection. *Nature*, 373(6510):123–126.

Huenecke, S., Behl, M., Fadler, C., Zimmermann, S. Y., Bochennek, K., Tramsen, L., Esser, R., Klarmann, D., Kamper, M., Sattler, A., Von Laer, D., Klingebiel, T., Lehrnbecher, T., and Koehl, U. (2008). Age-matched lymphocyte subpopulation reference values in childhood and adolescence: Application of exponential regression analysis. *European Journal of Haematology*, 80(6):532–539.

Hulstaert, F., Hannet, I., Deneys, V., Munhyeshuli, V., Reichert, T., De Bruyere, M., and Strauss, K. (1994). Age-related changes in human blood lymphocyte subpopulations. II. Varying kinetics of percentage and absolute count measurements. *Clinical Immunology and Immunopathology*, 70(2):152–158.

Ibrahim, M., Maswabi, K., Ajibola, G., Moyo, S., Hughes, M. D., Batlang, O., Sakoi, M., Auletta-Young, C., Vaughan, L., Lockman, S., Jean-Philippe, P., Yu, X., Lichterfeld, M., Kuritzkes, D. R., Makhema, J., and Shapiro, R. L. (2018). Targeted HIV testing at birth supported by low and predictable mother-to-child transmission risk in Botswana. *Journal of the International AIDS Society*, 21(5):e25111.

Jiang, C., Lian, X., Gao, C., Sun, X., Einkauf, K. B., Chevalier, J. M., Chen, S. M., Hua, S., Rhee, B., Chang, K., Blackmer, J. E., Osborn, M., Peluso, M. J., Hoh, R., Somsouk, M., Milush, J., Bertagnolli, L. N., Sweet, S. E., Varriale, J. A., Burbelo, P. D., Chun, T. W., Laird, G. M., Serrao, E., Engelman, A. N., Carrington, M., Siliciano, R. F., Siliciano, J. M., Deeks, S. G., Walker, B. D., Lichterfeld, M., and Yu, X. G. (2020). Distinct viral reservoirs in individuals with spontaneous control of HIV-1. *Nature*, 585(October 2019).

Joos, B., Fischer, M., Kuster, H., Pillai, S. K., Wong, J. K., Böni, J., Hirschel, B., Weber, R., Trkola, A., Günthard, H. F., Battegay, M., Bernasconi, E., Böni, J., Bucher, H. C., Bürgisser, P., Calmy, A., Cattacin, S., Cavassini, M., Dubs, R., Egger, M., Elzi, L., Fischer, M., Flepp, M., Fontana, A., Francioli, P., Furrer, H., Fux, C., Gorgievski, M., Günthard, H., Hirsch, H., Hirschel, B., Hösli, I., Kahlert, C., Kaiser, L., Karrer, U., Kind, C., Klimkait, T., Ledergerber, B., Martinetti, G., Martinez, B., Müller, N., Nadal, D., Paccaud, F., Pantaleo, G., Rauch, A., Regenass, S., Rickenbach, M., Rudin, C., Schmid, P., Schultze, D., Schüpbach, J., Speck, R., Taffé, P., Telenti, A., Trkola, A., Vernazza, P., Weber, R., and Yerly, S. (2008). HIV rebounds from latently infected cells, rather than from continuing low-level replication. *Proceedings of the National Academy of Sciences of the United States of America*, 105(43):16725–16730.

R

Kaufmann, G. R., Cunningham, P., Kelleher, A. D., Zaunders, J., Carr, A., Vizzard, J., Law, M., and Cooper, D. A. (1998). Patterns of viral dynamics during primary human immunodeficiency virus type 1 infection. *Journal of Infectious Diseases*, 178(6):1812–1815.

Kaufmann, G. R., Zaunders, J., and Cooper, D. A. (1999). Immune reconstitution in HIV-1 infected subjects treated with potent antiretroviral therapy. *Sexually Transmitted Infections*, 75(4):218–224.

Kelley, C. F., Barbour, J. D., and Hecht, F. M. (2007). The relation between symptoms, viral load, and viral load set point in primary HIV infection. *Journal of acquired immune deficiency syndromes (1999)*, 45(4):445–448.

Kiepiela, P., Ngumbela, K., Thobakgale, C., Ramduth, D., Honeyborne, I., Moodley, E., Reddy, S., De Pierres, C., Mncube, Z., Mkhwanazi, N., Bishop, K., Van Der Stok, M., Nair, K., Khan, N., Crawford, H., Payne, R., Leslie, A., Prado, J., Prendergast, A., Frater, J., McCarthy, N., Brander, C., Learn, G. H., Nickle, D., Rousseau, C., Coovadia, H., Mullins, J. I., Heckerman, D., Walker, B. D., and Goulder, P. (2007). CD8+ T-cell responses to different HIV proteins have discordant associations with viral load. *Nature medicine*, 13(1):46–53.

Kirschner, D. and Webb, G. F. (1996). A model for treatment strategy in the chemotherapy of aids. *Bulletin of Mathematical Biology*, 58(2):367–390.

Klein, N., Sefe, D., Mosconi, I., Zanchetta, M., Castro, H., Jacobsen, M., Jones, H., Bernardi, S., Pillay, D., Giaquinto, C., Walker, A. S., Gibb, D. M., and De Rossi, A. (2013). The Immunological and Virological Consequences of Planned Treatment Interruptions in Children with HIV Infection. *PLoS ONE*.

Koppensteiner, H., Brack-Werner, R., and Schindler, M. (2012). Macrophages and their relevance in Human Immunodeficiency Virus Type I infection. *Retrovirology*, 9(1):1–11.

Kuhn, L., Strehlau, R., Shiau, S., Patel, F., Shen, Y., Technau, K. G., Burke, M., Sherman, G., Coovadia, A., Aldrovandi, G. M., Hazra, R., Tsai, W. Y., Tiemessen, C. T., and Abrams, E. J. (2020). Early antiretroviral treatment of infants to attain HIV remission. *EClinicalMedicine*, 18:100241.

Laughton, B., Cornell, M., Kidd, M., Springer, P. E., Dobbels, E. F. M. T., Rensburg, A. J. V., Otwombe, K., Babiker, A., Gibb, D. M., Violari, A., Kruger, M., and Cotton, M. F. (2018). Five year neurodevelopment outcomes of perinatally HIV-infected children on early limited or deferred continuous antiretroviral therapy. *Journal of the International AIDS Society*, 21(5):e25106.

R

Laughton, B., Naidoo, S., Dobbels, E. F., Boivin, M. J., van Rensburg, A. J., Glashoff, R. H., van Zyl, G. U., Kruger, M., and Cotton, M. F. (2019). Neurodevelopment at 11 months after starting antiretroviral therapy within 3 weeks of life. *Southern African journal of HIV medicine*, 20(1).

Lawrie, D., Payne, H., Nieuwoudt, M., and Glencross, D. K. (2015). Observed full blood count and lymphocyte subset values in a cohort of clinically healthy South African children from a semi-informal settlement in Cape Town. *South African Medical Journal*, 105(7):589–595.

Levy, O. (2007). Innate immunity of the newborn: basic mechanisms and clinical correlates. *Nature reviews. Immunology*, 7(5):379–390.

Lewis, J., Payne, H., Sarah Walker, A., Otwombe, K., Gibb, D. M., Babiker, A. G., Panchia, R., Cotton, M. F., Violari, A., Klein, N., and Callard, R. E. (2017). Thymic output and CD4 T-cell reconstitution in HIV-infected children on early and interrupted antiretroviral treatment: Evidence from the children with HIV early antiretroviral therapy trial. *Frontiers in Immunology*, 8(SEP):1162.

Lewis, J., Walker, A. S., Castro, H., De Rossi, A., Gibb, D. M., Giaquinto, C., Klein, N., and Callard, R. (2012). Age and CD4 count at initiation of antiretroviral therapy in HIV-infected children: Effects on long-term T-cell reconstitution. *Journal of Infectious Diseases*, 205(4):548–556.

Li, K., Peng, Y. G., Yan, R. H., Song, W. Q., Peng, X. X., and Ni, X. (2020). Age-dependent changes of total and differential white blood cell counts in children. *Chinese medical journal*, 133(16):1900–1907.

Lindbäck, S., Karlsson, A. C., Mittler, J., Blaxhult, A., Carlsson, M., Briheim, G., Sönnerborg, A., and Gaines, H. (2000). Viral dynamics in primary HIV-1 infection. Karolinska Institutet Primary HIV Infection Study Group. *AIDS*, 14(15):2283–2291.

Little, S. J., McLean, A. R., Spina, C. A., Richman, D. D., and Havlir, D. V. (1999). Viral Dynamics of Acute HIV-1 Infection. *The Journal of Experimental Medicine*, 190(6):841.

Liu, L., Oza, S., Hogan, D., Chu, Y., Perin, J., Zhu, J., Lawn, J. E., Cousens, S., Mathers, C., and Black, R. E. (2016). Global, regional, and national causes of under-5 mortality in 2000-15: an updated systematic analysis with implications for the Sustainable Development Goals. *Lancet*, 388(10063):3027–3035.

Luzuriaga, K., Gay, H., Ziemniak, C., Sanborn, K. B., Somasundaran, M., Rainwater-Lovett, K., Mellors, J. W., Rosenbloom, D., and Persaud, D. (2015). Viremic Relapse

R

after HIV-1 Remission in a Perinatally Infected Child. *New England Journal of Medicine*, 372(8):786–788.

Luzuriaga, K., Tabak, B., Garber, M., Chen, Y. H., Ziemniak, C., McManus, M. M., Murray, D., Strain, M. C., Richman, D. D., Chun, T. W., Cunningham, C. K., and Persaud, D. (2014). HIV Type 1 (HIV-1) Proviral reservoirs decay continuously under sustained Virologic control in HIV-1-infected children who received early treatment. *Journal of Infectious Diseases*, 210(10):1529–1538.

Markowitz, M., Louie, M., Hurley, A., Sun, E., Di Mascio, M., Perelson, A. S., and Ho, D. D. (2003). A novel antiviral intervention results in more accurate assessment of human immunodeficiency virus type 1 replication dynamics and T-cell decay in vivo. *Journal of virology*, 77(8):5037–5038.

McBrien, J. B., Kumar, N. A., and Silvestri, G. (2018). Mechanisms of CD8 + T cell-mediated suppression of HIV/SIV replication. *European journal of immunology*, 48(6):898–914.

McIntosh, K., Ahevitz, A., Zaknun, D., Kornegay, J., Chatis, P., Karthas, N., and Burchett, S. K. (1996). Age- and Time-related Changes in Extracellular Viral Load in Children Vertically Infected by Human Immunodeficiency Virus. *The Pediatric Infectious Disease Journal*, 15.

Millar, J. R., Bengu, N., Vieira, V. A., Adland, E., Roider, J., Muenchhoff, M., Fillis, R., Sprenger, K., Ntlantsana, V., Fatti, I., Archary, M., Groll, A., Ismail, N., García-Guerrero, M. C., Matthews, P. C., Ndung'u, T., Puertas, M. C., Martinez-Picado, J., and Goulder, P. (2021). Early Initiation of Antiretroviral Therapy Following In Utero HIV Infection Is Associated With Low Viral Reservoirs but Other Factors Determine Viral Rebound. *The Journal of Infectious Diseases*, 224(11):1925–1934.

Morris, S. E., Dziobek-Garrett, L., Strehlau, R., Schröter, J., Shiau, S., Anelone, A. J., Paximadis, M., de Boer, R. J., Abrams, E. J., Tiemessen, C. T., Kuhn, L., and Yates, A. J. (2020). Quantifying the Dynamics of HIV Decline in Perinatally Infected Neonates on Antiretroviral Therapy. *Journal of acquired immune deficiency syndromes (1999)*, 85(2):209–218.

Morris, S. E., Strehlau, R., Shiau, S., Abrams, E. J., Tiemessen, C. T., Kuhn, L., Yates, A. J., study Team, t. E. C., and the LEOPARD (2022). Healthy dynamics of CD4 T cells may drive HIV resurgence in perinatally-infected infants on antiretroviral therapy. *medRxiv*, page 2022.02.09.22270686.

Mosier, D. E., Sprent, J., and Tough, D. (1995). CD4+ cell turnover. *Nature*, 375(6528):193–194.

Nagaraja, P., Gopalan, B. P., D'Souza, R. R., Sarkar, D., Rajnala, N., Dixit, N. M., and Shet, A. (2021). The within-host fitness of HIV-1 increases with age in ART-naïve HIV-1 subtype C infected children. *Scientific Reports*, 11(1):1–10.

National Institutes of Health (2022). Antiretroviral Management of Newborns with Perinatal HIV Exposure or HIV Infection.

Newell, M. L. (1998). Mechanisms and timing of mother-to-child transmission of HIV-1. *AIDS*, 12(8):831–837.

Nowak, M. A. and Bangham, C. R. (1996). Population dynamics of immune responses to persistent viruses. *Science*, 272(5258):74–79.

Nowak, M. A., Lloyd, A. L., Vasquez, G. M., Wiltrout, T. A., Wahl, L. M., Bischof-berger, N., Williams, J., Kinter, A., Fauci, A. S., Hirsch, V. M., and Lifson, J. D. (1997). Viral dynamics of primary viremia and antiretroviral therapy in simian immunodeficiency virus infection. *Journal of virology*, 71(10):7518–7525.

Nowak, M. A. and May, R. M. (2000). *Virus Dynamics: Mathematical Principles of Immunology and Virology*. Oxford University Press, Oxford; New York.

O'Gorman, M. R. and Zijenah, L. S. (2008). CD4 T cell measurements in the management of antiretroviral therapy - A review with an emphasis on pediatric HIV-infected patients. *Cytometry Part B - Clinical Cytometry*, 74(SUPPL. 1):19–26.

Okoye, A. A., Hansen, S. G., Vaidya, M., Fukazawa, Y., Park, H., Duell, D. M., Lum, R., Hughes, C. M., Ventura, A. B., Ainslie, E., Ford, J. C., Morrow, D., Gilbride, R. M., Legasse, A. W., Hesselgesser, J., Geleziunas, R., Li, Y., Oswald, K., Shoe-maker, R., Fast, R., Bosche, W. J., Borate, B. R., Edlefsen, P. T., Axthelm, M. K., Picker, L. J., and Lifson, J. D. (2018). Early antiretroviral therapy limits SIV reservoir establishment to delay or prevent post-treatment viral rebound. *Nature medicine*.

Pakker, N. G., Notermans, D. W., De Boer, R. J., Roos, M. T., De Wolf, F., Hill, A., Leonard, J. M., Danner, S. A., Miedema, F., and Schellekens, P. T. (1998). Biphasic kinetics of peripheral blood T cells after triple combination therapy in HIV-1 infection: A composite of redistribution and proliferation. *Nature Medicine*, 4(2):208–214.

Palma, P., Cotugno, N., Rossi, P., and Giaquinto, C. (2019). The mission is remission: Hope for controlling HIV replication without ART in early-treated perinatally HIV-infected children. *Pediatric Infectious Disease Journal*, 38(1):95–98.

R

Palma, P., Foster, C., Rojo, P., Zangari, P., Yates, A., Cotugno, N., Klein, N., Luzuriaga, K., Pahwa, S., Nastouli, E., Gibb, D. M., Borkowsky, W., Bernardi, S., Calvez, V., Manno, E., Mora, N., Compagnucci, A., Wahren, B., Muñoz-Fernández, M., De Rossi, A., Ananworanich, J., Pillay, D., Giaquinto, C., and Rossi, P. (2015). The EPIICAL project: an emerging global collaboration to investigate immunotherapeutic strategies in HIV-infected children. *Journal of virus eradication*, 1(3):134–139.

Parham, P. (2013). *The Immune System*. Garland Science, Taylor & Francis Group, New York, 4 edition.

Payne, H., Lawrie, D., Nieuwoudt, M., Cotton, M. F., Gibb, D. M., Babiker, A., Glencross, D., and Klein, N. (2020). Comparison of Lymphocyte Subset Populations in Children From South Africa, US and Europe. *Frontiers in Pediatrics*, 8(July):1–12.

Payne, H., Mkhize, N., Otwombe, K., Lewis, J., Panchia, R., Callard, R., Morris, L., Babiker, A., Violari, A., Cotton, M. F., Klein, N. J., and Gibb, D. M. (2015). Reactivity of routine HIV antibody tests in children who initiated antiretroviral therapy in early infancy as part of the Children with HIV Early Antiretroviral Therapy (CHER) trial: A retrospective analysis. *The Lancet Infectious Diseases*.

Penazzato, M., Townsend, C. L., Rakhmanina, N., Cheng, Y., Archary, M., Cressey, T. R., Kim, M. H., Musiime, V., Turkova, A., Ruel, T. D., Rabie, H., Sugandhi, N., Rojo, P., Doherty, M., Abrams, E. J., Abrams, E., Ananworanich, J., Andrieux-Meyer, I., Belew, Y., Best, B., Bologna, R., Burry, J., Carpenter, D., Clayden, P., Colbers, A., Conway, M., Cressey, T. R., Dangarembizi, M., Essajee, S., Gonzalez Tome, M., Hill, A., Khoo, S., Kim, M., Lewis, L., Lee, J., Lockman, S., Mahaka, I., Mirochnick, M. H., Mofenson, L., Muhimpundu, M., Mushavi, A., Obimbo, E., Pascual, F., Perez Casas, C., Pozniak, A., Ruel, T., Schapiro, J., Siberry, G., Simione, T. B., Tidiane Tall, C., Venter, F., Vicari, M., Walsh, J., Wambui, J., and Watkins, M. (2019). Prioritising the most needed paediatric antiretroviral formulations: the PADO4 list. *The Lancet HIV*, 6(9):e623–e631.

Perelson, A. S. (2002). Modelling viral and immune system dynamics. *Nature reviews. Immunology*, 2(1):28–36.

Perelson, A. S., Essunger, P., Cao, Y., Vesanen, M., Hurley, A., Saksela, K., Markowitz, M., and Ho, D. D. (1997). Decay characteristics of HIV-1-infected compartments during combination therapy. *Nature*, 387(6629):188–191.

Perelson, A. S. and Nelson, P. W. (1999). Mathematical Analysis of HIV-1 Dynamics in Vivo. *Society for Industrial and Applied Mathematics*, 41(1):3–44.

Perelson, A. S., Neumann, A. U., Markowitz, M., Leonard, J. M., and Ho, D. D. (1996). HIV-1 Dynamics in Vivo: Virion Clearance Rate, Infected Cell Life-Span, and Viral Generation Time. *Science*, 271(5255):1582–1586.

Persaud, D., Gay, H., Ziemniak, C., Chen, Y. H., Piatak, M., Chun, T.-W., Strain, M., Richman, D., and Luzuriaga, K. (2013). Absence of Detectable HIV-1 Viremia after Treatment Cessation in an Infant. *New England Journal of Medicine*, 369(19):1828–1835.

Picat, M. Q., Lewis, J., Musiime, V., Prendergast, A., Nathoo, K., Kekitiinwa, A., Nahirya Ntege, P., Gibb, D. M., Thiebaut, R., Walker, A. S., Klein, N., Callard, R., Munderi, P., Nahirya-Ntege, P., Katuramu, R., Matama, L., Nankya, F., Nabulime, G., Ruberantwari, A., Sebukyu, R., Tushabe, G., Nakitto-Kesi, D., Mugyenyi, P., Musiime, V., Keishanyu, R., Afayo, V. D., Bwomezi, J., Byaruhanga, J., Erimu, P., Karungi, C., Kizito, H., Namala, W. S., Namusanje, J., Nandugwa, R., Najjuko, T. K., Natukunda, E., Ndigendawani, M., Nsiyona, S. O., Robinah, K., Bainomuhwezi, B., Sseremba, D., Tezikyabbiri, J., Tumusiime, C. S., Balaba, A., Mugumya, A., Nathoo, K. J., Bwakura-Dangarembizi, M. F., Chidziva, E., Mhute, T., Vhembo, T., Mandidewa, R., Nyoni, D., Tinago, G. C., Bhiri, J., Muchabaiwa, D., Phiri, M., Masore, V., Marozva, C. C., Maturure, S. J., Tsikirayi, S., Munetsi, L., Rashirai, K. M., Steamer, J., Nhema, R., Bikwa, W., Tambawoga, B., Mufuka, E., Kekitiinwa, A., Musoke, P., Bakeera-Kitaka, S., Namuddu, R., Kasirye, P., Babirye, A., Asello, J., Nakalanzi, S., Ssemambo, N. C., Nakafeero, J., Tikabibamu, J., Musoba, G., Ssanyu, J., Kisekka, M., Gibb, D. M., Thomason, M. J., Walker, A. S., Cook, A. D., Naidoo, B., Spyer, M. J., Male, C., Glabay, A. J., Kendall, L. K., and Prendergast, A. (2013). Predicting Patterns of Long-Term CD4 Reconstitution in HIV-Infected Children Starting Antiretroviral Therapy in Sub-Saharan Africa: A Cohort-Based Modelling Study. *PLoS Medicine*, 10(10):e1001542.

Puthanakit, T., Ananworanich, J., Vonthanak, S., Kosalaraksa, P., Hansudewechakul, R., Van Der Lugt, J., Kerr, S. J., Kanjanavanit, S., Ngampiyaskul, C., Wongsawat, J., Luesomboon, W., Vibol, U., Pruksakaew, K., Suwarnlerk, T., Apornpong, T., Ratanadilok, K., Paul, R., Mofenson, L. M., Fox, L., Valcour, V., Brouwers, P., and Ruxrungtham, K. (2013). Cognitive function and neurodevelopmental outcomes in HIV-infected children older than 1 year of age randomized to early versus deferred antiretroviral therapy: The PREDICT neurodevelopmental study. *Pediatric Infectious Disease Journal*, 32(5):501–508.

R

R Development Core Team (2003). R: A language and environment for statistical computing.

Ribeiro, R. M., Hazenberg, M. D., Perelson, A. S., and Davenport, M. P. (2006). Naïve and Memory Cell Turnover as Drivers of CCR5-to-CXCR4 Tropism Switch in Human Immunodeficiency Virus Type 1: Implications for Therapy. *Journal of Virology*, 80(2):802–809.

Ribeiro, R. M., Qin, L., Chavez, L. L., Li, D., Self, S. G., and Perelson, A. S. (2010). Estimation of the Initial Viral Growth Rate and Basic Reproductive Number during Acute HIV-1 Infection. *Journal of Virology*, 84(12):6096–6102.

Richardson, B. A., Mbori-Ngacha, D., Lavreys, L., John-Stewart, G. C., Nduati, R., Panteleeff, D. D., Emery, S., Kreiss, J. K., and Overbaugh, J. (2003). Comparison of Human Immunodeficiency Virus Type 1 Viral Loads in Kenyan Women, Men, and Infants during Primary and Early Infection. *Journal of Virology*, 77(12):7120–7123.

Sáez-Cirión, A., Bacchus, C., Hocqueloux, L., Avettand-Fenoel, V., Girault, I., Lecuroux, C., Potard, V., Versmisse, P., Melard, A., Prazuck, T., Descours, B., Guergnon, J., Viard, J. P., Boufassa, F., Lambotte, O., Goujard, C., Meyer, L., Costagliola, D., Venet, A., Pancino, G., Autran, B., and Rouzioux, C. (2013). Post-Treatment HIV-1 Controllers with a Long-Term Virological Remission after the Interruption of Early Initiated Antiretroviral Therapy ANRS VISCONTI Study. *PLOS Pathogens*, 9(3).

Salzmann-Manrique, E., Bremm, M., Huenecke, S., Stech, M., Orth, A., Eyrich, M., Schulz, A., Esser, R., Klingebiel, T., Bader, P., Herrmann, E., and Koehl, U. (2018). Joint modeling of immune reconstitution post haploidentical stem cell transplantation in pediatric patients with acute leukemia comparing CD34+-selected to CD3/CD19-depleted grafts in a retrospective multicenter study. *Frontiers in Immunology*, 9(AUG):1–12.

Schmitz, J. E., Kuroda, M. J., Santra, S., Sasseville, V. G., Simon, M. A., Lifton, M. A., Racz, P., Tenner-Racz, K., Dalesandro, M., Scallon, B. J., Ghrayeb, J., Forman, M. A., Montefiori, D. C., Peter Rieber, E., Letvin, N. L., and Reimann, K. A. (1999). Control of viremia in simian immunodeficiency virus infection by CD8+ lymphocytes. *Science*, 283(5403):857–860.

Schröter, J., Anelone, A. J., Yates, A. J., and de Boer, R. J. (2020). Time to Viral Suppression in Perinatally HIV-Infected Infants Depends on the Viral Load and CD4 T-Cell Percentage at the Start of Treatment. *Journal of acquired immune deficiency syndromes (1999)*, 83(5):522–529.

R

Schröter, J., Borghans, J. A. M., Bitter, W. M., van Dongen, J. J. M., and de Boer, R. J. (2021). Age-dependent normalisation functions for T-lymphocytes in healthy individuals. *bioRxiv*, page 2021.12.01.470754.

Shearer, W. T., Quinn, T. C., Larussa, P., Lew, J. F., Mofenson, L., Almy, S., Rich, K., Handelsman, E., Diaz, C., Pagano, M., Smeriglio, V., and Kalish, L. A. (1997). Viral load and disease progression in infants infected with human immunodeficiency virus type 1. *New England Journal of Medicine*, 336(19):1337–1342.

Shearer, W. T., Rosenblatt, H. M., Gelman, R. S., Oyomopito, R., Plaeger, S., Stiehm, E., Wara, D. W., Douglas, S. D., Luzuriaga, K., McFarland, E. J., Yogev, R., Rathore, M. H., Levy, W., Graham, B. L., and Spector, S. A. (2003). Lymphocyte subsets in healthy children from birth through 18 years of age. *Journal of Allergy and Clinical Immunology*, 112(5):973–980.

Shiau, S., Abrams, E. J., Arpadi, S. M., and Kuhn, L. (2018). Early antiretroviral therapy in HIV-infected infants: can it lead to HIV remission? *The Lancet HIV*, 5(5):e250–e258.

Simms, V., Rylance, S., Bandason, T., Dauya, E., McHugh, G., Munyati, S., Mujuru, H., Rowland-Jones, S. L., Weiss, H. A., and Ferrand, R. A. (2018). CD4+ cell count recovery following initiation of HIV antiretroviral therapy in older childhood and adolescence. *AIDS*, 32(14):1977–1982.

Soetaert, K. and Petzoldt, T. (2010). Inverse modelling, sensitivity and monte carlo analysis in R using package FME. *Journal of Statistical Software*, 33(3):1–28.

Stafford, M. A., Coreya, L., Caob, Y., Daar " ", E. S., Hob, D. D., and Perelson, A. S. (2000). Modeling Plasma Virus Concentration during Primary HIV Infection. *Journal of Theoretical Biology*, 203:285–301.

Tagarro, A., Chan, M., Zangari, P., Ferns, B., Foster, C., De Rossi, A., Nastouli, E., Muñoz-Fernández, M. A., Gibb, D., and Rossi, P. (2018a). Early and highly suppressive antiretroviral therapy are main factors associated with low viral reservoir in European perinatally HIV-infected children. *Journal of Acquired Immune Deficiency Syndromes*, 79(2):269–276.

Tagarro, A., Chan, M., Zangari, P., Ferns, B., Foster, C., De Rossi, A., Nastouli, E., Muñoz-Fernández, M. A., Gibb, D., Rossi, P., Giaquinto, C., Babiker, A., Fortuny, C., Freguja, R., Cotugno, N., Judd, A., Noguera-Julian, A., Navarro, M. L., Mellado, M. J., Klein, N., Palma, P., Rojo, P., Tagarro, A., Watters, S., Marcelin, A. G., Calvez, V., Wahren, B., Cotton, M., Robb, M., Ananworanich, J., Claiden, P., Pillay, D.,

Persaud, D., De Boer, R. J., Puthanakit, T., Ceci, A., Giannuzzi, V., Luzuriaga, K., Chomont, N., Cameron, M., Cancrini, C., Yates, A., Kuhn, L., Violari, A., Otwombe, K., and Rocchi, F. (2018b). Early and highly suppressive antiretroviral therapy are main factors associated with low viral reservoir in European perinatally HIV-infected children. In *Journal of Acquired Immune Deficiency Syndromes*, volume 79, pages 269–276. Lippincott Williams and Wilkins.

Terrade, G., Huot, N., Petitdemange, C., Lazzerini, M., Resendiz, A. O., Jacquelin, B., and Müller-Trutwin, M. (2021). Interests of the Non-Human Primate Models for HIV Cure Research. *Vaccines*, 9(9).

Thapa, P., Guyer, R. S., Yang, A. Y., Parks, C. A., Brusko, T. M., Brusko, M., Connors, T. J., and Farber, D. L. (2021). Infant T cells are developmentally adapted for robust lung immune responses through enhanced T cell receptor signaling. *Science Immunology*, 6(66):1–14.

Tobin, N. H. and Aldrovandi, G. M. (2013). Immunology of pediatric HIV infection. *Immunological reviews*, 254(1):143–169.

Tuaillon, E., Kania, D., Pisoni, A., Bollore, K., Taieb, F., Ontsira Ngoyi, E. N., Schaub, R., Plantier, J. C., Makinson, A., and Van de Perre, P. (2020). Dried Blood Spot Tests for the Diagnosis and Therapeutic Monitoring of HIV and Viral Hepatitis B and C. *Frontiers in Microbiology*, 11:373.

UNAIDS (2020). Global HIV & AIDS statistics — Fact sheet.

Valiathan, R., Ashman, M., and Asthana, D. (2016). Effects of Ageing on the Immune System: Infants to Elderly. *Scandinavian Journal of Immunology*, 83(4):255–266.

van den Heuvel, D., Jansen, M. A., Nasserinejad, K., Dik, W. A., van Lochem, E. G., Bakker-Jonges, L. E., Bouallouch-Charif, H., Jaddoe, V. W., Hooijkaas, H., van Dongen, J. J., Moll, H. A., and van Zelm, M. C. (2017). Effects of nongenetic factors on immune cell dynamics in early childhood: The Generation R Study. *Journal of Allergy and Clinical Immunology*, 139(6):1923–1934.e17.

van Dongen, J. J., van Der Burg, M., Kalina, T., Perez-Andres, M., Mejstrikova, E., Vlkova, M., Lopez-Granados, E., Wentink, M., Kienzler, A. K., Philippé, J., Sousa, A. E., Van Zelm, M. C., Blanco, E., and Orfao, A. (2019). EuroFlow-based flowcytometric diagnostic screening and classification of primary immunodeficiencies of the lymphoid system. *Frontiers in Immunology*, 10(JUN):1–21.

R

van Dorp, C. H., van Boven, M., and Boer, R. j. D. (2020). Modeling the immuno-logical pre-adaptation of HIV-1. *bioRxiv*, page 2020.01.08.897983.

van Gent, R., van Tilburg, C. M., Nibbelke, E. E., Otto, S. A., Gaiser, J. F., Janssens-Korpela, P. L., Sanders, E. A., Borghans, J. A., Wulffraat, N. M., Bierings, M. B., Bloem, A. C., and Tesselaar, K. (2009). Refined characterization and reference values of the pediatric T- and B-cell compartments. *Clinical Immunology*, 133(1):95–107.

Van Rossum, A. M., Scherpbier, H. J., Van Lochem, E. G., Pakker, N. G., Slieker, W. A., Wolthers, K. C., Roos, M. T., Kuijpers, J. H., Hooijkaas, H., Hartwig, N. G., Geelen, S. P., Wolfs, T. F., Lange, J. M., Miedema, F., De Groot, R., Jurriaans, S., Hoetelmans, R., Veerman, A. J., Vossen, J. M., Schrander, J. J., Burger, D. M., Weemaes, C. M., Niester, H. G., Osterhaus, A. D., Vulto, A. G., Boucher, C., and Rijkers, G. T. (2001). Therapeutic immune reconstitution in HIV-1-infected children is independent of their age and pretreatment immune status. *Aids*, 15(17):2267–2275.

Veel, E., Westera, L., van Gent, R., Bont, L., Otto, S., Ruijsink, B., Rabouw, H. H., Mudrikova, T., Wensing, A., Hoepelman, A. I., Borghans, J. A., and Tesselaar, K. (2018). Impact of aging, cytomegalovirus infection, and long-term treat-ment for human immunodeficiency virus on CD8+ T-Cell subsets. *Frontiers in Immunology*, 9(MAR):572.

Veldsman, K. A., Rensburg, A., Isaacs, S., Naidoo, S., Laughton, B., Lombard, C., Cotton, M. F., Mellors, J. W., and Zyl, G. U. (2019). HIV-1 DNA decay is faster in children who initiate ART shortly after birth than later. *Journal of the International AIDS Society*, 22(8):1–7.

Vieira, V. A., Millar, J., Adland, E., Muenchhoff, M., Roider, J., Guash, C. F., Peluso, D., Thomé, B., Garcia-Guerrero, M. C., Puertas, M. C., Bamford, A., Brander, C., Carrington, M., Martinez-Picado, J., Frater, J., Tudor-Williams, G., and Goulder, P. (2022). Robust HIV-specific CD4+and CD8+T-cell responses distinguish elite control in adolescents living with HIV from viremic nonprogressors. *AIDS*, 36(1):95–105.

Violari, A., Cotton, M. F., Gibb, D. M., Babiker, A. G., Steyn, J., Madhi, S. A., Jean-Philippe, P., McIntyre, J. A., and CHER Study Team (2008). Early Antiretroviral Therapy and Mortality among HIV-Infected Infants. *New England Journal of Medicine*, 359(21):2233–2244.

R

Violari, A., Cotton, M. F., Kuhn, L., Schramm, D. B., Paximadis, M., Loubser, S., Shalekoff, S., Da Costa Dias, B., Otwombe, K., Liberty, A., McIntyre, J., Babiker, A., Gibb, D., and Tiemessen, C. T. (2019). A child with perinatal HIV infection and long-term sustained virological control following antiretroviral treatment cessation. *Nature Communications*, 10(1):1–11.

Vrisekoop, N., van Gent, R., de Boer, A. B., Otto, S. A., Borleffs, J. C. C., Steingrover, R., Prins, J. M., Kuijpers, T. W., Wolfs, T. F. W., Geelen, S. P. M., Vulto, I., Lansdorp, P., Tesselaar, K., Borghans, J. A. M., and Miedema, F. (2008). Restoration of the CD4 T Cell Compartment after Long-Term Highly Active Antiretroviral Therapy without Phenotypical Signs of Accelerated Immunological Aging. *The Journal of Immunology*, 181(2):1573–1581.

Wade, A. M. and Ades, A. E. (1994). Age-related reference ranges: Significance tests for models and confidence intervals for centiles. *Statistics in Medicine*, 13(22):2359–2367.

Walker, A. S., Doerholt, K., Sharland, M., and Gibb, D. M. (2004). Response to highly active antiretroviral therapy varies with age: The UK and Ireland Collaborative HIV Paediatric Study. *Aids*, 18(14):1915–1924.

Wei, X., Ghosh, S. K., Taylor, M. E., Johnson, V. A., Emini, E. A., Deutsch, P., Lifson, J. D., Bonhoeffer, S., Nowak, M. A., Hahn, B. H., Saag, M. S., and Shaw, G. M. (1995). Viral dynamics in human immunodeficiency virus type 1 infection. *Nature*, 373(6510):117–122.

Whitney, J. B., Lim, S. Y., Osuna, C. E., Kublin, J. L., Chen, E., Yoon, G., Liu, P. T., Abbink, P., Borducci, E. N., Hill, A., Lewis, M. G., Geleziunas, R., Robb, M. L., Michael, N. L., and Barouch, D. H. (2018). Prevention of SIVmac251 reservoir seeding in rhesus monkeys by early antiretroviral therapy. *Nature Communications 2018 9:1*, 9(1):1–8.

Wodarz, D. and Nowak, M. A. (2002). Mathematical models of HIV pathogenesis and treatment. *BioEssays*, 24(12):1178–1187.

Ygberg, S. and Nilsson, A. (2012). The developing immune system – from foetus to toddler. *Acta Paediatrica*, 101(2):120–127.

Zhang, Z.-Q., Schuler, T., Zupancic, M., Wietgrefe, S., Staskus, K. A., Reimann, K. A., Reinhart, T. A., Rogan, M., Cavert, W., Miller, C. J., Veazey, R. S., Notermans, D., Little, S., Danner, S. A., Richman, D. D., Havlir, D., Wong, J., Jordan, H. L., Schacker, T. W., Racz, P., Tenner-Racz, K., Letvin, N. L., Wolinsky, S., and Haase,

R

A. T. (1999). Sexual Transmission and Propagation of SIV and HIV in Resting and Activated CD4+ T Cells. *Science*, 286(5443):1353–1357.

R

Summary

When an HIV-infected mother gives birth, the virus may be passed on to the child. Fortunately, an HIV infection is not a death sentence anymore. Since international guidelines changed in 2008 to always start treatment immediately after birth, many children nowadays survive into adolescence. They, however, depend lifelong on drugs, so called antiretroviral therapy (ART), to control the virus, and have to attend regular medical check-ups to ensure that the HIV infection remains under control.

Viral load (VL) and CD4+ T-cell data are the routine HIV measures taken from blood samples. While the VL directly indicates the amount of active virus material in the blood, the CD4+ T-cell level is an indirect measurement reflecting the health status of our immune system. CD4+ T cells are an important cell type of our immune system, which protect us from developing severe infections. These cells are, however, targeted by HIV. Thus, HIV-infected CD4+ T-cells are getting destroyed by their own immune system, which weakens the immune system over time. Consequently, if the CD4+ T cells are too low, the immune system is no longer functional, and usually harmless infections become more severe and eventually may lead to death. This last state of an HIV infection is then referred to as AIDS. ART prevents the virus to multiply and to infect further cells. Successful ART allows the immune system to recover, or, if ART is taken early enough, it helps to maintain a "healthy" immune system, recognisable by stable CD4+ T-cell levels within a healthy range.

VL and CD4+ T-cell measurements are the basis for the studies presented within this thesis. We describe previously collected longitudinal measurements by mathematical models to characterise and quantify viral and immunological dynamics in response to early treatment initiation. While previous studies have tried to find factors predicting fast viral suppression based on the whole population, we aimed to gain a better understanding of the underlying mechanisms leading to a successful viral suppression and the subsequent recovery of the immune system on a case-by-case basis. Since children are

very different, and hence a population average combines too many factors, we describe the measurements for each individual child.

In **Chapter 2**, we mainly focused on VL dynamics of children who are born with HIV and started treatment within 6 months after birth. As most children suppress VL upon treatment initiation, we have been interested how fast the VL declines, and to mathematically determine the time when VL becomes undetectable in blood for each individual child. Measurements by itself do not capture the moment of viral suppression, as measurements intervals are usually broadly distributed. Fitting an exponential decay model allowed us to better estimate the time to viral suppression. Further, we defined different patterns of the VL decay dynamics – clean and erratic. We could show that children with an erratic decay pattern have experienced more changes in their drug schedules, and concluded that those children are more likely to have had treatment complications, which would contribute to the erratic VL decline. For those children with a clean VL decay pattern, we could associate a shorter time to viral suppression with a lower VL and a healthier immune system (higher numbers of CD4+ T-cells) at the start of treatment onset. Even though previous studies have found age at start of treatment as a predictor for time to viral suppression, we surprisingly could not confirm this finding in our analysis. To note, the age range in our study is very narrow and covers only 6 months. The time of infection more or less matches with time of birth such that VL increases and CD4+ T-cell declines with the progress of an HIV infection. The age factor is thereby captured by these two variables, and no further age effect on time to viral suppression is required. Hence, we show that it is important to interfere early in an HIV infection to gain a fast control over the virus, and to also prevent treatment complications.

In the next two chapters (**Chapter 3 and 4**), we focused more on the immune system and its recovery after a successful early ART initiation. We have to be aware that the numbers of immune cells in a microliter (μL) of blood are not constant over life and that they are very dynamic, particularly in childhood. This is mainly due to the maturation of the immune system, during which immune cells proliferate. Additionally, children gain body weight and consequently blood volume, which implies a dilution process of the immune cells in blood. Thus, the number of T-cells in a μL of blood overall declines with age, which we have to take into account when quantifying CD4+ T-cells during an HIV infection.

In current literature, there are tables available listing counts and percentages of immune cells for different age categories. These categories are, however,

usually quite broad, and thus not reflecting natural T-cell dynamics on a smaller scale. In **Chapter 3** we therefore studied the healthy immune cell dynamics from birth to 60 years of age in a continuous manner to gain proper reference functions of T-cell dynamics over age. We had individual measurements of healthy individuals available, and in contrast to a previous study we ensured to make use of sufficiently accumulated paediatric measurements. This allowed us to distinguish two phases in the natural dynamics of T-cells. During an initial phase, which we have determined to last for half a year, T-cell counts linearly increase. This is followed by a second phase, in which T-cells exponentially decay. The composition of a T-cell subset varies with the exposure of pathogens. Naïve T-cells get transiently activated and become effector cells, before they then differentiate into so-called memory T-cells, which patrol and accelerate the clearance of a reinduced infection with the same pathogen. Thus, the subpopulation of naïve T-cell counts decline over time, while the memory T-cell counts increase until they both reach a balancing equilibrium (homeostasis). We were able to capture these opposite dynamics with the same mathematical model. A novelty of our study has been the way how we gained fits for the cell counts. Instead of fitting the often computed cell counts directly, we have taken the laboratory procedure into account. Thus, we have fitted the truly measured percentages of T-cell subsets and derived from there the function for the counted data. This procedure has the advantage that counts and percentages of one subset are dependent, resulting in a consistent set of parameters, which can be used to describe both dynamics of count data and percentages. Hence, we obtained reference functions for healthy T-cell dynamics, which provide the basis for the quantification of CD4+ T-cell dynamics in response to early ART initiation in the next chapter.

In **Chapter 4**, we normalised CD4+ T cells to the reference functions obtained in Chapter 3, and we thereby defined a distance to "healthy" levels. We are interested if CD4+ T-cells recover during successful treatment, and if so, how fast they recover. During the untreated phase of HIV, these distances to healthy had become negative. With treatment initiation, the CD4 courses follow a model with an initial increase, and then reaching a stable level. This model allows us to identify the recovery rate, the time of stabilisation of CD4+ T cells and the level of CD4 stabilisation. We showed that healthy CD4+ T-cell levels are typically restored during treatment. CD4+ T-cell counts and percentages show similar recovery dynamics, suggesting that mainly CD4+ T-cells recover compared to other lymphocyte subsets. CD4 recovery is rather slow compared to the natural production of new cells and usually occurs after viral load is suppressed, i.e.,

3-13 months after treatment initiation. We could identify a density dependence in CD4 recovery, meaning that the lower the initial CD4+ T-cell levels were at start of treatment the faster their recovery. We could not find any direct evidence that CD4+ T-cell reconstitution is age dependent. Furthermore, we have seen in children with an erratic VL decay pattern, that CD4 recovery is delayed but still tend to normalise after the VL is controlled. Hence, an early treatment initiation helps to keep CD4 depletion typically low and supports a "full" CD4+ T-cell recovery in numbers.

While we studied the impact of early initiated treatment in the previous chapters, **Chapter 5** is a more hypothetical study of the paediatric viral load dynamics in the case of no treatment. We focused on the differences in VL dynamics between young children and adults, and investigated in which ways these can be mechanistically explained. Untreated children often experience a higher VL that they are maintaining for years, while adult's VL decline to a somewhat lower stable level, the so-call setpoint VL. In general, high VLs are associated with a more rapid disease progression and children die within 2 years if remain untreated. Based on a mathematical model for an adult acute HIV infection, we swept parameters to identify which component of the model results in a high peak VL but a poor contraction to a high setpoint VL. We showed that the viral replication rate is comparable to adults. We further saw that a virus without cytopathic effects can dampen the VL contraction in the absence of an immune response. In the absence of an immune response, a lower VL contraction ratio is also achieved by a higher turnover of the target cells. Lastly, we showed that the immune response itself influences the VL contraction the most. Hence, a weak cytotoxic immune response explains the observed phenomena the best, indicating that early treatment is essential to allow the infant immune system to mature, and contribute to the control of the virus.

Taken together, we paved a path towards a better understanding of the viral and immunological dynamics in children born with HIV, who have started treatment early. We showed that an early treatment initiation in children is beneficial in controlling the virus in a quick and clean manner and allow the immune system either to be maintained, or to recover to almost healthy levels. A successful control of the virus and a healthy immune system are important to ensure a healthy development for each child and are required for future clinical approaches, such as establishing a "functional" cure.

S

Samenvatting

Wanneer een moeder met HIV een kind krijgt, kan het virus worden doorgegeven aan het kind. Gelukkig is een HIV-infectie geen doodvonnis meer. Sinds 2008 schrijven de internationale richtlijnen voor om dit soort kinderen direct vanaf hun geboorte te behandelen met antiretrovirale geneesmiddelen (antiretrovirale therapie, ART). Hierdoor overleven veel kinderen tegenwoordig de infectie. Zij blijven echter wel levenslang afhankelijk van medicijnen om het virus onder controle te houden. Daarnaast krijgen zij regelmatig medische controles om het virus in de gaten te houden.

Tijdens deze medische controles wordt onder andere gekeken naar twee bloedwaarden: de viruslast (VL) en de hoeveelheid CD4+ T-cellen in een milliliter bloed. Terwijl de VL een directe indicator is van de hoeveelheid actieve virusdeeltjes in het bloed, is de CD4-waarde een indirecte indicator van de gezondheid van het immuunsysteem. CD4+ T-cellen zijn namelijk witte bloedcellen die een belangrijke rol spelen in ons immuunsysteem en ons helpen beschermen tegen infecties. Het zijn echter ook de cellen die besmet worden door HIV. Het virus dringt deze cellen binnen en gebruikt ze vervolgens om zichzelf te vermeerderen. Hierdoor sterven de CD4-cellen af: ze worden of van binnenuit kapot gemaakt door het virus, of ze worden aangevallen door het immuunsysteem dat geïnfecteerde cellen aanvalt om infecties uit het lichaam te verwijderen. Door het afsterven van CD4-cellen wordt het immuunsysteem steeds zwakker, tot het uiteindelijk niet goed meer functioneert en normaal gesproken onschuldige infecties kunnen leiden tot ernstige symptomen en zelfs de dood. Op dat moment spreken we van AIDS. ART onderdrukt de vermeerdering van HIV in het lichaam, en voorkomt dat het virus CD4-cellen infecteert. Als de ART goed aanslaat kan het immuunsysteem zich herstellen, of, wanneer patiënten ART nemen ruim voor zij AIDS ontwikkelen, voorkomen dat het immuunsysteem achteruitgaat. Dit is dan terug te zien in stabiele, gezonde CD4-waarden.

In dit proefschrift worden VL-metingen en CD4-waarden gebruikt uit een eerder onderzoek waarin kinderen met HIV langdurig werden gevolgd. We gebruiken

S

deze data in combinatie met wiskundige modellen om een kwantitatief begrip te krijgen van hoe het virus en het immuunsysteem zich ontwikkelen over de tijd als de kinderen jong beginnen met ART. Eerdere studies zochten meestal naar voorspellende factoren voor een goede en snelle onderdrukking van het virus op basis van gemiddelden in een populatie HIV-patiënten. Maar omdat kinderen erg van elkaar kunnen verschillen, laat zo'n populatiegemiddelde niet het hele beeld zien. In dit proefschrift wordt daarom de VL- en CD4-dynamica van elk kind apart beschreven en geanalyseerd. Zo hopen wij meer te weten te komen over de mechanismen die zorgen voor onderdrukking van het virus en herstel van het immuunsysteem.

Het onderzoek in **hoofdstuk 2** richt zich op de VL-dynamica bij kinderen die geboren werden met HIV en binnen zes maanden na hun geboorte begonnen zijn met hun ART-behandeling. Bij de meeste van deze kinderen gaat de VL scherp omlaag na het begin van de behandeling, tot het virus niet meer te zien is in het bloed. Wij waren onder andere geïnteresseerd in hoelang het duurt voordat het virus niet langer te detecteren is. Omdat de VL slechts op een aantal momenten wordt gemeten, en deze momenten niet voor alle kinderen hetzelfde zijn, kan "de tijd tot suppressie" niet goed direct worden afgelezen uit de VL-data. Door een wiskundig model van exponentieel verval te fitten aan de data per kind, konden wij een betere schatting geven van de *tijd tot suppressie*. Daarnaast zagen we dat de afname van de VL op verschillende manieren kon verlopen – *clean* of juist onregelmatig. We lieten zien dat kinderen met een onregelmatig VL-patroon vaker veranderingen hebben ondergaan in hun behandelingsschema's, wat erop wijst dat deze kinderen waarschijnlijk meer complicaties hebben met hun medicijnen. Dit draagt vervolgens bij aan de onregelmatige afname van de VL. Bij de kinderen met een *clean* VL-patroon zagen we een associatie tussen een kortere *tijd tot suppressie* en een gezonder immuunsysteem (hogere CD4-waarden) aan het begin van de behandeling. Terwijl in eerdere studies de leeftijd van het kind bij het begin van ART een voorspeller bleek te zijn voor *tijd tot suppressie* (waarbij jongere kinderen het virus sneller onderdrukten), vonden wij dit leeftijdseffect niet terug. Dit komt waarschijnlijk omdat de leeftijd van een (tot dan toe onbehandeld) kind ook samenhangt met de VL, die toeneemt als het kind ouder wordt, en met de CD4-waarde, die afneemt over de tijd. Wanneer je de CD4-waarde en VL aan het begin van de behandeling meeneemt, voegt een extra leeftijdseffect weinig meer toe aan de voorspelling van de *tijd tot suppressie*. Samenvattend laten we in dit hoofdstuk zien dat het belangrijk is om jong te beginnen met de behandeling van HIV-besmette kinderen, omdat dit leidt tot snellere controle over het virus

en het risico op complicaties in de behandeling kan verlagen.

In hoofdstuk 2 keken we naar de onderdrukking van het virus als gevolg van ART. In **hoofdstuk 3 en 4** richtten we ons op het herstel van het immuunsysteem. We moeten er daarbij rekening mee houden dat het aantal immuuncellen in een microliter (μL) bloed sterk kan veranderen over de tijd, met name bij jonge kinderen. Hoewel het totaal aantal immuuncellen namelijk toeneemt terwijl het immuunsysteem zich ontwikkelt, neemt het lichaamsgewicht en daardoor het bloedvolume van groeiende kinderen ook toe, wat zorgt voor een verdunningseffect. Hierdoor neemt het aantal T-cellen per μL bloed af naarmate kinderen ouder worden. Deze natuurlijke, gezonde afname moeten we meenemen wanneer we kijken naar de CD4-waarden van jonge kinderen met HIV.

In de medische vakliteratuur zijn tabellen beschikbaar met aantallen en percentages van verschillende typen immuuncellen voor verschillende leeftijdscategorieën. Deze leeftijdscategorieën zijn echter meestal vrij grof, waardoor we geen volledig beeld hebben van het natuurlijk verloop van T-cel-concentraties over de tijd. In **hoofdstuk 3** ontwikkelden wij daarom een wiskundig model voor de gezonde dynamica van verschillende typen T-cellen van geboorte tot een leeftijd van zestig jaar. We konden daarvoor gebruik maken van metingen die gedaan zijn in gezonde proefpersonen, waarbij we erop letten dat we ook voldoende metingen uit de vroege kindertijd meenamen. We zagen dat we de natuurlijke dynamica van T-cel-concentraties in het bloed kunnen opdelen in twee fasen. In de eerste fase, die ongeveer een half jaar duurt, neemt het totale aantal immuuncellen per μL bloed lineair toe. In de tweede fase daarna zagen we juist een exponentieel verval van het totaal aantal T-cellen per μL bloed. De dynamica van verschillende typen T-cellen hangt af van de blootstelling aan ziekteverwekkers. Naïeve T-cellen worden geactiveerd als ze worden blootgesteld aan een ziekteverwekker, waarna een deel van deze cellen zich ontwikkelt tot geheugencellen die weer in actie komen bij een nieuwe blootstelling aan dezelfde ziekteverwekker. Door blootstelling aan steeds nieuwe ziekteverwekkers neemt het aantal naïeve T-cellen af over de tijd, terwijl het aantal geheugencellen toeneemt totdat er een evenwicht is bereikt. Wij lieten zien dat zowel deze afname als toename met hetzelfde wiskundige model beschreven kan worden. We maakten hierbij gebruik van een nieuwe methode om het model de geschatte celaantallen te laten beschrijven door de percentages in plaats van de aantallen direct te fitten. Hiermee komen we tot consistente parameters voor zowel de aantallen als de percentages. Op deze manier konden we referentiefuncties opstellen die een gezond verloop van de T-cel-dynamica over het leven beschrijven.

S

In **hoofdstuk 4** gebruikten we deze referentiefuncties als uitgangspunt om de CD4+ T-celdynamica in kinderen met HIV te bestuderen. Door de CD4-waarden van deze kinderen te vergelijken met de referentiefuncties konden we bepalen in hoeverre zij afwijken van een gezond niveau. Vervolgens onderzochten we of de CD4-waarden zich herstellen tijdens een ART-behandeling, en zo ja, hoe snel dat gaat. We zagen dat wanneer de kinderen nog niet behandeld werden, hun CD4-waarden lager waren dan de gezonde referentie. Na het begin van de ART-behandeling namen de CD4-waarden toe, tot zij op een bepaald stabiel niveau bleven hangen. Door deze dynamica te beschrijven met een wiskundig model, konden wij de snelheid van het herstel, het moment van stabilisatie, en het uiteindelijke stabiele niveau beschrijven. We lieten zien dat ART meestal zorgt voor herstel van het aantal CD4+ T-cellen naar een gezonde waarde. We zagen echter ook dat dit herstel relatief langzaam verloopt in vergelijking met de natuurlijke productie van nieuwe cellen. Het herstel van de CD4-waarde werd meestal pas gezien 3-13 maanden nadat het virus in het bloed onderdrukt was. Daarnaast vonden we een dichtheidsafhankelijkheid in het CD4-herstel: hoe lager de CD4-waarde op het moment dat de behandeling begon, hoe hoger de snelheid waarmee de CD4-waarde toenam. Het CD4-herstel hing niet direct af van de leeftijd van de kinderen. Bij de kinderen met een onregelmatige VL-afname ging het CD4-herstel langzamer dan bij kinderen met een *clean* VL-afname, maar ook bij deze kinderen normaliseerden de CD4-waarden als de VL eenmaal onder controle was. Deze studie laat zien dat een vroege ART-behandeling bijdraagt aan het voorkomen van uitputting van de CD4+ T-cellen en kan zorgen voor volledig herstel naar gezonde CD4-waarden.

Tot nu toe hebben we gekeken naar het effect van een vroege ART-behandeling bij kinderen met HIV. In **hoofdstuk 5** onderzochten we juist hoe de VL zich zou ontwikkelen als de kinderen niet behandeld zouden worden, hoe dit verschilt met geïnfecteerde volwassenen en welke mechanismen de verschillen kunnen verklaren. Als kinderen geen ART-behandeling krijgen, blijft de VL vaak erg hoog, terwijl de VL in volwassenen na de eerste besmettingspiek meestal afneemt naar een lager stabiel niveau dat per persoon verschilt en de *set-point viral load* wordt genoemd. Patiënten met een hoge VL krijgen over het algemeen sneller AIDS. Als kinderen geen ART krijgen, sterven zij vaak binnen twee jaar. In deze studie gebruikten we een wiskundig model van een acute HIV-infectie bij volwassenen. We bestudeerden het model voor een reeks verschillende parameterwaarden om te onderzoeken welke mechanismen kunnen zorgen voor de dynamica die wordt gezien in jonge kinderen: een hoge piek in de VL

die vervolgens niet of weinig afneemt. We konden allereerst laten zien dat de replicatiesnelheid van het virus niet hoger lijkt te zijn in jonge kinderen dan in volwassenen om het verschil te verklaren. We zagen dat een hoge turn-over van de CD4+ T-cellen (bijvoorbeeld doordat de CD4+ T-cellen zich snel delen) ervoor kan zorgen dat de VL weinig afneemt. Maar de afname van de VL bleek vooral afhankelijk te zijn van de immuunrespons tegen het virus. Wanneer het lichaam niet in staat is om een goede immuunrespons op te zetten, bijvoorbeeld omdat het immuunsysteem daarvoor nog niet ver genoeg ontwikkeld is, gaat de VL niet of nauwelijks omlaag. Dit laat zien dat een belangrijk effect van een vroege ART-behandeling is dat het immuunsysteem van het kind zich kan ontwikkelen, zodat het daarna kan bijdragen aan het onderdrukken van het virus.

De studies in dit proefschrift dragen bij aan een beter begrip van de ontwikkeling over de tijd van HIV en het immuunsysteem in jonge kinderen met HIV. Ze laten zien dat het vroeg beginnen van een ART-behandeling voordeel oplevert op meerdere vlakken: een vroege start van de behandeling hangt samen met een snelle en regelmatige afname van de VL, en met een kleiner negatief effect op het zich nog ontwikkelende immuunsysteem of met herstel tot een bijna gezond niveau. Onderdrukking van het virus en een gezond immuunsysteem zijn belangrijk voor een goede ontwikkeling van ieder kind. Daarnaast is het een eerste voorwaarde voor een "functionele" genezing van HIV-infectie.

S

Zusammenfassung

Eine HIV-infizierte Mutter kann bei der Geburt das Virus an ihr Kind weitergeben. Glücklicherweise ist eine HIV-Infektion heute kein Todesurteil mehr. Seit 2008 schreiben internationale Richtlinien vor, dass Kinder, die bei der Geburt mit HIV infiziert wurden, sofort behandelt werden müssen. Dadurch überleben heutzutage viele Kinder und wachsen mit einer HIV-Infektion auf. Diese Kinder sind aber darauf angewiesen Medikamente einzunehmen. Sie müssen sich einer sogenannten antiretroviralen Therapie (ART) unterziehen, um das Virus zu kontrollieren, und regelmäßige Untersuchungen erdulden, um sicher zu stellen, dass die HIV-Infektion unter Kontrolle bleibt.

Zu den Routineuntersuchungen bei einer HIV-Infektion gehört die Blutentnahme zur Bestimmung der Viruslast (VL) und zur Messung der CD4+ T-Zellen. Über die VL wird eine direkte Angabe der Menge von aktiven Viruspartikeln im Blut gemacht, während der CD4-Wert eine indirekte Angabe für den Gesundheitszustand des Immunsystems ist. CD4+ T-Zellen sind ein wichtiger Bestandteil unseres Immunsystems, die uns vor schweren Infektionen schützen. Diese Zellen werden jedoch von HIV angegriffen und zur Vermehrung verwendet. HIV-infizierte CD4+ T-Zellen werden wiederum vom eigenen Immunsystem erkannt und zerstört. Über längere Zeit schwächt sich das Immunsystem somit selbst, was zur Folge hat, dass normalerweise harmlose Infektionen schlimmer werden und sogar zum Tod führen können. Diesen Endzustand einer HIV-Infektion bezeichnet man dann als AIDS. In diesem Zusammenhang verhindert ART, dass sich das Virus vermehren kann und weiterhin Zellen infiziert. Erfolgreiche ART ermöglicht dem Immunsystem sich zu erholen, oder, wenn ART früh angesetzt wird, hilft es sogar, das Immunsystem „gesund" zu erhalten, was an einer stabilen Anzahl von CD4+ T-Zellen im Normalbereich zu erkennen ist.

Diese Doktorarbeit verwendet VL-Messungen und CD4-Werte aus früheren Studien, in denen Kinder mit HIV über längere Zeit beobachtet wurden. Wir verwenden diese Daten in Kombination mit mathematischen Modellen, um ein quantitatives Verständnis dafür zu bekommen, wie sich das Virus und das

Immunsystem im Laufe der Zeit entwickeln, wenn Kinder in einem frühen Alter mit ART beginnen. Frühere Studien haben hauptsächlich nach Faktoren gesucht, die für eine gute und schnelle Unterdrückung des Virus voraussagend sind und basierten sich auf die Durchschnittswerte in einer Population von HIV-Patienten. Da sich Kinder aber stark voneinander unterscheiden können, zeigt ein solcher Bevölkerungsdurchschnitt nicht das Gesamtbild. Daher beschreibt und analysiert diese Arbeit die VL- und CD4-Verläufe jedes Kindes separat. Auf diese Weise hoffen wir, mehr über die Mechanismen zu erfahren, die das Virus unterdrücken und das Immunsystem wiederherstellen.

In **Kapitel 2** nehmen wir den Verlauf der VL von Kindern in den Blick, die mit HIV geboren wurden und deren Medikation innerhalb der ersten sechs Monate begann. Da die meisten Kinder die VL während der Behandlung unterdrücken, sind wir daran interessiert zu erfahren, wie schnell die VL abfällt und bestimmen mathematisch den Zeitpunkt, ab dem das Virus nicht weiter im Blut nachgewiesen werden kann. Messdaten selbst, erfassen oft den Zeitpunkt der Unterdrückung des Virus nicht, da die Abstände zwischen den Messzeitpunkten in der Regel zu groß sind. Indem wir ein mathematisches Modell, das einem exponentiellen Zerfall folgt, an die Daten anpassen, können wir den "Zeitpunkt der VL-Unterdrückung" genauer bestimmen. Des Weiteren unterscheiden wir verschiedene Muster der VL-Abnahme – regelmäßige und unregelmäßige. Wir konnten zeigen, dass Kinder mit einem unregelmäßigen Abnahme mehrere Wechsel im Medikamentenplan aufwiesen. Daraus schließen wir, dass diese Kinder womöglich häufiger Komplikationen mit ihrer ART aufzeigten, was wiederum eine unregelmäßige VL-Abnahme bestätigen würde. Bei Kindern mit einer regelmäßigen VL-Abnahme konnten wir eine kürzere Zeit bis zur VL-Unterdrückung mit einer niedrigeren VL und einem gesünderen Immunsystem (höhere Anzahl von CD4+ T-Zellen) am Anfang der Behandlung in Zusammenhang bringen. Auch wenn frühere Studien das Alter vom Behandlungsstart als Prädikator für die Zeit der VL-Unterdrückung als ausschlaggebend angesehen haben, konnten wir das Alter zu Beginn der Behandlung als einen eigenständigen Faktor in unseren Analysen nicht bestätigen. Dies liegt wahrscheinlich daran, dass der Zeitpunkt der Infektion nur schwer vom Zeitpunkt der Geburt zu unterscheiden ist. Das Alter eines (bis dahin unbehandelten) Kindes stimmt somit mit dem Fortschreiten der HIV-Infektion überein, wobei die VL zunimmt, während der CD4-Wert mit der Zeit abnimmt. Wenn man nun den CD4-Wert und die VL zu Beginn der Behandlung betrachtet, trägt ein zusätzlicher Alterseffekt nur wenig zur Vorhersage der Zeit bis zur Unterdrückung der VL bei. Anzumerken ist hierbei auch, dass die Altersspanne in unserer Studie sehr schmal ist und nur

sechs Monate umfasst. Zusammenfassend zeigen wir in diesem Kapitel, dass es wichtig ist, mit der Behandlung HIV-infizierter Kinder in einem frühen Alter zu beginnen, da dies zu einer schnelleren Kontrolle des Virus führt und das Risiko von Behandlungskomplikationen verringern kann.

In den nächsten beiden Kapiteln (**Kapitel 3 und 4**), konzentrieren wir uns mehr auf das Immunsystem und seine Erholung, nach erfolgreichem frühen Behandlungsbeginn. Dabei muss berücksichtigt werden, dass sich die Anzahl der Immunzellen in einem Mikroliter (μL) Blut im Laufe des Lebens stark verändern kann, insbesondere bei Kleinkindern. Obwohl die Gesamtzahl der Immunzellen mit der Entwicklung des Immunsystems zunimmt, nimmt auch das Körpergewicht und damit das Blutvolumen heranwachsender Kinder zu, was zu einem Verdünnungseffekt der Immunzellen im Blut führt. Dadurch nimmt die Anzahl der T-Zellen pro μL Blut mit zunehmendem Alter der Kinder ab. Wir müssen diesen natürlichen, gesunden Rückgang berücksichtigen, wenn wir den CD4-Spiegel bei Kleinkindern mit HIV betrachten.

In der medizinischen Fachliteratur sind Tabellen mit Anzahlen und Prozentsätzen verschiedener Arten von Immunzellen für unterschiedliche Alterskategorien verfügbar. Diese Alterskategorien sind jedoch in der Regel recht breit angelegt und reflektieren deswegen nicht die natürlichen T-Zellverläufe auf einer feineren Skala. In **Kapitel 3** haben wir daher ein mathematisches Modell für die gesunden Verläufe verschiedener T-Zellen von der Geburt bis zum 60. Lebensjahr entwickelt. Dabei konnten wir auf Messungen gesunder Probanden zurückgreifen und haben darauf geachtet, auch genügend Messungen aus der frühen Kindheit mit einzubeziehen. Wir können die natürliche Dynamik der T-Zell-Konzentration im Blut in zwei Phasen einteilen. In der ersten Phase, die etwa sechs Monate dauert, steigt die Gesamtzahl der Immunzellen pro μL Blut linear an. In der darauffolgenden zweiten Phase sehen wir einen exponentiellen Abfall der Gesamtzahl der T-Zellen pro μL Blut. Die Dynamik verschiedener Arten von T-Zellen hängt von der Exposition gegenüber Krankheitserregern ab. Naive T-Zellen werden vorübergehend aktiviert, wenn sie einem Krankheitserreger ausgesetzt werden, woraufhin sich Teile dieser Zellen zu sogenannten Gedächtniszellen weiterentwickeln. Gedächtniszellen patrouillieren im Körper und beschleunigen die Beseitigung von wiederkehrenden Infektionen mit demselben Krankheitserreger. Aufgrund der Exposition gegenüber neuen Krankheitserregern nimmt die Anzahl der naiven T-Zellen im Laufe der Zeit ab, während die Anzahl der Gedächtniszellen zunimmt, bis ein Gleichgewicht (Homöostase) erreicht ist. Wir haben gezeigt, dass sowohl diese Abnahme

als auch diese Zunahme von T-Zellen mit demselben mathematischen Modell beschrieben werden können. Wir haben eine neue Methode verwendet, um das Modell, die in der Regel experimentell geschätzten Zellzahlen beschreiben zu lassen. Anstatt das Modell direkt an die Anzahl der Zellen anzupassen, berücksichtigten wir die labormäßige Gewinnung der Daten. So passten wir das Modell zunächst an die experimentell gemessenen Prozentsätze der Zellen an und leiteten dann davon die Funktionen für die absolute Anzahl der Zellen ab. Dies ermöglicht es uns, sowohl für absolute Zahlen als auch für Prozentsätze von T-Zellen konsistente Parameter zu erhalten. Auf diese Weise konnten wir Referenzfunktionen etablieren, die einen gesunden Verlauf der T-Zell-Dynamik im Laufe des Lebens beschreiben.

In **Kapitel 4** haben wir diese Referenzfunktionen als Ausgangspunkt verwendet, um die Dynamik von CD4+ T-Zellen bei Kindern mit HIV zu untersuchen. Durch den Vergleich der CD4-Werte dieser Kinder mit den Referenzfunktionen, konnten wir feststellen, inwieweit sie von einem gesunden Wert abweichen. Anschließend untersuchten wir, ob sich der CD4-Spiegel während der ART-Behandlung erholt, und wenn ja, wie schnell. Wir haben gesehen, dass die CD4-Werte der Kinder, als sie noch nicht behandelt wurden, niedriger waren als die gesunde Referenz. Nach Beginn der ART-Behandlung stiegen die CD4-Spiegel an, bis sie auf einem bestimmten stabilen Niveau blieben. Durch die Beschreibung dieser Dynamik mit einem mathematischen Modell konnten wir die Geschwindigkeit der Erholung, den Moment der Stabilisierung und das endgültige stabile Niveau beschreiben. Wir zeigten, dass ART normalerweise die Anzahl der CD4+ T-Zellen auf einen gesunden Wert zurückbringt. Wir haben jedoch auch gesehen, dass diese Erholung im Vergleich zur natürlichen Produktion neuer Zellen, relativ langsam ist. Eine Erholung der CD4-Zahlen wurde normalerweise erst 3-13 Monate nach der Unterdrückung des Virus im Blut beobachtet. Darüber hinaus fanden wir eine Dichteabhängigkeit der CD4-Erholung: Je niedriger der CD4-Wert zum Zeitpunkt des Behandlungsbeginns war, desto schneller stieg der CD4-Wert an. Die CD4-Erholung war nicht direkt vom Alter der Kinder abhängig. Bei den Kindern mit einer unregelmäßigen VL-Abnahme war die CD4-Erholung langsamer als bei Kindern mit einer regelmäßigen VL-Abnahme, aber die CD4-Werte normalisierten sich auch bei diesen Kindern, sobald die VL kontrolliert wurde. Diese Studie zeigt, dass eine frühzeitige ART-Behandlung zur Verhinderung einer CD4+-T-Zell-Abnahme beiträgt und eine vollständige (zumindest zahlenmäßige) Erholung auf gesunde CD4-Spiegel sicherstellen kann.

Bisher haben wir uns mit der Wirkung einer frühen ART-Behandlung bei Kindern

mit HIV befasst. In **Kapitel 5** haben wir untersucht, wie sich die VL entwickeln würde, wenn die Kinder nicht behandelt würden, wie sie sich von infizierten Erwachsenen unterschieden und welche Mechanismen diese Unterschiede erklären könnten. Wenn Kinder keine ART-Behandlung erhalten, bleibt die VL oft sehr hoch, während die VL bei Erwachsenen normalerweise nach einer anfänglichen sich zuspitzenden Infektionsphase auf ein niedrigeres stabiles Niveau abfällt, das von Person zu Person variiert und als *VL-Sollwert* bezeichnet wird. Patienten mit einer hohen VL entwickeln im Allgemeinen schneller AIDS. Wenn Kinder keine ART erhalten, sterben sie oft innerhalb von zwei Jahren. In dieser Studie verwendeten wir ein mathematisches Modell für eine akute HIV-Infektion bei Erwachsenen. Wir haben das Modell für eine Reihe verschiedener Parameterwerte verändert, um zu untersuchen, welche Mechanismen, für die bei Kleinkindern beobachtete Dynamik (ein hoher Spitzenwert der VL, der anschließend wenig oder gar nicht abnimmt) verantwortlich sein können. Zunächst einmal konnten wir zeigen, dass die Replikationsrate des Virus bei Kleinkindern nicht höher zu sein scheint, als bei Erwachsenen, um den Unterschied zu erklären. Wir haben gesehen, dass ein hoher Umsatz der CD4+ T-Zellen (z.B., weil sich die CD4+ T-Zellen schnell teilen) dafür sorgen kann, dass die VL wenig abnimmt. Aber die Abnahme der VL schien hauptsächlich von der Immunantwort gegen das Virus abhängig zu sein. Wenn der Körper keine gute Immunantwort aufbauen kann, zum Beispiel weil das Immunsystem noch nicht ausreichend entwickelt ist, sinkt die VL nicht oder kaum. Dies zeigt, dass ein wichtiger Effekt einer frühen ART-Behandlung darin besteht, dass sich das Immunsystem des Kindes so entwickeln kann, dass es dazu beitragen kann das Virus zu unterdrücken.

Die Studien dieser Arbeit tragen zu einem besseren Verständnis der zeitlichen Entwicklung von HIV und des Immunsystems bei Kleinkindern mit HIV bei. Sie zeigen, dass ein früher Beginn der ART-Behandlung mehrere Vorteile hat: Ein früher Beginn der Behandlung ist mit einer schnellen und regelmäßigen Abnahme der VL und mit einer geringeren negativen Wirkung auf das sich entwickelnde Immunsystem oder mit seiner Erholung auf nahezu gesunde Werte verbunden. Die Unterdrückung des Virus und ein gesundes Immunsystem sind wichtig für die gesunde Entwicklung jedes Kindes. Außerdem schaffen sie die Voraussetzung für zukünftige klinische Anwendungen, die eine „funktionelle" Heilung der HIV-Infektion verfolgen.

S

Acknowledgements

A PhD journey is never linear, and so has not been mine. Through the up and downs (which are also reflected by the waves on the cover) quite some people have accompanied, encouraged, supported and have kept believing in me along the way, and it is now about time to say thank you for that all.

First of all, I would like to thank my supervisor, Rob de Boer. Rob, even though you told me several times to keep it short, you totally deserve this space here to let everyone know what kind of great mentor you have been for me. You taught me how to fly, by slowly but surely pushing me out of the nest. Leaving my comfort zones helped me to become more confident in my abilities, but only because I could always rely on you to back me up in any case of emergency. Your calm state of mind, "First do then think", was exactly what I needed when things were not going as planned or when my nerves were once more playing tricks on me. I could definitely not have asked for a better "Doktorvater", and no words can properly reflect my appreciation.

Second, I would like to thank my thesis advisor committee, Can and José. You both have always had a sympathetic ear for me, and you were there with help and advice. From casual chats to scientific feedback over career advises to personal growth, I could come with any subject to you and always met friendliness and benevolence. Thank you for that!

Third, a big thank you goes to the whole TBB. Every single one of you is unique and makes TBB to the speciality that it is. You were my scientific family and home over the last years. You gave me the opportunity and provided me the stage to grow and to develop. You are a bunch of like-minded people that I will favourably keep in memory.
At this point, I would also like to thank Paola, who opened me the doors to TBB, and facilitated with her connections my TBB beginning.

Paulien, you are the rock of the TBB family. It has been an honour to get to know you, you are an outstanding figure in the world of science with an incredible down-to-earthness. I very much appreciated our little chats on the sidelines.

Thank you, Berend, for keeping my spirits up with your authenticity, your openness, and your indispensable eager to make this world to a better place; I am sorry I could not help you more often when you randomly entered our office.

Rutger, Michael, Bas and Kirsten were always available for advice on statistics, university politics, scientific careers and self-care. Thank you for the support and chats along the way!

A significant thank you must also go to Jan Kees, whose technical support was indispensable for ensuring that I always had the required IT-tools available (and working) to complete my work. Thank you especially for your quick and straightforward help in some critical moments, you rescued me more than once!

Peter, Arpit and Erdem – my boys – were at my side during the ups and downs of my PhD: always ready to share a cup of coffee and a sympathetic ear. I will miss our countless dinners including chilli contest, fisheyes, the one or other glass of wine, tears and laughers, serious conversations and of course international delicacies, which varied the composition of my PhD to the better. It was an awesome and intense time, thank the three of you for sharing this path together! Good luck for finishing up your PhDs, I have managed and so will you.

My (two eras of) office mates Julian, Sam, John, Bastiaan, and Eelco deserve special thanks: you experienced my day-to-day moments of joy and difficulty; you were always quick to encourage me to keep on and push through. Thank you also for your invaluable feedback on my charts and figures, without you my colour compositions would have just been a shadow of black and some shades of grey.

Chris and Laurens, thank you for the mathematical discussions and your advice on the correct use of some statistical procedures. You were always willing to help me out when I was appearing at your doors. Thanks a lot!

Laura, Bas, Marleen, and Sarah – thank you for sharing your knowledge with me, and for your time discussing different aspects of work and life.

My "predecessors" Hilje and Bram inspired me to follow after their example; thank you Hilje for all the Dutch translations you provided and Bram for being my native guide to the social ecosystem of TBB. You both made it very easy for me to settle into the Dutch lifestyle, not only at work as colleagues but also outside of work, such as during ice skating or social gatherings.

My project partners Andy, Sinead and Anet were the people who collaborated most in this endeavour; thank you so much for your great teamwork, communication and personal support at all stages of this work. Without you it would have been much less fun!

The hospital members of the IJCLUB Aridaman, Nila, Rianne, Weiyang, and Abhi deserve special thanks for the discussions about hot topics in immunology and bringing me closer to the practical application of flow cytometry analysis. The exchange with you was always informative and very enjoyable. I have learnt a lot!

Thank you, Julia, for the friendship we built throughout countless conferences, joint tutorials, lunches, coffee and garden breaks. Work related or not, we have always found a topic to talk about.

Claudia, Adele, and Sophia: thank you for listening to me elaborate on this project; and then making sure that I would spend an evening away from science doing Pilates, having a coffee walk, or just chit-chatting about topics that do not require a p-value.

Special thanks belong to my paranymphs Eva and Susi; thank You for having my back on more than just my defence: being it for handy stress management flow-charts or learning Dutch together – without you I could not have done it. Eva, from day one on we have been on this path together, and Susi, you ensured that the homesickness never became a problem.

Dear Tina, your friendship has been a continuous source of strength during the composition of this thesis; thank you for your untiring emotional support over this challenging period of my life. Thank you for being my chosen family, my COVID asylum and my partner in crime. Durch dick und dünn: wir haben es immer zusammen gemeistert. Wir sind zu einem unschlagbaren Team geworden, dies ist nur schwer zu toppen!

Ein großer Dank geht an Melina für die Umsetzung und Gestaltung meines Covers. Danke für deine Detailgenauigkeit und deine unaufhörliche Geduld in diesem langwierigen Prozess.

Jule, Fabi, Franzi und Lukas – ihr habt schon früh meinen Werdegang mit verfolgt und seid auch während den schweren Zeiten immer für mich da gewesen. Danke dafür!

Carmen und Dominik (ich hoffe du bekommst es da oben auch mit), ihr habt immer an mich geglaubt und mich ermutigt meinen eigenen Weg zu gehen, in

schwierigen Zeiten nicht aufzugeben, sondern die Gelegenheit, die sich entlang des Weges bieten zu nutzen. Ich bin euch unendlich dankbar dafür, dass ihr so wichtige und großartige Wegweiser gewesen seid.

Jana und Liane, vielen Dank für eure langjährige Freundschaft. Bei euch kann und darf ich einfach ich sein. Danke für all die Gespräche, Aufmunterungen, und gemeinsamen Aktivitäten über die Jahre. Auch wenn ich in der Weltgeschichte herumirre, gebt ihr mir immer das Gefühl für mich da zu sein. Vor allem die Pandemiezeit hat mir aufgezeigt, was für ein unglaubliches Geschenk diese Freundschaft ist. Liane, danke auch dir für das unzählige Korrekturlesen.

Und zu guter Letzt, geht mein Dank an meine Familie: Mama, Papa, Sebastian, Oma und Opa, was wäre ich nur ohne euch. Das alles hier wäre nicht machbar gewesen, wenn ich nicht eure Unterstützung gehabt hätte. Ich weiß, dass ihr voll und ganz hinter mir steht und ich immer auf euch zählen kann! Oma und Opa, ich möchte die wöchentlichen Anrufe mit euch nicht missen, eure Ermutigungen und Weisheiten habe ich mir immer zu Herzen genommen. Ein ganz spezielles Dankeschön geht an Mama; du warst zu jeder Tages- und Nachtzeit für mich erreichbar und hast die unterschiedlichen Stationen dieser Doktorarbeit hautnah mitbekommen. Danke, dass ihr mir immer mit Rat und Tat zur Seite standet und meine Leuchttürme wart in Zeiten des Sturms!

List of Publications

Schröter J, Anelone AJN, de Boer RJ; EPIICAL Consortium. Quantification of CD4 recovery in early-treated infants living with HIV. *J Acquir Immune Defic Syndr.* 2022;89(5):546-557 doi: 10.1097/QAI.0000000000002905

Schröter J, Borghans JAM, Bitter WM, van Dongen JJM, de Boer RJ. Age-dependent normalisation functions for T-lymphocytes in healthy individuals. *bioRxiv.* 2021. doi: 10.1101/2021.12.01.470754.

Morris SE, Dziobek-Garrett L, Strehlau R, **Schröter J**, Shiau S, Anelone AJN, Paximadis M, de Boer RJ, Abrams EJ, Tiemessen CT, Kuhn L, Yates AJ; EPIICAL Consortium and the LEOPARD study team. Quantifying the dynamics of HIV decline in perinatally infected neonates on antiretroviral therapy. *J Acquir Immune Defic Syndr.* 2020;85(2):209-218. doi: 10.1097/QAI.0000000000002425.

Schröter J, Anelone AJN, Yates AJ, de Boer RJ; EPIICAL Consortium. Time to viral suppression in perinatally HIV-infected infants depends on the viral load and CD4 T-cell percentage at the start of treatment. *J Acquir Immune Defic Syndr.* 2020;83(5):522-529. doi: 10.1097/QAI.0000000000002291.

Piontek T, Harmel C, Pawlita M, Carow K, **Schröter J**, Runnebaum IB, Dürst M, Graw F, Waterboer T. Post-treatment Human Papillomavirus antibody kinetics in cervical cancer patients. *Philos Trans R Soc Lond B Biol Sci.* 2019;374(1773):20180295. doi: 10.1098/rstb.2018.0295.

Loenenbach AD, Poethko-Müller C, Pawlita M, Thamm M, Harder T, Waterboer T, **Schröter J**, Deleré Y, Wichmann O, Wiese-Posselt M. Mucosal and cutaneous Human Papillomavirus seroprevalence among adults in the prevaccine era in Germany - Results from a nationwide population-based survey. *Int J Infect Dis.* 2019;83:3-11. doi: 10.1016/j.ijid.2019.03.022.

Curriculum vitae

Juliane Schröter (*21 April 1989) grew up in the little village Loffenau in the northern part of the Black Forest, Germany. After her Abitur at the Albert-Schweitzer-Gymnasium in Gernsbach (Germany) in 2008, she has become a little globetrotter. She spent a year in New Zealand as an au-pair, before she started her studies in Biomathematics at the University of Greifswald, Germany. A DAAD PROMOS stipend allowed her to return to New Zealand to complement her Bachelor studies with a semester abroad at Massey University in Palmerston North. In 2012, she concluded her Bachelor's studies with an interdisciplinary thesis about "Metabolic Flux analysis of Streptococcus pneumoniae" at the department of Molecular Genetics and Infection Biology, where she also gained her first wet lab experience. Before continuing with her Master's degree, she spent another half year at Massey University for an internship in Computational Biology financed by a Royal New Zealand Grant. Juliane worked there in the field of population genetics to reveal the mosaic genome structure of admixed Pacific populations, while also improving her programming skills. In 2015, she obtained her Master's degree with distinction in Mathematical Biology at University of Dundee, Scotland. For her thesis, she developed a mathematical model about Auger induced double-strand break propagation in cells. Juliane's interest to apply mathematics as a tool in an interdisciplinary and medical context led her then to the DKFZ (German cancer research centre) for 2 years. She worked there as a research fellow in the area of molecular epidemiology, where she gained some more wet lab experience and was involved in large nationwide serology studies. In 2017, she started her PhD in the Theoretical Biology group at Utrecht University, NL. The results of her research are presented in this thesis.

Juliane's next stop is New York City (USA), where she has accepted a postdoc position at Columbia University starting in January 2023.